ABSENCE OF MYOSTATIN IMPROVES CARDIAC FUNCTION AFTER MYOCARDIAL INFARCTION

Thesis submitted in partial fulfilment of the requirements for the Degree of

Doctor of Medicine

By

SARINA LIM

MB ChB, FRACP

University of Auckland

New Zealand 2014

ABSTRACT

Myostatin is a well-established inhibitor of skeletal muscle development. However, the role of myostatin in cardiac muscle, specifically in acute myocardial infarction (MI), is less clear. Therefore, the aim of this thesis is to determine the potential effects of myostatin following an acute MI.

Methods: The first study examined the concentration of myostatin mRNA at different time points following an induction of MI in an ovine model. Using a murine model with a constitutive deletion of the myostatin gene ($Mstn^{-/-}$) and compared with WT controls, the second study investigated several clinical outcomes in the absence of myostatin at 28 days following an acute MI via ligation of the left anterior descending (LAD) artery. At 28 days post-MI, mice were injected with BrdU, then euthanized and their hearts were excised and weighed, followed by histological examination, immunohistochemistry and indirect immunofluorescence.

Findings: When compared with non-infarcted ovine controls, the concentration of myostatin mRNA was reduced and reached a nadir at day one post-MI in the peri-infarct region of the myocardium before a progressive restoration of the concentration of myostatin mRNA to that of the controls ($P < 0.01$). This dynamic change was not observed in the distant region of the myocardium post-MI ($P < 0.01$). In the $Mstn^{-/-}$ mice, the total body weight was larger than WT mice (39.21 ± 0.57g vs 24.66 ± 0.37g, $P <$

0.001) and remained so during the study period. The mortality rate in Mstn$^{-/-}$ mice was lower compared with WT mice post-surgery (0% vs 20%, $P < 0.05$). Ligation of the LAD artery resulted in a similar infarct size in both the Mstn$^{-/-}$ and WT mice (9.9 ± 1.9% vs 12.5 ± 1.7%, $P = 0.38$). Cardiac ejection fraction (EF) as determined by echocardiography was similar at baseline between the genotypes (61.5 ± 1.2% vs 60.6 ± 1.3%, $P = 0.15$) and following induction of MI, a similar degree of reduction in EF resulted (-8.6 ± 2.2% vs -7.3 ± 2.7%, $P = 0.6$). However, at 28 days post-MI, EF was restored to baseline in Mstn$^{-/-}$ but not in the WT mice (61.8 ± 1.1% vs 57.1 ± 2.3%, $P < 0.01$). Mstn$^{-/-}$ mice had a lower mean increased in heart rate post-surgery compared with WT mice (+23.6 ± 13.7bpm vs +109.5 ± 14.3bpm, $P < 0.01$). Induction of MI resulted in a lower increased in mean arterial pressure in Mstn$^{-/-}$ mice compared with WT mice (-7 ± 3.9mmHg vs +4.4 ± 3.9mmHg, $P < 0.05$). There was no difference in the number of BrdU positive cells, the percent of apoptotic cardiomyocytes, and the size of cardiomyocytes between Mstn$^{-/-}$ and WT mice. However, a reduction in the extent of collagen deposition was observed in the Mstn$^{-/-}$ mice compared with WT mice (41.9 ± 2.8% vs 54.7 ± 3.4%, $P < 0.05$).

Conclusion: The absence of myostatin protects the function of the heart following an acute MI likely via inhibiting the extent of fibrosis. Further studies are needed to determine whether administration of myostatin antagonists could be used as an effective adjunct to the current management of acute MI.

ACKNOWLEDGMENTS

The surgical procedures and laboratory experiments conducted in this thesis were undertaken in Ruakura Research Centre, Hamilton, New Zealand. My supervisors Associate Professor John V Conaglan and Dr Chris McMahon contributed significantly to the design of the study and I am deeply grateful for their mentorship and guidance over the years. This thesis would not have been possible without their constant encouragement and support. Thank you both.

For the surgical procedures, I thank Dr Gerard Devlin for his work in the induction of myocardial infarction in the ovine model. Dr Devlin is also my advisor and provided valuable suggestions on obtaining and interpretation of the echocardiogram data. I am grateful to Dr Leigh Ellmers who taught me the surgical techniques in a murine model, from ventilation through to induction of myocardial infarction. The technique of echocardiography was learned from Juliet Jenson, a clinical echocardiographer at Waikato Hospital, Hamilton. A special thanks to Dr Kenneth Matthews who had assisted me in the collection of the histological samples. Dr Matthews was also one of the first persons who had shown me the various laboratory skills and techniques when I first embarked in this thesis. Thank you, Ken.

In the laboratory, every member of the Growth and Development team had, one way or another, provided their valuable time and advice in facilitating the success of this thesis. I

am therefore, grateful to Frank Jeanplong, Jenny Oldham, Shelley Falconer, Mônica Senna Salerno, Alex Hennebry, Mark Thomas, Jeremy Bracegirdle, Trevor Watson, Gina Nicholas, and Carole Berry. I also thank staff of the Small Animal Colony unit, Ric Broadhurst, Bobby Smith, and Genevieve Baildon, for their care of the animals. I would also acknowledge Harold Henderson, the statistician at Ruakura Research Centre for his advice on the statistical data presented in this project.

I also thank colleagues from Waikato Clinical School, including Professor Ross Lawrenson, Gillian Hunn, and Raewyn Wooderson for their support and administrative assistance. A special thank you also goes to my colleague Dr Marianne Elston, for her encouragement and constructive criticism of the thesis.

Finally, a special thank you to my husband, Kong, for his unconditional support, emotionally and financially. Thank you for his time off work in the final months of this thesis in taking care of household chores and looking after our two-year old daughter. I would not have succeeded without your loving support. Thank you.

GRANTS AND FUNDING

This thesis was supported by funding from the following body and organisations -

- Cardiology Research Charitable Trust.
- NZ RACP Grant Advisory Subcommittee.
- Research Fellowship from the Sarah Fitzgibbon Trust, Waikato Clinical School, University of Auckland.
- Waikato Medical Research Foundation.

PUBLICATIONS AND PRESENTATIONS

Oral presentations at learned scientific meetings:

1. Lim S, Matthews K, Devlin GP, Conaglen JV, McMahon CD. Absence of myostatin improves cardiac function following myocardial infarction. **RACP Annual Scientific Meeting, November 2009, Auckland**
2. Lim S, Matthews K, Ellmers L, Devlin GP, Conaglen JV, McMahon CD. Absence of myostatin improves cardiac function following myocardial infarction – animal studies. **ESA-SRB Annual Scientific Meeting, August 2009, Adelaide Convention Centre, Abstract Number 200**

TABLE OF CONTENTS

LIST OF ABBREVIATIONS

α-SMA	α-smooth muscle actin
Akt	Protein kinase B
Alks	Activin-like kinases
ANF	Atrial natriuretic factor
BMD	Becker muscular dystrophy
BMP	Bone-morphogenetic protein
Cdk2	Cyclin dependent kinase 2
CHD	Coronary heart disease
DM	diabetes mellitus
DMD	Duchenne muscular dystrophy
Fst	Follistatin
GDF-8	Growth and differentiation factor -8
GDF-11	Growth and differentiation factor -11
HR	Heart rate
IGF-1	Insulin-like growth factor-1
JNK	c-Jun N-terminal kinase
LAD	Left anterior descending
LAP	Latent associated peptide
LVESD	Left ventricle end systolic diameter
LVEDD	Left ventricle end diastolic diameter
MAP	Mean arterial pressure

MAPK	Mitogen-activated protein kinase
MEF2	Myocyte enhancer factor 2
MI	Myocardial infarction
Mstn	Myostatin
mTOR	Mammalian target of rapamycin
NYHA	New York Heart Association
PARP	Poly-ADP ribose polymerase
PBS	Phosphate buffered saline
PCR	Polymerase chain reaction
PI3K	Phosphoinositide-3-kinase
Rb	Retinoblastoma
TAC	transverse aortic constriction
TGF-β	Transforming growth factor-beta
TMP	Tolloid family of metalloproteinases
TNF-α	Tumour necrosis factor-α

LIST OF TABLES

LIST OF FIGURES

1

Overview of myostatin and myocardial infarction

1.1 Introduction

Ischaemic heart disease (IHD) was the second leading cause of death in New Zealand in 2009, accounting for 5553 deaths (96.6/100,000 in men, 48.6/100,000 in women) [1]. Furthermore, the investigation and management of ischaemic heart disease, including coronary angiography, angioplasty and coronary artery bypass surgery, contributed to a significant rate of hospitalisation in New Zealand [2]. Primary percutaneous coronary intervention remains the most effective treatment following an episode of acute myocardial infarction (MI) [3], contributing to an overall decline in the mortality from IHD, with a 68.3% and 67.4% reduction respectively from 1980 to 2009 in the male and female age-standardised death rate [1]. However, substantial morbidity remains with survivors being at risk of recurrent MI and developing acute or chronic heart failure [4, 5]. Indeed, the prevalence of heart failure, which increases with age, has risen substantially as a result of an overall increase in life expectancy [6]. Furthermore, as one of the major causes of chronic heart failure [6], preventing or reducing the severity and impact of ischaemic heart disease is essential in the management of chronic heart failure.

The pathophysiological consequences of ischaemic heart disease and the resultant heart failure are cellular inflammation and proliferation, apoptosis, regeneration, hypertrophy and remodelling of the myocardium, as well as fibrosis and formation of extracellular matrix in the interstitium [7, 8]. As a result, several novel therapeutic approaches have been considered to target these pathways in an attempt to reduce the burden of the disease. Specifically, one of the areas of interest is the transforming growth factor-β (TGF-β)

superfamily and its downstream cellular pathways, which play a role in hypertrophic signalling as well as modulation of fibrotic responses [9, 10].

Myostatin was discovered in 1997 following a screen of mouse genomic DNA to identify new members of the TGF-β superfamily [11]. Genetically modified mice with a disruption in the myostatin gene were found to be at least 30% larger than wild-type (WT) counterparts with individual muscles weighing two to three times heavier than WT controls [11]. Naturally, this led to an interest in developing a myostatin inhibitor to combat debilitating disorders of skeletal muscle such as Duchenne muscular dystrophy [12-15]. The subsequent detection of myostatin in cardiomyocytes and an up-regulation of myostatin expression in the peri-infarct tissue after MI suggested that, like other members of the TGF-β superfamily, myostatin may be a key player in cardiac pathology [16]. Indeed, a recent study had demonstrated that loss of myostatin slowed the progression of the growth of atheromatous lesions in low density lipoprotein (LDL) receptor-null (*Ldlr-/-)* mice [17]. Other studies had demonstrated that the expression of myostatin (either mRNA, protein or both) was up-regulated in various pathological models of chronic heart failure [18-20]. Myostatin was also shown to directly regulate the proliferation of normal and dystrophic skeletal muscle fibroblasts [21, 22]. However, little is known about the effects of myostatin in an acute phase of myocardial injury, such as following an acute MI. Whether myostatin has a different role in cardiomyocytes or cardiac fibroblasts is also unclear. It is also not known if the frequently reported up-regulation of myostatin expression following cardiac injury is beneficial, detrimental, or neutral to the heart. Therefore, the aim of this thesis is to determine whether the absence of myostatin will improve the recovery of

cardiac function post-MI and, if so, whether the mechanism involves regulating the hypertrophy of cardiomyocytes or through a reduction in fibrosis or possibly both.

To introduce the role of myostatin in the heart, this chapter will firstly address the characteristics, structure and biosynthesis of myostatin. A brief overview of the TGF-β receptors and post-receptor signalling pathways will be discussed. This will be followed by an overview of the role of myostatin at a cellular level, and the clinical applications published to date. The chapter will conclude with a critical analysis of the current literature, reviewing the effects of myostatin on the heart in normal and pathophysiological states, followed by the hypothesis and aims of the study.

1.2 Characteristics, structure, biosynthesis and regulation of myostatin

The human myostatin gene maps to chromosome 2q.32.2 and is highly conserved across the vertebrate species [23]. It is a small gene of 7.8kb and consists of three exons and two intervening introns (Figure 1-1). The gene is processed to produce a single 3.1kb mRNA species which is translated into a protein of 375 amino acids (aa) in humans [23, 24].

In mice, myostatin can be detected in the early developing somites and is expressed throughout embryogenesis and, probably, throughout life [11, 25]. The expression of

myostatin was originally described as being almost exclusively expressed in skeletal muscle, although a lower level of detection was observed in adipose tissue [11]. With the advent of more sensitive detection techniques, subsequent studies have shown that myostatin is also expressed in cardiac tissue [16] and in the serum of multiple species including humans [26, 27].

The biological function of myostatin also appears to be highly conserved across species (Figure 1-2). As previously mentioned, genetically engineered mice lacking the receptor binding moiety of myostatin are 30% larger than heterozygotes and wild type counterparts with individual muscles of myostatin-null mice weighing two to three fold more than wild type mice [11]. In Belgian Blue and Piedmontese cattle, there are naturally occurring loss-of-function mutations in the myostatin gene which result in a double-muscling phenotype [28, 29]. Similarly, an inactivating mutation in the myostatin gene was discovered in the whippet dog breed, resulting in a double-muscle phenotype known as the 'bully whippet' [30]. Several polymorphisms in the myostatin gene were detected in Piétrain pigs and may be responsible for the increased muscularity seen [31]. In several fish species, mutations in the myostatin gene were also thought to be responsible for increased growth and development of the muscle [32-34]. In 2004, a myostatin loss-of-function mutation was reported in a child with muscle hypertrophy [35]. These collective observations support the role of myostatin as a negative regulator of the skeletal muscle mass.

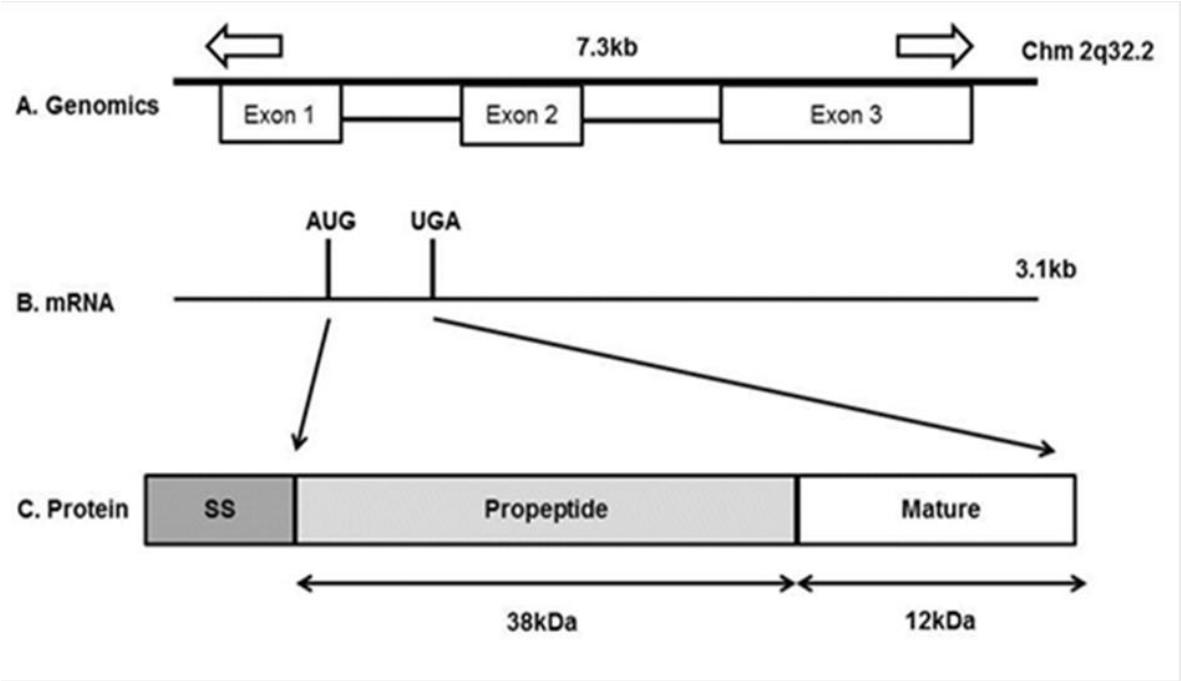

Figure 1-1. Human myostatin and its gene product. (A) Position of the three exons; (B) mRNA transcriptional initiation sites; (C) Structure of the myostatin protein. *Modified with permission from Patel K. et al. Neuromuscular disorders 2005;15:117-126*

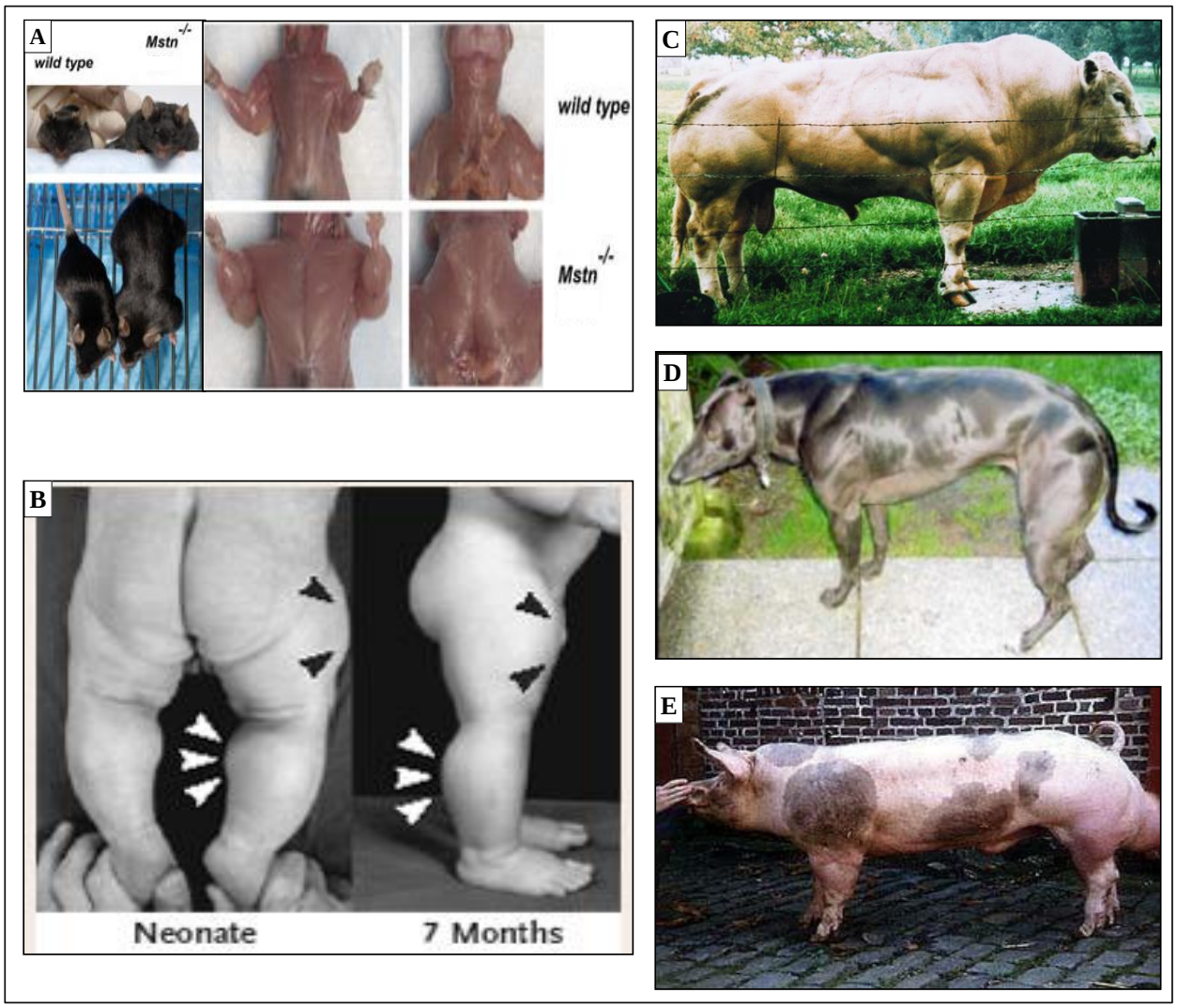

Figure 1-2. Alteration in the myostatin gene resulting in the double muscling phenotype seen in various species. (A) Genetically engineered myostatin-null mouse compared to wild-type mouse. Mutation of the myostatin gene in a (B) human child, (C) Belgian blue cattle, (D) Whippet dog, and (E) Piétrain pig. *Images compiled with permission from various references – see text.*

Myostatin shares characteristic hallmarks common to members of the TGF-β superfamily: an N-terminal signal peptide for secretion, a pro-region followed by an RSRR sequence representing a proteolytic processing site, and a C-terminal domain containing nine cysteine residues, six of which are integral to forming a cysteine knot structure [11]. Myostatin is synthesized as a precursor protein, known as prepromyostatin and requires at least three proteolytic events to generate the biologically active mature myostatin (Figure 1-3). The first cleavage removes the 24 amino acid signal peptide to form promyostatin [36]. The second cleavage by the furin family of protein convertases occurs at the RSRR site at amino acid 240-243 [36]. This processing event generates the N-terminal fragment known as the latent associated peptide (LAP or propeptide) and the C-terminal fragment which eventually gives rise to the mature myostatin, both of which remained non-covalently bound and are collectively referred to as the latent complex. Release of the mature myostatin from this latent complex requires a third proteolytic cleavage immediately N-terminal to aspartate 76 by the bone morphogenetic protein (BMP)-1/tolloid family of metalloproteinases (TMP) [36].

It was originally thought that generation of the latent complex occurred constitutively within the Golgi apparatus and, therefore, secretion of myostatin into circulation was thought to occur as a latent complex from myostatin producing cells [37]. However, recently it has been shown that the predominant form of myostatin in skeletal myocytes is promyostatin and this promyostatin is present extracellularly [37]. After secretion, this inactive promyostatin is held in the extracellular matrix by latent TGF-β binding proteins (LTBPs) with LTBP-3 being the predominant LTBP family in skeletal muscle [37].

Promyostatin is then converted to the latent complex through cleavage by furin convertases in the extracellular space (Figure 1-4). In contrast, myostatin already exists as a latent complex in serum and requires only cleavage by BMP-1/TMP for activation [26, 27]. Therefore, two different pools of myostatin exist in regulating muscle growth: a local pool in skeletal muscle and a systemic pool in serum, the latter which could potentially be derived from heart or adipose tissue [38].

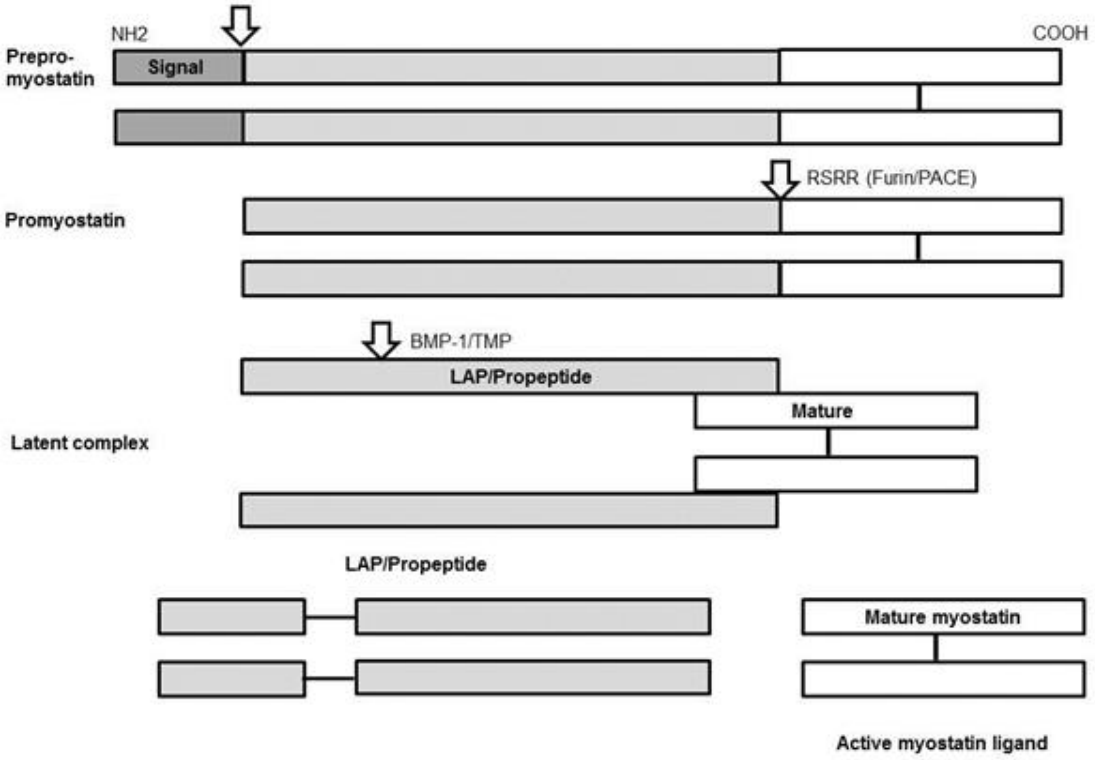

Figure 1-3. Schematic structure of the myostatin protein and the proteolytic processing sites. *Reproduced with permission from Breitbart A et al. Am J Physio Heart Circ Physio 2011;300:H1973-H1982*

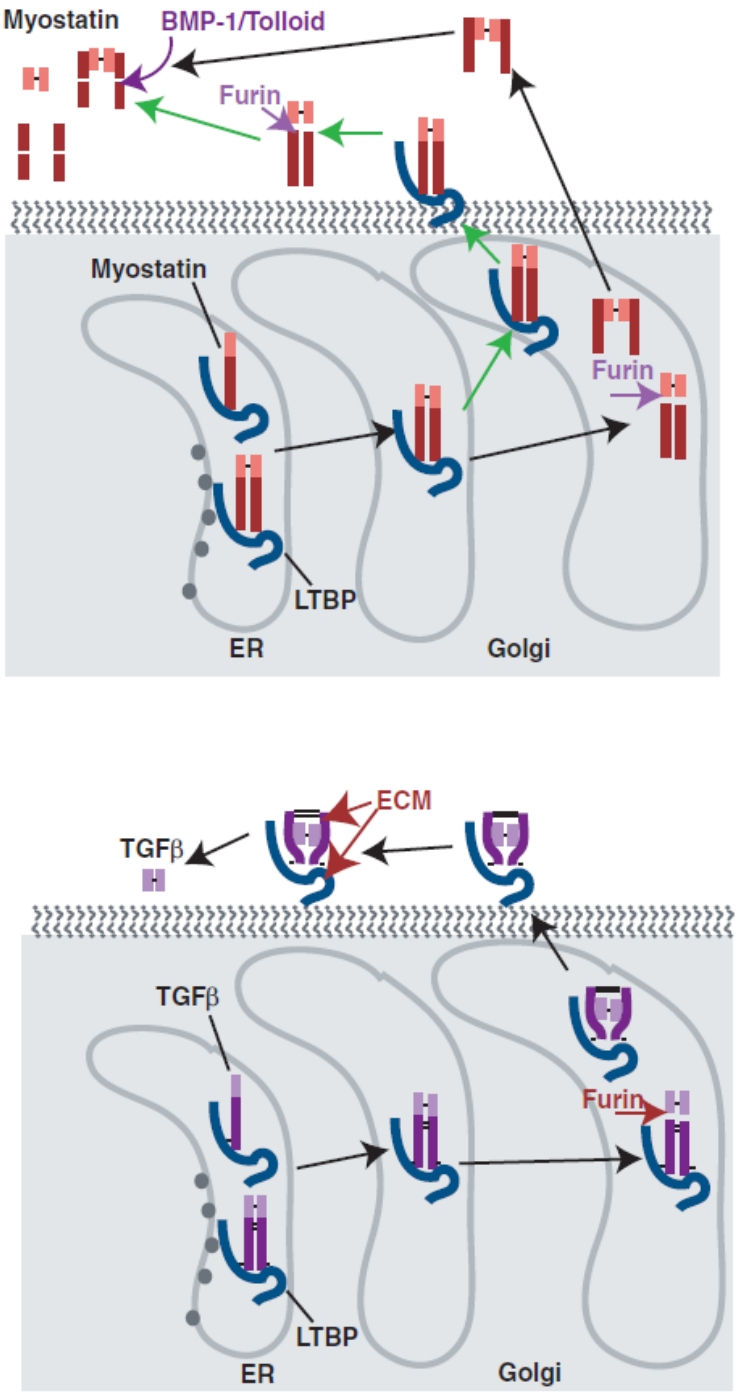

Figure 1-4. Model of myostatin and TGF-β ligand maturation and secretion. Green arrows indicate the proposed model. *Reproduced with permission from Anderson et al. J Bio Chem 2008;283(11):7027-35*

The C-terminal region of mature myostatin exists as a disulphide linked dimer, as demonstrated by McPherron and co-workers [11]. Under non-reducing conditions, an antibody directed against the C-terminus detected two protein species with apparent molecular masses (M_r) of 101,000 and 25,000, which is consistent with the dimeric forms of the unprocessed and processed myostatin respectively [11].

The propeptide form of myostatin facilitates the correct folding of the C-terminal domain into a cysteine knot structure [36]. Correct folding of the protein is important for myostatin action [36]. The often cited example of incorrect folding of mature myostatin came from the Piedmontese breed of cattle which have a high frequency of the double-muscling phenotype [28]. The Piedmontese cattle phenotype arises from a naturally occurring single nucleotide polymorphism that substitutes a guanine (G) to an adenine (A) in exon 3, resulting in a cysteine to tyrosine substitution in the mature region of the protein (amino acid 313) [28]. This cysteine residue is crucial for the correct formation of the cysteine knot structure. The mutation in this region results in a misfolded peptide which forms a dominant negative protein that cannot activate the receptors [28]. Therefore, muscle development is not inhibited, and the resulting increase in muscle mass is referred to as 'double muscling' [28]. The myostatin propeptide is also able to regulate the activity of the C-terminal dimer following proteolytic processing [36]. *In vitro* studies have shown that the myostatin propeptide is able to block the biological activity of the C-terminal dimer through inhibition of receptor binding [39, 40]. This inhibitory effect has also been demonstrated *in vivo* in which transgenic mice overexpressing myostatin propeptide have increased muscling, arising from both an increase in the number and size of muscle fibres

that were comparable to that of myostatin knockout mice, and the increase in muscle weight corresponded to the expression of the myostatin propeptide [39].

In addition to the propeptide, the activity of myostatin is regulated at several levels. As mentioned earlier, the expression of myostatin is limited to only a few cell types such as skeletal muscle, cardiac and adipose tissue [11, 16]. Secondly, myostatin is synthesized as a precursor protein and remains inactive until the subsequent proteolytic cleavages take place, as previously described [36]. Thirdly, several extracellular inhibitors that control the binding of myostatin to cell surface receptors have been implicated in the regulation of myostatin activity [36]. These proteins, which have the potential to develop as potent inhibitors of myostatin, include follistatin (Fst), follistatin-like related gene (FLRG), and growth and differentiation factor-associated serum protein-1 (GASP-1). Follistatin is a multi-domain protein with an N-terminal domain and three subsequent Fst domains (FSD1-3) [41]. Follistatin is thought to inhibit the activity of myostatin by binding to the C-terminal dimer and blocks its ability to bind to the receptor [39]. Transgenic mice overexpressing follistatin develop hypermuscularity similar to that of the myostatin knockout mice [39]. The roles of FLRG and GASP-1 in the regulation of myostatin activity are less clear and several possibilities were speculated. These include the ability of these regulators forming higher order complexes with the myostatin C-terminal dimer and maintaining myostatin latency, or the ability of these proteins in terminating myostatin signalling post-receptor binding [36]. As a result, these endogenous inhibitors may potentially alter the concentration of myostatin protein and this would, therefore, explain some of the discrepancies seen between myostatin mRNA and protein expression

reported in the literature. Nevertheless, understanding and appreciating that the activity of myostatin can be regulated at multiple levels is essential, particularly when an inhibitor of myostatin is to be developed for therapeutic use.

1.3 TGF-β receptors and SMAD signalling pathways

The TGF-β superfamily has been broadly divided into two main groups based on the phylogenetic relationship of the ligands: (1) TGF-β and activin/inhibin, and (2) bone morphogenetic protein (BMP)/growth and differentiation factor (GDF) [42]. Upon activation of the mature ligand from its latent complex, members of the TGF-β superfamily exert their effects through a series of cell-surface serine/threonine transmembrane receptors, known as receptor types I and II [43]. There are seven type I and five type II receptors in vertebrates, classified based on their sequence similarities (Table 1-1). Binding of the ligand firstly to a type II receptor induces the association between type I and II receptors. The type II receptor transphosphorylates the inactive GS box, a highly conserved region immediately preceding the protein kinase domain located in the type I receptor, and activates its kinase domain [44]. It is thought that different TGF-β ligands use specific receptors for signalling, although some receptors may display a more promiscuous behaviour [41]. For example, TGF-β uses type II receptor TGF-βRII and type I receptor Activin like kinase-5 (Alk5) [45], while activin signals through Act RII or Act RIIB and Alk4 [46]. However, Alk4 can also mediate GDF1 and Nodal signals, while Act RIIB mediates Nodal, BMP2, BMP 6/7 and Inhibin A/B signals (Table 1-1). In the case of myostatin (also known as GDF8), the active ligand preferentially binds to type II

receptors Act RII or Act RIIB (with higher affinity to the latter) and recruits type I receptors Alk4 or Alk5 to activate downstream signals (Figure 1-5).

The activated ligand-receptor complex phosphorylates the first group of the SMAD family of transcription factors, the receptor-regulated or R-Smads and forms the receptor-Smad complex (Figure 1-6). The binding of the type I receptor to R-Smads is facilitated by the SMAD anchor for receptor activation (SARA), a protein that recruits SMADs to the membrane [43]. Different R-Smads are recognised by different receptors wherein Smads 1, 5 and 8 are recognised by BMP receptors whilst Smads 2, 3 by TGF-β and Activin receptors [47]. The phosphorylated R-Smads accumulate in the nucleus and associate with the second class of the SMAD family of transcription factors, the Co-Smad of which Smad 4 is the only member, to form a functional heteromeric complex [43]. In the nucleus, this transcriptional complex associates with one of the many DNA-binding cofactors and various coactivators and corepressors of gene expression [43]. The third class of the SMAD family of transcription factors, the Inhibitory Smads (Smads 6 and 7) counteract the effects of R-Smads and antagonise TGF-β signalling. Despite belonging to the subgroup of BMP family, myostatin has been shown to preferentially signal through TGF-β/activin dependent intracellular pathway by phosphorylation of Smads 2 and 3 and activate downstream signal transduction [48, 49].

This combination of complex receptor binding capacities, the presence of binding proteins, the effects of coactivators and co-repressors, and other accessory receptors may explain how members of the TGF-β family manage to produce diverse cellular responses

and why they are regarded as multifunctional hormones. Moreover, there are thoughts to be interactions between the TGF-β and other signalling cascades and receptor crosstalk, and possibly SMAD-independent pathways, which have started to be described [50, 51] .

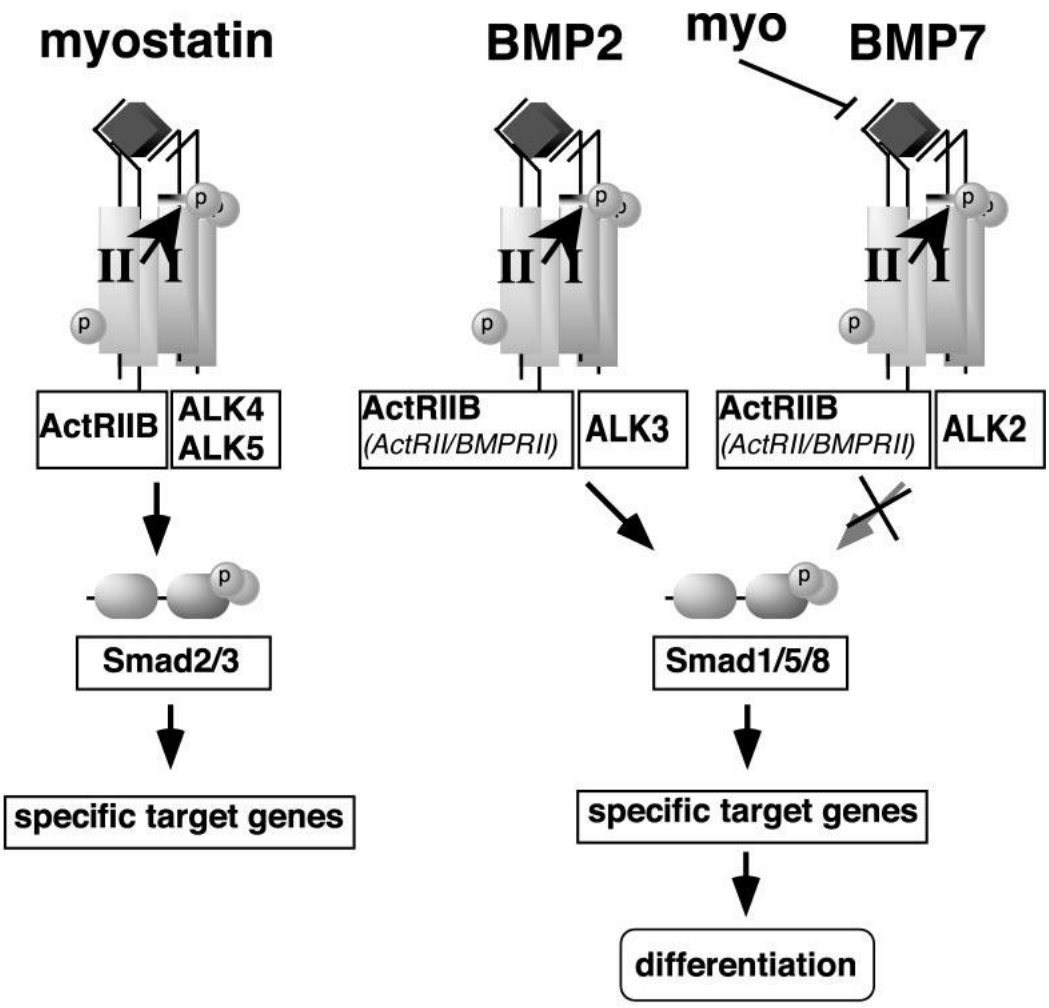

Figure 1-5. TGF-β receptors affinity and selective SMAD signalling. *Reproduced with permission from Rebbapragada A. et al. Mol. Cell. Biol. 2003;23(20):7230-42*

Table 1-1. Known ligand-binding properties and nomenclature for the TGF-β superfamily receptors. *Modified with permission from de Caestecker M. Cytokine & Growth Factor Reviews 2004;15:1-11*

Receptors	Ligands
Type 1 Receptors	
Alk 1 Group	
Alk 1	TGF-β, Activin A
Alk 2	TGF-β, Activin A, MIS, BMP6/7
Alk 3 Group	
Alk 3	BMP2/4, BMP6/7
Alk 6	BMP2/4, GDF5/6, GDF9b, MIS, BMP6/7
Alk 5 Group	
Alk 4	Activin A, GDF1 and Nodal, GDF 11
Alk 5	TGF-β
Alk 7	Nodal
Type II Receptors	
TGF-β RII	TGF-β
BMP RII	Inhibin A, BMP2/4, BMP6/7, GDF5/6, GDF9b
Act RII (Activin type II receptor)	Activin A, Inhibin A/B, GDF1 and Nodal, BMP2, BMP6/7, GDF5, GDF9b, GDF8/11
Act RIIB	Activin A, Inhibin A/B, Nodal, BMP2, BMP6/7, GDF5, GDF8/11
MIS RII (Mullerian inhibiting substance type II receptor	MIS

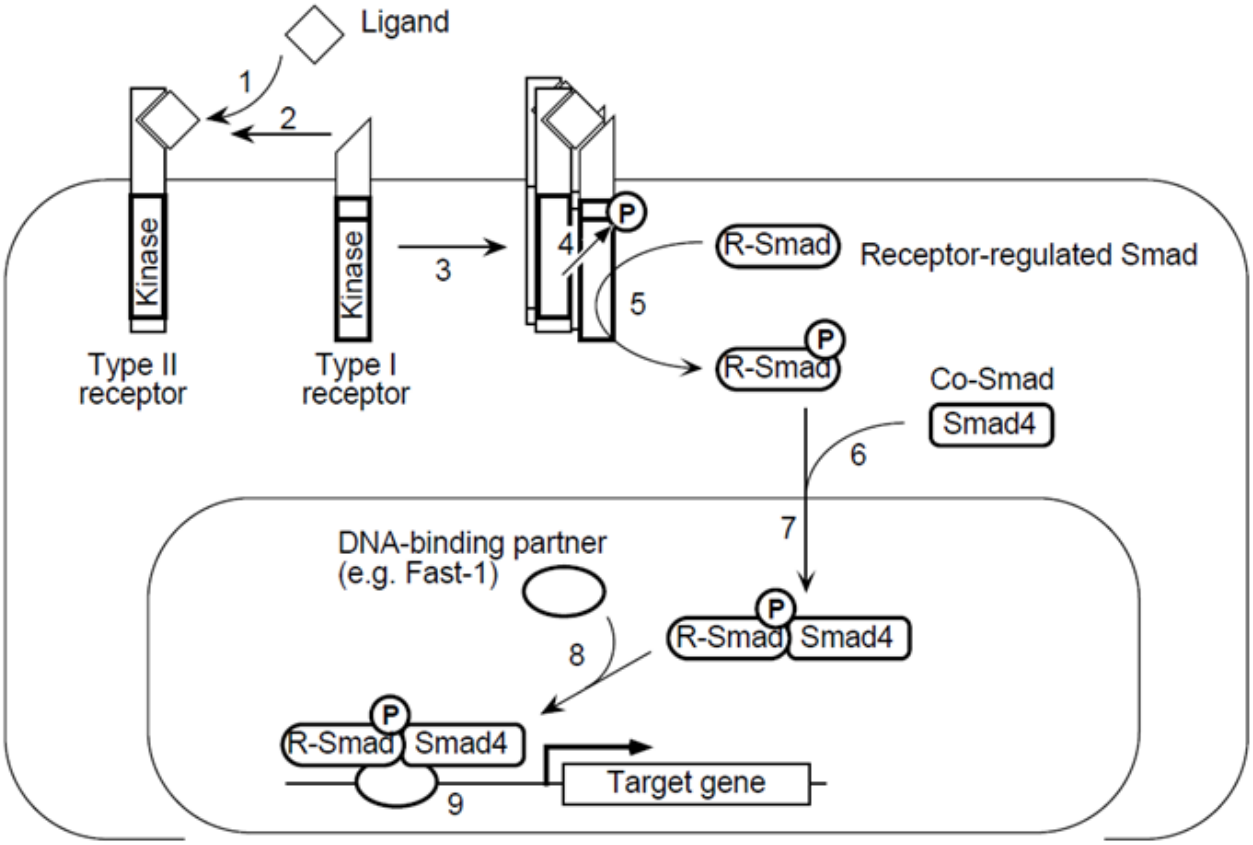

Figure 1-6. The TGF-β and SMAD pathway. Binding of a TGF-β family member to its type II receptor (*1*) in concert with a type I receptor (*2*) leads to formation of a receptor complex (*3*) and phosphorylation of the type I receptor (*4*). Thus activated, the type I receptor subsequently phosphorylates a receptor-regulated SMAD (R-Smad) (*5*), allowing this protein to associate with Smad4 (*6*) and move into the nucleus (*7*). In the nucleus, the SMAD complex associates with a DNA-binding partner, such as Fast-1 (*8*), and this complex binds to specific enhancers in targets genes (*9*), activating transcription. *Reproduced with permission from Massagué J. Ann Rev Biochem 1998;67:753-91*

1.4 The role of myostatin in proliferation and differentiation of cells

A number of studies have examined the effects of myostatin on proliferation of cells. Thomas and co-workers have shown that myostatin protein is synthesized and proteolytically processed in myoblasts [52]. They also reported that myostatin inhibited the proliferation not only of C_2C_{12} myoblasts, but also of primary ovine myoblasts, and that this inhibition was reversible once myostatin protein was removed from the culture media [52]. Taylor and colleagues have shown that both the full-length 375aa and the 110aa C-terminal recombinant myostatin protein inhibit the proliferation of C_2C_{12} myoblasts in a dose-dependent manner [53]. Ríos and co-workers were able to transiently transfect C_2C_{12} myoblasts with a transgenic myostatin construct, which subsequently synthesized the protein and induced a 50% reduction in the rate of myoblast proliferation [54]. Collectively, these data indicate that myostatin inhibits the growth of skeletal muscle by reducing the number of cells and myofibres. Myostatin appears to achieve this reduction in cell number by inhibiting the activity of cyclin-dependent kinases (Cdks) of which Cdk2 is the primary target [52]. A concomitant up-regulation of the cyclin-dependent kinase inhibitor p21 was observed [52]. Together, these resulted in hypophosphorylation of retinoblastoma (Rb) protein and arrest of the progression of the cell cycle at the G1-S phase.

The effects of myostatin on differentiation have also been extensively studied. For cellular differentiation to occur, undifferentiated mesoderm cells must commit to the myogenic lineage, followed by proliferation and irreversible withdrawal from the cell cycle [55]. A number of muscle-specific transcription factors collectively known as the MyoD family of muscle regulatory factors (MRF) are critical for the formation of multinucleated myotubes [55]. Within the MRF family, MyoD and Myf5 are classified as primary MRFs as they are involved in the determination of the myogenic lineage, whereas myogenin and MRF4 are considered secondary MRFs as they control the process of terminal differentiation [56].

Using C_2C_{12} and primary ovine myoblasts, Langley and co-workers showed that myostatin inhibited differentiation of myoblasts in a dose-dependent manner [55]. They also examined whether this inhibition was mediated through MRFs and found that the expression of MyoD, Myf5 and myogenin were significantly increased in the control myoblasts when myostatin was not added to the differentiation media, whilst the expression of these factors was down-regulated in the myostatin-treated myoblasts. Similarly, Joulia and colleagues were able to overexpress myostatin in C_2C_{12} myoblasts and showed that in cultures expressing antisense to myostatin, myotubes had formed earlier and were of greater length than that of control cells [57]. Furthermore, it was shown that myostatin inhibited protein synthesis in myotubes of C_2C_{12} culture cells [53]. Taken together, these data support the role of myostatin in regulating muscle mass through inhibition of cell replication, differentiation and protein synthesis.

The findings from *in vitro* studies were supported by animal research in which the composition of different muscle groups was examined histologically. Skeletal muscles from myostatin null ($Mstn^{-/-}$) mice were found to have a significantly increased number of myocytes and the synthesis of DNA was 50% higher than wild-type muscle [11]. Moreover, the cross-sectional area of the fibres were larger in $Mstn^{-/-}$ muscle compared with wild-type muscle, indicating that hypertrophy of the muscle fibre also contributed to the overall increased in skeletal muscle mass [11]. Conversely, overexpression of myostatin in male transgenic mice was associated with lower skeletal mass, and a reduction in fibre size and myonuclear numbers [58].

1.5 Clinical applications of myostatin

The increased mass of skeletal muscle in the absence of myostatin has a significant agricultural impact, especially in the meat industry. Specifically, meat from Belgian Blues and Piedmontese cattle are prized for the quantity, tenderness and palatability [59]. However, whether this increased in the mass of skeletal muscle results in improvement in muscle performance is unclear. Indeed, forced exercise in double muscle cattle resulted in precocious exhaustion, with significant elevation in lactic acid and serum creatinine kinase [60]. In mice, inhibiting the activity of myostatin either by genetic manipulation of the myostatin gene or the administration of myostatin antibody in otherwise normal skeletal muscles result in inconsistent performance of the muscle strength that is disproportional to the effects of an increase in the mass of skeletal muscle [61, 62]. In some cases, the increase in the mass of skeletal muscle in $Mstn^{-/-}$ mice has not resulted in any

strength advantage over WT mice [63]. Nevertheless, it is possible that a functional benefit may be gained in dystrophied or atrophied muscle such as that seen in primary and secondary muscle disorders.

1.5.1 Primary and secondary muscle disorders

Primary muscle disorders include muscular dystrophies [Duchenne muscular dystrophy (DMD), Becker muscular dystrophy (BMD), facioscapulohumeral dystrophy (FSHD), and limb-girdle muscular dystrophy (LGMD)], congenital myopathies, metabolic and inflammatory myopathies. Secondary muscle diseases encompass age-related sarcopenia, cachexia, denervation and the effects of medications such as glucocorticoids [64]. While inhibiting the activity of myostatin does not correct the underlying pathology, it has the potential to ameliorate these disorders by increasing muscle mass and strength. For example, using animal models of DMD, deletion of myostatin was associated with a functional improvement of muscle by increasing muscle mass and reducing the extent of fibrosis in the diaphragm [12, 14, 65]. Animal models of several other forms of muscular dystrophy, however, have produced less consistent results [66-69]. These differences in efficacy may be explained by the mode of myostatin inhibition applied (eg. prenatal vs postnatal inhibition, myostatin antibody vs endogenous inhibitor of myostatin etc.) and the severity of the underlying muscle dystrophy. In humans, a phase I/II double-blind, placebo-controlled, dose-escalation safety study of a myostatin inhibitor, MYO-29 was conducted in 2006 involving 116 subjects with primary muscle diseases [13]. MYO-29 or Stamulumab was the first neutralizing antibody to myostatin to be used in clinical trials.

MYO-29 was reported to be safe and well tolerated with only cutaneous reactions reported in the highest dose cohort [13]. However, there was no improvement in muscle strength and function in the study, although the authors commented that the study was underpowered to determine efficacy. A subsequent study demonstrated that improvement in muscle strength may have occurred at the cellular level which was not apparent at the whole muscle or functional level [70].

The cause of age-related sarcopenia is multifactorial, resulting in loss of skeletal muscle mass and overall decreased performance in muscle and increase frailty with aging [71]. The pathophysiology is complex with contributing factors including age-associated reduction of anabolic hormones, increase in inflammatory insults and oxidative stress, apoptosis in myofibres and a reduction in nutritional status and physical activity [71]. A significant structural reorganisation of muscle fibre occurs with aging, with loss of both type I (slow oxidative) and accelerated loss of type II (fast glycolytic) myofibres along with an infiltration of lipid into the intracellular and intramyocellular space [72]. In addition, age-related neurodegeneration causing atrophy of muscle fibres has also contributed to the overall reduction in muscle performance [72].

When aged Mstn$^{-/-}$ mice were compared with their WT controls as well as their respective adult cohorts, the total body weight was not different between the senescent Mstn$^{-/-}$ and WT mice [73]. However, aged WT mice had a greater body mass compared with adult WT mice as a result of an increase in fat mass, while no difference in body weight was observed between the senescent and adult Mstn$^{-/-}$ mice [73]. The senescent Mstn$^{-/-}$ mice

maintained more muscle mass and lower percentage of body fat compared with senescent WT mice [73]. A later study reported similar findings wherein aged Mstn$^{-/-}$ mice had greater lean fat-free mass and less total and percentage of body fat content compared with the aged WT controls [74]. While the effects of longevity were not examined in these studies, a favourable aging phenotype in the Mstn$^{-/-}$ mice is established, with a possible advantage of myostatin deletion in ameliorating age-related sarcopenia.

The content of myostatin varies in different skeletal muscles of aging rodents, depending upon the age and type of muscle studied. In mice up to 92 weeks of age, there was no significant changes in myostatin protein in the soleus muscle (50% type I and 50% type IIa fibres) [75]. An initial increase in the abundance of myostatin protein as determined by western blot analysis was observed in combined gastrocnemius and plantaris (Gast/Plant) muscles (predominantly type II fibres) until 11 weeks of age, followed by a gradual reduction up to 92 weeks of age [75]. Similarly, the concentration of myostatin mRNA was reduced in gastrocnemius muscle of the old adult rats (30 month old) compared to young adult rats (6 month old) [76]. In humans, however, the concentrations of myostatin mRNA and the abundance of myostatin protein in vastus lateralis muscles of healthy older individuals (70-89 year old, men or women) were increased under resting conditions compared with young adults (18-30 year old, men or women) [77, 78]. An earlier report detected no difference in myostatin mRNA expression in vastus lateralis of older men (62-77 year old) compared with young men (21-31 year old), although the author could not exclude the possibility of an increased in the abundance of myostatin protein in the older cohort [79]. These conflicting results in myostatin mRNA expression may be

explained by a gender difference, the age group studied and possibly difference in body weight. In serum, the abundance of myostatin protein has been reported to be increased [80] or decreased [81] in older population (60-92 year old) than in young adults (18-35 year old). One possible explanation is the methodological challenges in measuring serum myostatin using an appropriate and reliable assay. Nevertheless, administering anti-myostatin antibody to aged mice resulted in an increased in muscle mass and grip strength, suggesting that inhibition of myostatin may have the potential to improve the function of aging muscles [82, 83].

Cachexia is another important secondary muscle disorder that is described as a '*complex metabolic syndrome associated with underlying illness and characterised by loss of muscle with or without loss in fat mass*' [84]. It is often seen in patients with chronic diseases such as heart failure, renal failure, chronic obstructive airway diseases or inflammatory disorders such as cancer, AIDS, or sepsis [85, 86]. Cachexia in patients is associated with a higher mortality and a poorer response to treatment compared with control cohorts [87, 88]. Myostatin was considered to be a potential mediator of cachexia [85, 89]. Systemic administration of myostatin in mice resulted in severe wasting with an average of 33% total body weight loss compared to controls [27]. In HIV-infected men with AIDS-wasting syndrome, the abundance of myostatin protein in serum and skeletal muscle was significantly greater than that in HIV-infected men without weight loss or healthy adults [23]. Based on this finding, those authors suggested that myostatin may be contributing to the pathophysiology of muscle protein wasting seen in AIDS-wasting syndrome [23]. Although the precise mechanism is unknown, it was speculated by the

investigators that myostatin down-regulates the expression of MyoD in both *in vitro* and *in vivo* models of cachexia [90]. The induction of cachexia by myostatin appears to be mediated independent of the nuclear factor-kappa B (NF-κB) transcription factors, a pathway that is critical in the initiation of cachectic conditions [90].

1.5.2 Obesity

When myostatin was first discovered in skeletal muscle, a lower expression was also detected in adipose tissue [11]. The role of myostatin in adipose tissue is unclear, but subsequent studies have demonstrated a reduction in the accumulation of fat with increasing age in $Mstn^{-/-}$ mice compared with wild-type controls [91]. In addition, when $Mstn^{-/-}$ mice were fed a high-fat diet, the increase in body fat was significantly less than that in wild-type mice [92]. When the $Mstn^{-/-}$ allele was crossed with two genetic mouse models of obesity, the *Agouti lethal yellow* (A^y/a) or the leptin *ob/ob* mice, the double mutants mice had lower mass of adipose tissue, a decrease in the mass of the fat pad and improved fasting glucose and glucose tolerance compared with their single mutant counterparts [91]. Furthermore, other metabolic consequences associated with diet-induced obesity, such as serum leptin, cholesterol and triglycerides were also ameliorated by the inhibition of myostatin when fed a high-fat diet [92, 93].

In humans, morbidly obese subjects who underwent biliopancreatic diversion surgery, the weight loss post-surgery was associated with a significant reduction in the expression of

myostatin mRNA [94]. The precise mechanism by which myostatin influences the accumulation or metabolism of fat remains unclear. Emerging evidence suggests that the reduction in fat mass appears to be an indirect effect of lack of myostatin in skeletal muscle rather than adipose tissue [95]. However, a recent study reported that treatment with myostatin inhibited the differentiation of brown adipocytes and that this inhibition occurred early in the stages of brown adipogenic differentiation [96]. Given the increasing interest in using cold-induced thermogenesis to activate brown adipocytes and combat obesity, antagonising the effects of myostatin is a promising target in the treatment of obesity by promoting the differentiation of brown adipocytes [97, 98].

1.5.3 Type 2 DM and insulin resistance

Along with the role of myostatin in the metabolism of fat and energy expenditure, a parallel improvement in glucose metabolism has also been shown in the absence of myostatin [91]. When $Mstn^{-/-}$ mice were compared with WT littermates following a standard diet, the fasting serum glucose and insulin were lower in the $Mstn^{-/-}$ mice together with a significant improvement in the glucose tolerance (GTT) and insulin tolerance (ITT) tests [95]. Using a hyperinsulinaemic-euglycaemic clamp, $Mstn^{-/-}$ mice had a lower plasma glucose and insulin concentrations at baseline, and required a higher infusion of glucose to maintain euglycaemia during the clamp compared with WT mice [95]. Taken together, these data suggest greater insulin sensitivity in $Mstn^{-/-}$ mice, and an enhanced response in the peripheral tissues of the $Mstn^{-/-}$ mice to take up glucose during hyperinsulinaemia.

In humans, the age- and gender-adjusted expression of myostatin mRNA and protein concentration in skeletal muscle was significantly increased in patients with Type 2 DM compared with healthy controls, whilst no difference in the plasma myostatin concentration was observed [99]. The skeletal muscle content of myostatin mRNA correlated positively with impaired insulin sensitivity, increased triglycerides, obesity and poor fitness level [99]. However, this correlation was only apparent in healthy controls, and not in Type 2 DM patients, and the authors suggested that the metabolic effects of myostatin is likely confounded by other factors in Type 2 DM [99]. In contrast, another study examining similar clinical manifestations and the concentration of plasma myostatin between Type 2 DM and healthy controls reported a different result [100]. The plasma concentration of myostatin was significantly increased in patients with Type 2 DM compared with healthy controls [100].

1.5.4 Bone

It has long been recognized that a positive correlation exists between muscle mass and bone mineral density (BMD) in humans and that '*the weight of a muscle reflects the forces it exerts on the bones to which it is attached, and a reduction or increase in muscle weight results in a corresponding loss or increase of bone*' [101]. Being a potent regulator of skeletal muscle mass, naturally the effects of myostatin on bone have been examined. Compared with wild-type littermates, $Mstn^{-/-}$ mice with increase muscle mass were found to have increased cortical area and bone mineral content (BMC) in the muscle attachment site of the humerus, without an increase in BMD [102]. A later study by the same author

found an increase in femoral BMD compared with control mice [103]. Induction of fibular fracture resulted in a greater increase in callus size and bone volume in $Mstn^{-/-}$ mice compared to wild-type mice, indicating that inhibition of myostatin may enhance the repair of fracture [104].

In summary, the potential beneficial role of myostatin is not limited to skeletal muscle alone. Indeed, systemic circulation of myostatin implies that the effects of myostatin are broader than previously thought, that the inhibition of myostatin can be an effective adjunct to the current management of metabolic and bone diseases, in addition to skeletal muscle disorders. Importantly, pertinent to this thesis are the possible effects of myostatin on the heart.

1.6 Ischaemic heart disease, cardiomyopathy and myostatin

The historical management of acute MI in humans has evolved significantly from a largely palliative approach with strict bed rest to a curative intent with primary revascularisation and secondary prevention [105]. As a result, a steady decline in mortality has been observed following these therapeutic advances and modification of cardiovascular risk factors (Figure 1-7). However, the in-patient and one-year mortality following acute coronary syndrome remains high as described in a recent Scandinavian observational study [106]. The in-patient mortality for STEMI (ST elevation myocardial

infarction), NSTEMI (non-ST elevation myocardial infarction) and UA (unstable angina) in a cohort of unselected patients was 9.6%, 13% and 2.6% respectively [106]. Notably, the mortality rate during the follow-up period (median follow up of 10 months) increased to 19%, 27% and 12% respectively [106]. These data suggest that further gains in the acute management of coronary heart diseases to improve morbidity and mortality have yet to be achieved.

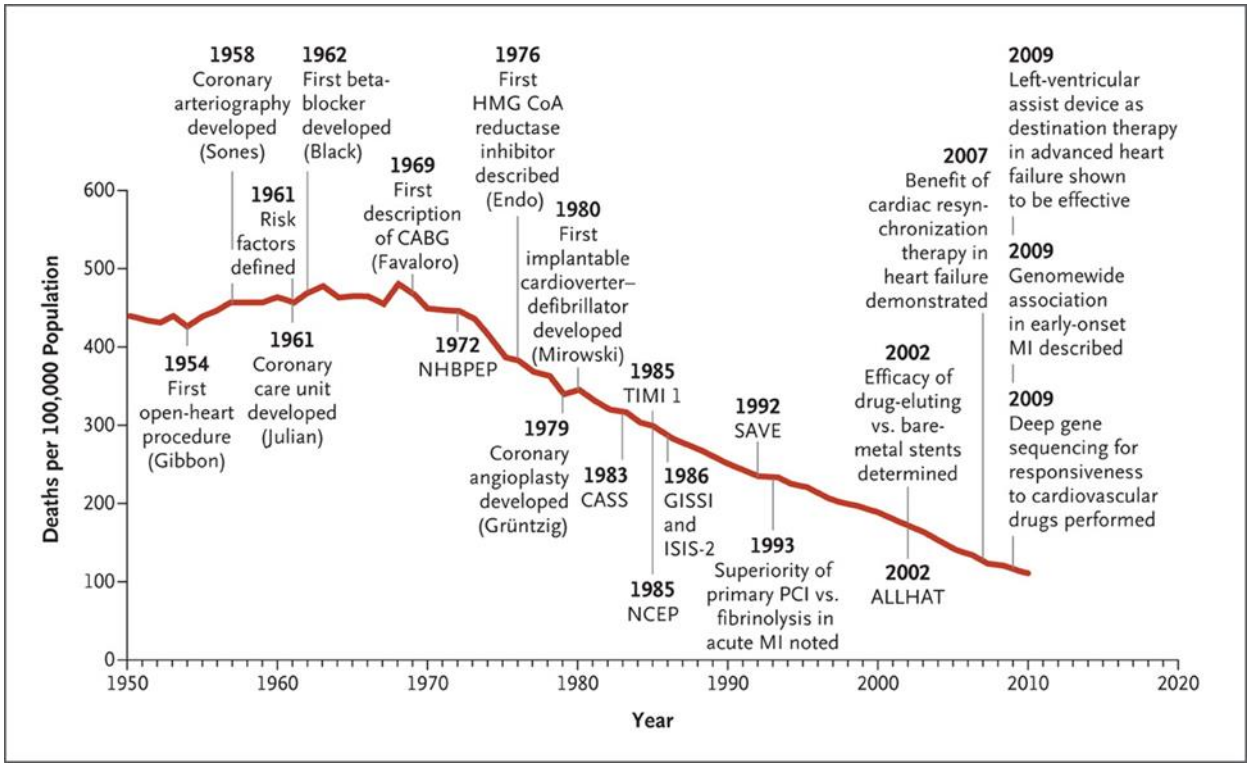

Figure 1-7. Decline in deaths from cardiovascular disease in relation to scientific advances. *Reproduced with permission from Nabel et al. NEJM 2012;366:54-63*

1.6.1 Pathogenesis of MI and heart failure

To improve treatment outcomes for MI requires an understanding of the pathogenesis of coronary artery diseases. Coronary heart disease (CHD), as defined by the ICD-10 codes I20-I25, includes acute MI, other acute ischaemic (coronary) heart disease, angina pectoris, atherosclerotic cardiovascular disease and all other forms of chronic ischaemic CHD [107]. Each of these represents a spectrum in severity of what is essentially caused by underlying atherosclerosis of the coronary arteries. For the purpose of this thesis, attention will be focused on acute MI.

Atherosclerosis is a chronic inflammatory process involving a complex interplay between the endothelium, smooth muscle of the arterial walls, monocytes and macrophages, and T-lymphocytes [7]. Following insults such as oxidative, haemodynamic and biochemical stimuli (eg. cigarette smoking, hypercholesterolameia, hypertension), the permeability of the intact endothelial cells changes [108]. This results in invasion of the intima by lipid rich macrophages and T-lymphocytes, forming the earliest recognisable atherosclerotic lesion, the "fatty streak" [7]. With ongoing inflammation, endothelial and smooth muscle cells proliferate, and the "fatty streak" develops into a more advanced and complex occlusive lesion known as a fibrous plaque [7]. The fibrous plaques gradually increase in size with formation of a connective tissue matrix. These fibrous plaques then project into the lumen and eventually restrict the blood flow either temporarily (unstable angina) or permanently (in the case of MI) (Figure 1-8). Rupture of these plaques exposes pro-coagulant material to coagulation proteins and platelets, predisposing the vessels to thrombosis [108].

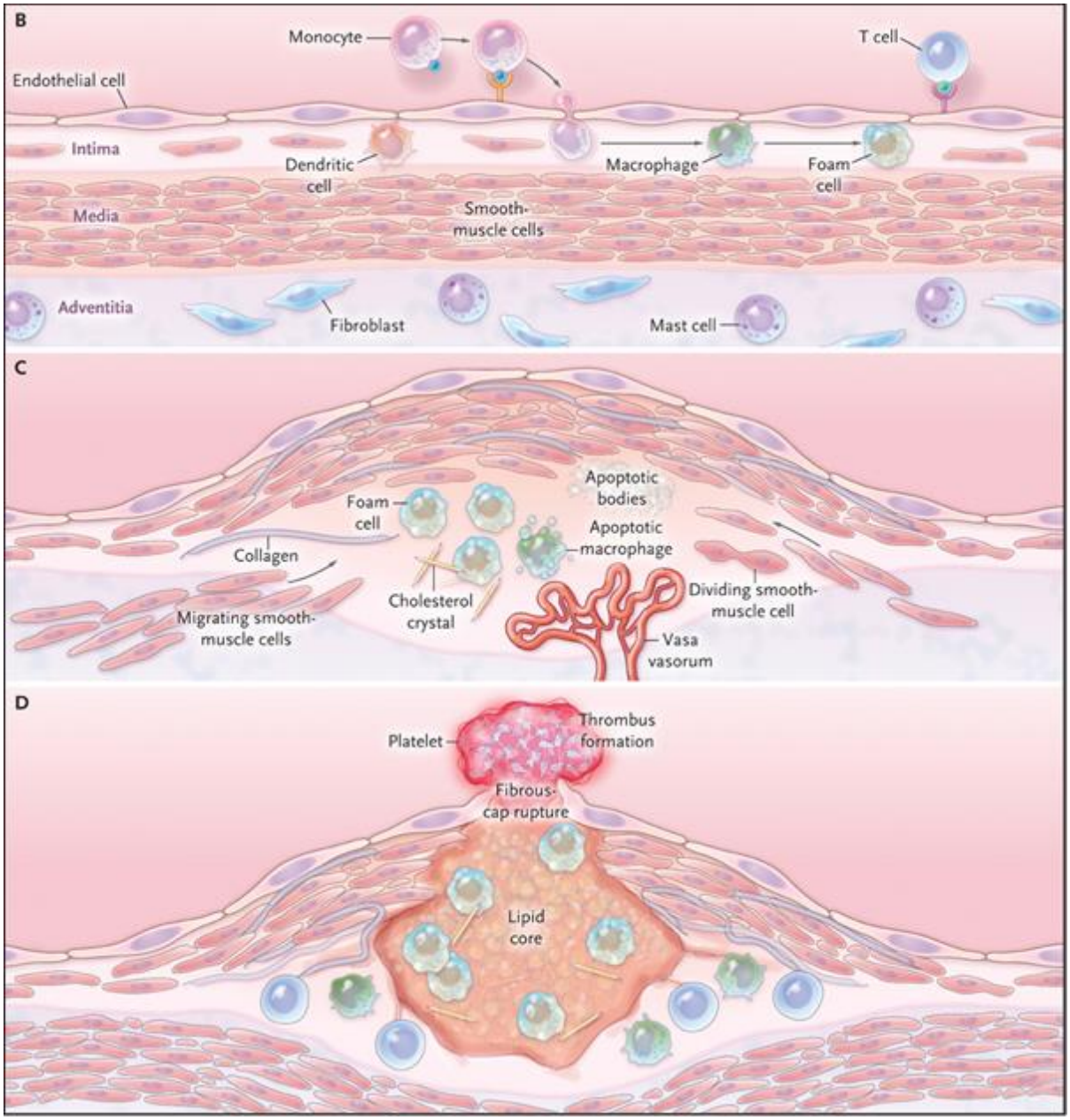

Figure 1-8. Stages of atherosclerosis development. *Reproduced with permission from Nabel et al. NEJM 2012;366:54-63*

After the initial myocardial ischaemia/infarction, reperfusion may occur (if death does not ensue), either naturally or through therapeutic intervention, followed by healing and repair of the myocardium [109]. Ventricular remodelling following an infarct is a complex and evolving process, resulting in an alteration in the size, shape and function of the ventricle, and is regulated by mechanical, neurohormonal, and genetic factors [110]. Post-infarction remodelling is a continuous event that initially begins in the infarcted region, but with time, secondary changes also occur in the non-infarcted tissue [111, 112]. The process of remodelling can be arbitrarily divided into several phases (Figure 1-9) and involves the three key components of the myocardium: cardiomyocytes, cardiac fibroblasts and extracellular matrix, and the capillary microcirculation [110]. The initial apoptosis and necrosis of cardiomyocytes triggers a cascade of immuno-inflammatory responses including degradation of extracellular matrix, inhibition of tissue proliferation and release of inflammatory mediators [8]. Expansion of the infarct follows which is a result of thinning and dilatation of the infarcted myocardial wall, and may predispose the ventricle to early rupture and formation of an aneurysm [9, 109]. In late phases of healing, a global rearrangement of the surviving myocardium occurs with the development of cardiomyocyte hypertrophy, interstitial fibrosis, and dilatation of the LV resulting in the impairment of the ventricle and heart failure. The dilatation of the LV post-MI is thought to be an adaptive response of the ventricle to injury in order to maintain stroke volume despite a decline in ejection fraction [109]. This is achieved by a series of chronotropic and inotropic activities and stimulate the sympathetic adrenergic system to maintain the pump function [109]. However, the augmented ventricular wall stress triggers further dilatation of the ventricle, resulting in a greater increase in the volume of the cavity, which will require an even greater augmentation of ventricular wall stress and a vicious cycle is created [109].

Furthermore, during the late phase of remodelling, hypertrophy of the cardiomyocytes occurs to compensate for loss of cells post-MI in an attempt to overcome the increased load and progressive dilatation of the ventricle [109].

While cardiomyocytes contribute to the major myocardial tissue volume, cardiac fibroblasts surround the cardiomyocytes and bridge the areas between the myocardial tissue layers [113]. Fibroblasts are the major player in the maintenance of the extracellular matrix and contribute to the myocardial remodelling process [113]. In response to injury, cardiac fibroblasts in the myocardium proliferate and differentiate into myofibroblasts [9], a specialised fibroblast which are only found in the granulation tissue in the infarcted region and not in healthy, uninjured myocardium [114]. Myofibroblasts retain the characteristics of fibroblasts and produce extracellular matrix (predominantly collagen) to replace necrotic cardiomyocytes and form a scar [115]. Myofibroblasts are also able to contract and are associated with a smaller and stronger scar area to prevent expansion of the infarct [115]. While initially beneficial, excessive fibroblast proliferation and deposition of extracellular matrix in the interstitium and surrounding non-infarcted myocardium eventually leads to increased myocardial stiffness, impaired relaxation and progressive diastolic and systolic dysfunction [9]. Therefore, efforts in interrupting these deleterious remodelling processes either directly or through modulation of hypertrophic signalling pathways or neurohormonal responses will be the basis for effective treatment of ischaemic heart disease and heart failure. Indeed, new therapeutic approaches to manage HF, including targeting microRNAs, stem and progenitor cells, gene therapy, anti-inflammatory and anti-fibrotic responses have shown promising results [9, 10].

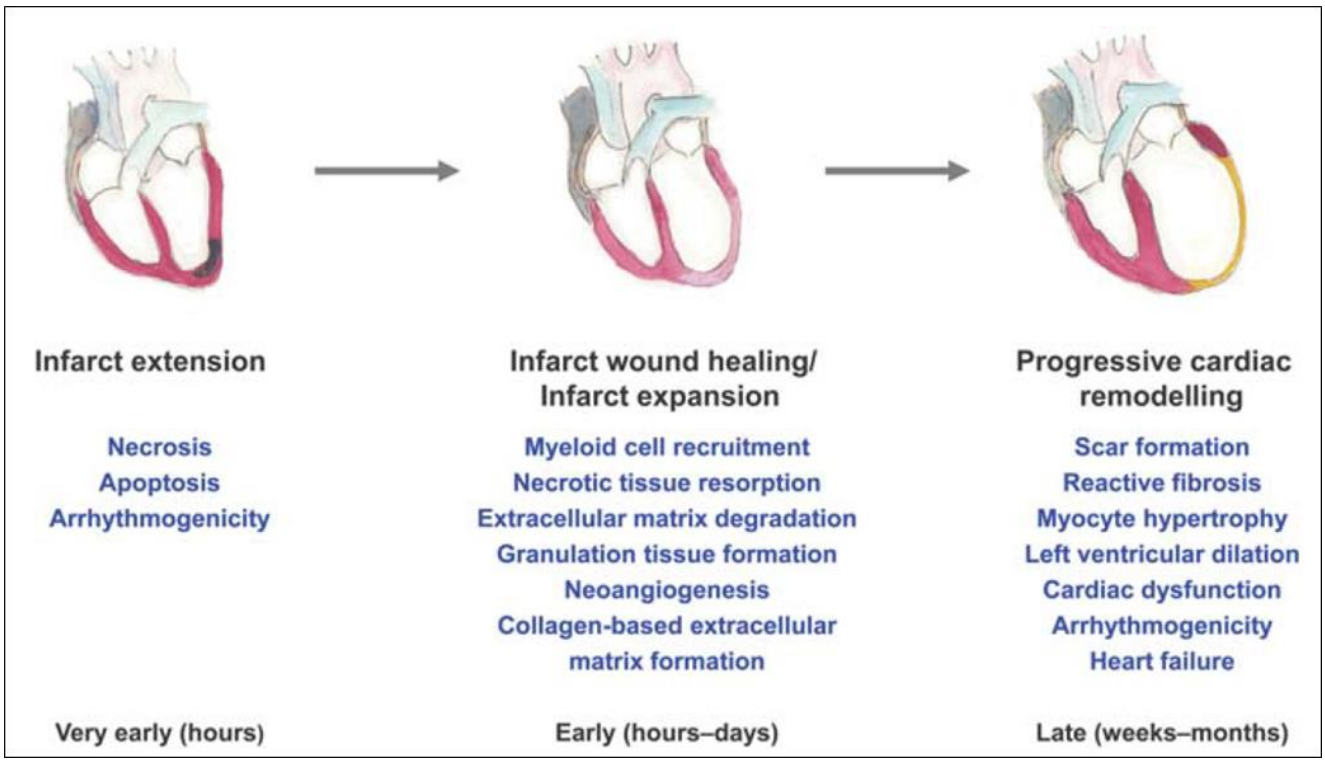

Figure 1-9. Stages of cardiac remodelling post-infarction. *Reproduced with permission from Fraccarollo et al. Cardiovascular Research 2012;94:293-303*

1.6.2 Myostatin and the heart

In 1999, Sharma and co-workers were the first to report that myostatin may play a role in the heart, having detected myostatin in murine and sheep heart tissue [16]. Since then, myostatin has been detected in the hearts of different species of fish [116, 117], chickens [118], rats [119], pigs [120] and humans [20]. However, for almost 15 years since its detection, the precise function of myostatin in the heart remains to be elucidated. Specifically, it remains unclear as to whether myostatin is beneficial or detrimental to the process of healing following myocardial damage. It is also not known whether the effects of myostatin in the heart are different at baseline or after a stimulus. Hence, for the purpose of the thesis, this section will firstly provide an overview of the current literature relating to the effects of myostatin in the heart, which led to the hypothesis and aims of the study. The systemic and skeletal muscle effects of myostatin will not be addressed in this work.

1.6.2.1 Where is myostatin found in the heart?

The expression of myostatin can be detected in the developing foetal heart, suggesting a possible role in early heart development [16]. This expression continues into adulthood and is well conserved in mammals [16]. In normal cardiac tissue, myostatin protein is detected in higher abundance in Purkinje fibres with a lower abundance also seen in cardiomyocytes and the smooth muscles of coronary arteries [16]. Within the ventricular myocardium, a differential LV/RV expression of myostatin mRNA is found with a two- and six-fold increase in myostatin mRNA expression in the left ventricle of newborn and 20-day piglets, respectively, compared to the right ventricle [120].

1.6.2.2 Is the effect of myostatin on the proliferation and differentiation of cardiac cells similar to that seen in skeletal muscle?

While the expression of myostatin mRNA and protein was observed in rat cardiomyocytes from embryonic day 18 (E18) through to post-natal life (Days 0, 2, 5 and 10), the abundance was much lower in the actively proliferating cardiomyocytes at E18, compared with postnatal day 10, when the majority of the cardiomyocytes lose the ability to proliferate [119]. Thereafter, a reduction in both the mature myostatin protein and mRNA expression (two-fold and 15-fold respectively) were observed in adult cardiomyocytes compared with foetal cardiomyocytes at E18 in the same study. These data indicate that the expression of myostatin is inversely proportional to the proliferation of cardiomyocytes and that myostatin modulates hypertrophic growth rather than hyperplastic growth post-natally [119].

In *in vitro* studies, the addition of recombinant myostatin inhibited the proliferation of dividing foetal and neonatal cardiomyocytes, via blocking the transition through the G1-S phase of the cell cycle and this effect was reversed when myostatin was removed [119]. Similarly, myostatin is expressed predominantly in the nuclei of the H9c2 rat embryonic cardiomyocytes, and proliferation of cells is reduced by either endogenous or exogenous recombinant myostatin protein [121]. Furthermore, addition of myostatin is shown to partially suppress equilibrative nucleoside transporter-1 (ENT-1) mRNA, which is a marker of cellular differentiation, indicating that myostatin also inhibits the

differentiation of cardiomyoblasts [122]. Collectively, these results support the role of myostatin in inhibiting cardiac cellular proliferation and differentiation, in a manner similar to that observed in skeletal muscle myoblasts.

1.6.2.3 What is the physiological role of myostatin in the heart?

Morphologically, the hearts of $Mstn^{-/-}$ mice were normal even at 24 months of age when compared with wild-type (WT) littermates [123]. The heart weights of adult $Mstn^{-/-}$ mice, however, have been reported to be similar [123], increased [121, 122] or even decreased [124] when compared with age-matched controls. These conflicting results for heart weight are likely due to the different age groups of adult mice used, and the variable body weights measured. Nevertheless, it appears that the weight of the heart is related to an autocrine or paracrine function of myostatin in the myocardium rather than the endocrine effects from circulating myostatin [121]. This was demonstrated by transgenic mice with overexpression of myostatin with a muscle-specific creatinine kinase (MCK) promoter (which is active in both skeletal and heart muscle) to have smaller hearts compared with controls [121]. This difference in heart weight was not observed in transgenic over-expresser mice with a myostatin mutation in the MCK-3E promoter which is only active in skeletal muscle [121].

Rather intriguingly, despite the differences in heart weight between $Mstn^{-/-}$ and myostatin over-expresser mice, and severe cardiomyopathy in the hearts of dystrophin-deficient (*mdx)* mice, most studies reported similar resting cardiac function among the groups

studied when compared with controls [121, 123, 124]. In other words, cardiac muscle retains its functional efficacy at rest irrespective of the change in morphology and muscle mass. One postulate suggested was that while myostatin reduced the size of the heart during embryonic development, factors that trigger changes in cardiac function in early post-natal life are either absent or non-operative, thereby maintaining normal tissue composition and function at rest [121]. On the other hand, Rodgers and co-workers demonstrated that the heart weights in adult Mstn$^{-/-}$ mice (7 month old) of both sexes were greater than WT controls, but that this was associated with significantly reduced resting fractional shortening (FS) and ejection fraction (EF) [122]. However, the internal diameters and volumes of the left ventricle at diastole and systole were greater in Mstn$^{-/-}$ mice, and intraventricular septum wall thickness and stroke volume (SV) were similar in both groups consistent with eccentric hypertrophy of the myocardium [122]. When stimulated with a sympathomimetic agent isoproterenol, Mstn$^{-/-}$ mice performed better with a greater reduction in systolic volumes and greater increased in FS and EF compared with WT mice [122]. Based on these findings, it was concluded that the increase in heart size in Mstn$^{-/-}$ mice is most likely a physiological, and not pathological hypertrophy of the myocardium [122].

While the effects of longevity have not been reported, the effects of myostatin in the hearts of the normal aging mice have been examined recently [73, 74]. In one study, the mass of the hearts in WT and Mstn$^{-/-}$ mice increased with age (from 4 through to 30 months) but no difference between the two genotypes was observed [73]. Resting cardiac function was better preserved in aged Mstn$^{-/-}$ mice compared with WT mice [73]. A reduction in

cardiac fibrosis and an increased in the ratio of phosphorylated to total phospholamban activity, which is important for maintaining contractile function, were thought to be responsible for this preservation in cardiac function seen in aged $Mstn^{-/-}$ mice [73]. Conversely, another study reported an increase in heart weights and a dilated cardiomyopathy phenotype at rest in the aging $Mstn^{-/-}$ mice compared with WT controls [74]. The apparent pathological cardiac function in these aging $Mstn^{-/-}$ mice was shown to have an enhanced contractile ability following isoproterenol stress test, consistent with a physiological hypertrophy of the myocardium, that was not seen in aged WT controls [74]. These data were in line with their earlier reports in adult $Mstn^{-/-}$ mice [122] but was different from that obtained by Morissette *et al* [73]. The difference in cardiac function may be explained by the way the echocardiography was performed – both studies used a 10 MHz transducer, but one was performed on anaesthetized mice [74] while the other was carried out on conscious mice [73].

In summary, the literature provides conflicting evidence as to the effects of myostatin in physiologically normal hearts. Nevertheless, it appears that a unique cardiac phenotype which is different from the WT mice does exist in the absence of myostatin. It is likely that this phenotype leads to a growing interest of a possible role of myostatin in cardiac pathology.

1.6.2.4 What about the role of myostatin in diseased state?

Interestingly, while the abundance of myostatin protein was reported to be low in normal cardiomyocytes [16], the expression of myostatin can be re-induced in the presence of pathological stimulation [38].

1.6.2.4.1 Acute myocardial infarction

The literature on the effects of myostatin following acute MI was limited. One of the earlier reports was demonstrated by Sharma *et al.* using three year old Romney ewes and induction of acute MI was achieved by occluding the distal left anterior descending (LAD) artery with sterile gel foam [16]. The hearts were excised at 0.5, 1, 2, 6, 12 and 30 days post-infarct and the immunointensity of myostatin was examined. The immunointensity of myostatin was increased in the peri-infarct cardiomyocytes from 0.5 day and persisted throughout the study [16]. Immunostaining in the viable cardiac tissue and in the cardiomyocytes in the infarcted area was at a very low level and similar to non-infarcted controls [16]. Another study adopted an ischaemic-reperfusion model to induce MI in WT mice, and the expression of myostatin mRNA 28 days post-MI was similar in the non-infarcted, peri-infarcted and infarcted zone of the cardiac muscle [122]. However, that study did not include sham-operated mice as controls, which may limit the interpretation of results.

1.6.2.4.2 Volume-overload heart failure

The expression of myostatin was studied in a rat model of volume-overload induced by aorto-caval shunt followed by treatment with carvedilol, a non-selective vasodilating beta blocker [19]. Both myostatin protein and mRNA expression were up-regulated (approximately three fold) in the myocardium of the shunt group compared with sham-operated animals and this increased expression of myostatin was inhibited following treatment with carvedilol [19]. Similarly, in the skeletal muscle of the shunt group, the abundance of myostatin protein was increased and this increase was blocked by treatment with carvedilol. It is not known whether or not carvedilol acts directly on the cardiomyocytes or through its effects on the sympathetic nervous system to inhibit the expression of myostatin. It is also possible that the haemodynamic changes resulting from carvedilol exposure alters the expression of myostatin. Lenk and co-workers examined the effects of myostatin expression in rats with chronic heart failure induced by ligation of LAD artery and compared with sham-operated controls [18]. Once CHF was confirmed in the ligation animals, the two groups were further divided into either exercise-trained or sedentary arms, and the expression of both myostatin protein and mRNA was examined eight weeks later. The expression of myostatin mRNA was increased in skeletal and heart muscles following induction of heart failure, although this did not reach significance [18]. The abundance of myostatin protein, on the other hand, was significantly increased in both tissues in animals with CHF [18]. The discrepancy between the myostatin mRNA and protein findings may be related to post-transcriptional or post-translational modifications which the authors did not elucidate further. Importantly, while no difference was observed between exercise-trained and sedentary rats in sham-operated controls, exercise-trained CHF rats had a significant reduction in the abundance of myostatin protein back to baseline compared with sedentary CHF controls [18]. The authors speculated that this

reduction in myostatin protein could be linked to a reduction in TNF-α seen following exercise-training. In a larger animal model of CHF (i.e. beagle dogs), tachycardia-induced dilated cardiomyopathy via over-pacing did not alter the expression of myostatin mRNA and that the authors suggested that the up-regulation of myostatin is only seen in cardiac diseases characterized by hypertrophic process [125]. However, this unchanged expression of myostatin mRNA could simply be explained by the fact that the endomyocardial biopsies were taken from the septal region of the right ventricle, an area already reported to have a low concentration of myostatin [120], therefore making it more difficult to identify any significant changes.

In humans, the expression of myostatin in CHF patients has also been reported to be up-regulated in several studies [20, 126, 127]. George and co-workers examined various myostatin proteins, including the full-length precursor promyostatin, the propeptide and the latent complex in normal human myocardial tissue and serum and compared with patients in advanced HF [20]. While no difference was seen in the full length precursor, the abundance of myostatin propeptide, which is a marker of myostatin activation, was increased in the myocardial tissue of ischaemic (ICM) and non-ischaemic (DCM) dilated cardiomyopathy patients compared with normal subjects [20]. The concentration of myostatin latent complex in blood was also increased in DCM HF patients compared with healthy controls [20]. Consistent with these findings, downstream of myostatin, the Smad2/3 signalling was also increased in ICM and DCM patients [20]. The expression of BMP-1 was increased in both ICM and DCM patients, and correlated with higher concentrations of cleaved propeptide [20]. The unchanged concentrations of myostatin precursor but increased

concentrations of propeptide indicated that generation of mature active myostatin for signal transduction is enhanced in diseased hearts. In addition, the increased concentrations of circulating myostatin latent complex may serve as a reservoir for local activation in the heart by BMP-1 which was increased in advanced HF patients [20]. Gruson and co-workers measured plasma myostatin concentration in CHF patients and healthy control subjects using a competitive myostatin immunoassay [126]. The concentration of plasma myostatin was increased in CHF patients compared with healthy controls, and the increase was positively correlated with New York Heart Association (NYHA) classification and other biomarkers of heart failure [126]. Interestingly, the group has also found a higher concentration of plasma myostatin in healthy men than women, although the level of significance was not mentioned in their report [126].

While exercise-training reduced the elevated expression of myostatin in CHF rats, a similar result was also observed in CHF patients [127]. Following 12 weeks of endurance exercise training, Lenk and co-workers demonstrated that CHF patients with NYHA class III symptoms and an increase in baseline concentration of myostatin mRNA and protein compared with healthy controls, had a significant reduction in both the myostatin mRNA (by 36%) and protein (by 23%) compared with sedentary CHF patients [127]. An improvement in the exercise capacity and clinical symptoms have also been shown in their study confirming that exercise training is an important strategy in the treatment of heart failure.

1.6.2.4.3 Pressure-overload cardiac hypertrophy

In pressure-overload CHF such as that induced by transverse aortic constriction (TAC) in mice, the expression of myostatin mRNA and protein concentration did not change in the skeletal muscle post-TAC compared with sham-operated controls. The lack of up-regulation in the expression of myostatin post-TAC suggests a differential reaction of myostatin towards different models of CHF (ie. volume-overload vs pressure-overload). The circulating plasma myostatin protein, on the other hand, increased by two to three fold compared with sham-operated mice [128]. This increase in circulating myostatin post-TAC was abrogated in transgenic mice with cardiac muscle-specific deletion of myostatin (Mstn fl/fl$^{Nkx2.5\text{-}cre}$), indicating that the heart was responsible for the increase abundance of plasma myostatin observed post-TAC [128]. Importantly, a reduction in skeletal muscle mass which was seen in control mice after TAC was not observed in Mstn fl/fl$^{Nkx2.5\text{-}cre}$ after TAC [128]. Based on this finding, the author concluded that deletion of myostatin in the heart mitigates the atrophy of skeletal muscle seen following chronic pressure-overload.

1.6.2.4.4 Cardiac cachexia

One of the major debilitating consequences in cardiac disease such as CHF is the development of cardiac cachexia [87]. In clinical practice, cardiac cachexia is defined as a documented non-oedematous weight loss of over 6% of the previous normal weight observed over a period of six months and is associated with an increased in mortality [129]. As discussed in Section 1.5.1, myostatin is thought to be a mediator of cardiac cachexia

[89]. Genetic deletion of cardiomyocyte-specific myostatin ameliorates the skeletal muscle atrophy seen following pressure-overload hypertrophy of the myocardium as described earlier [128].

1.6.2.4.5 Summary

In summary, while myostatin appears to play a minor role in normal cardiac development and physiology, its expression is enhanced in cardiac diseases. However, the degree of expression seems highly dependent on the underlying stimuli (i.e. volume-overload vs. pressure-overload). In addition, circumstantial evidence suggests that myostatin produced from the heart contributes to the increased in the pool of plasma myostatin. It is this pool of myostatin that likely accounts for, or contributes to the atrophy of skeletal muscle seen in chronic cardiac pathology. Furthermore, reversibility of the increase in the expression of myostatin seems possible such as that observed following endurance exercise or medication such as beta blockade in heart failure. However, little evidence is available on the effect of myostatin post-acute MI, and whether the frequently reported up-regulation in the expression of myostatin translates into any demonstrable functional changes. Moreover, it remains unclear whether the increased endogenous expression of myostatin seen in cardiac pathology is a direct release from the damaged cells and merely serves as a prognostic indicator, or is a counter-regulatory factor limiting the growth of muscle mass following injury.

1.7 Hypothesis and aims

The hypothesis of this thesis is that the absence of myostatin is beneficial to the heart following an acute MI. To test the hypothesis, the following aims are examined:

Aim one: to determine if the expression of myostatin changes at various time points post-MI. This aim will be achieved in the first study using an ovine model of MI induction via intracoronary injection of microspheres into the LAD coronary artery. The concentration of myostatin mRNA at different time points will be measured in the peri-infarct and distant viable regions of the myocardium and compared with the non-infarcted controls.

Aim two: to determine if the absence of myostatin will improve cardiac function post-acute MI. This is achieved in the second study using $Mstn^{-/-}$ and WT mice. An acute MI will be induced via ligation of the LAD artery and the haemodynamic changes at baseline and 28 days post-MI between $Mstn^{-/-}$ and WT mice will be examined. Echocardiography will be used to determine the underlying left ventricular function at baseline and post-surgery in the $Mstn^{-/-}$ and WT mice. The size of the infarct and the extent of fibrosis will be determined histologically between $Mstn^{-/-}$ and WT mice after MI.

Aim three: to determine the potential cellular mechanism(s) contributing to any clinical improvement observed in the absence of myostatin following an acute MI. This will be achieved by performing immunohistochemistry and indirect immunofluorescence on the

cardiac sections collected from the second study. The mechanisms of interest include assessment of the number and size of the cardiomyocytes, determination of the number of myofibroblasts, and semi-quantification of cellular survival, apoptosis and programmed necrosis.

2

Materials and methods

2.1 Introduction

This chapter is divided into two parts. The first part describes the animals used and the development of the surgical procedures required. The second part outlines the laboratory methods used in the study. Specific methods are detailed in each relevant chapter.

All animals and surgical procedures were handled in accordance with guidelines of the AgResearch Ruakura Animal Ethics Committee, Hamilton, New Zealand.

2.2 Animals, surgical procedures and clinical parameters

2.2.1 The murine model

Adult male (12 week old) $Mstn^{-/-}$ and WT (C57BL/6) mice were used in this study. Generation of $Mstn^{-/-}$ mice by Se-Jin Lee and colleagues at John Hopkins University School of Medicine has previously been described [11]. Briefly, the structure of the myostatin (GDF-8) gene was deduced from restriction mapping and partial sequencing of phage clones isolated from a murine 129 SV/J genomic library. Homologously targeted clones of myostatin were injected into C57BL/6 blastocysts and transferred into pseudopregnant females [11]. A pair of heterozygote ($Mstn^{-/+}$) mice of C57BL/6

background were obtained as a gift from Se-Jin Lee. Mice were genotyped and bred to homozygosity ($Mstn^{-/-}$) at the Ruakura Small Animal Colony unit. Mice had ad libitum access to standard chow and water.

2.2.2 The ovine model

Romney ewes (3 year old) were housed indoors and acclimated to a commercially available pelleted feed for two weeks prior to the study. The feed provided the complete nutritional requirements for sheep and was available, along with water, ad libitum.

2.2.3 Induction of myocardial infarction in the ovine model

Romney ewes (as above) were obtained from the Ruakura farm at AgResearch Limited. The surgical procedure has been described previously [130]. Briefly, general anaesthesia was induced with intravenous 5% sodium thiopentone. Sheep were intubated, and under fluoroscopic guidance, MI was induced by intracoronary injection of 0.6 ml of 45 µm microspheres into the left LAD of the coronary artery immediately distal to the first major branch. Samples of the peri-infarct and distant viable cardiac muscle were obtained from the left ventricle at three hours, six hours, one day, two days, four days and eight days post-infarct from sheep in which a MI was induced and from non-infarcted controls (n = 3 per group).

2.2.4 Procedures for the murine model

The technique of animal intubation and induction of myocardial infarction were modified from that described by Dr Leigh Ellmers [131] as follows:

2.2.4.1 Anaesthesia

General anaesthesia was achieved using a combination of 1 ml of ketamine (100 mg/ml), 0.5 ml of xylazine (20 mg/ml) and 0.5 ml of acepromazine (2 mg/ml) diluted in 8 ml of distilled water to make up a total volume of 10 ml as this combination was found to have the highest safety margin and longest time of surgical tolerance [132]. A full dose (ie. 0.1 ml/10g body weight) was initially administered, but this resulted in high numbers of mice (~40%) dying immediately following anaesthesia. Therefore, the dose was reduced by 30% (i.e. 0.07 ml/10g body weight) and while deep anaesthesia was maintained at the appropriate level, no further pre-operative deaths were observed.

2.2.4.2 Intubation

Mice were placed in a supine position on a 37 °C heated pad to maintain normothermia. The paws were taped to the heated pad to prevent lateral movement and a 5-0 silk black braided suture was placed behind the front lower incisors and pulled taut so that the neck

was slightly extended for better visualisation of the trachea. Endotracheal intubation was carried out under direct laryngoscopy using a rodent ventilator (Harvard Apparatus Inspira HSV) and a 22g intravenous cannula used as the ventilator tube. Mice were ventilated with room air at a rate of 107 breaths per minute with a tidal volume of 1.5 ml. This was in excess of the actual tidal volume (0.15 ml) to allow escape of part of the delivered volume while allowing optimal lung expansion without overexpansion. During the trial period, failed intubation had occurred and resulted in the death of mice. In addition, the time taken to intubate a mouse varied between 2 and 30 min. Therefore, in order to avoid any bias, the study commenced when successful intubation was achieved and the procedure consistently took less than 5 min to perform.

2.2.4.3 Induction of myocardial infarction

Numerous approaches have been described to induce MI in small animals, with ligation of the LAD artery being the procedure of choice with the greatest reproducibility [133, 134]. It took three months to learn and refine the surgical procedures, testing various suture materials and needles and orientation of the animal to achieve optimal results.

Following general anaesthesia and endotracheal intubation, a left thoracotomy of approximately 10 mm in length was performed at the fourth intercostal space. Forceps were used to delicately dissect through the chest opening and to expand the initial incision. The chest cavity was exposed using 5-0 braided silk sutures *(SOFSILK,*

Syneture), the distal ends of which were taped to the heat pad to act as retractors. Ligation of the LAD artery was made midway between the left atrium and the apex of the left ventricle using a 6-0 black braided silk ligature tapered needle *(ETHICON)*. The estimation of blood loss was determined by counting the number of cotton sticks used to swab blood during the surgery. Successful ligation was evident when blanching of the distal myocardium was observed. The intercostal muscles and chest wall were closed with 5-0 braided silk ligature *(SOFSILK, Synerture)*. Care was taken throughout the procedure to avoid contact with the lungs. Assisted ventilation was maintained until spontaneous breathing was restored post-operatively. Mice were kept on the heated pad at all times during the surgery and during recovery from the anaesthesia. For sham animals, a left thoracotomy was performed without ligating the coronary artery. Food and water were not withheld prior to surgery. Analgesia with Ibuprofen (100 mg/5ml) was added at a dose of 0.25 mg/ml of drinking water post-operatively. Total procedure time was between 20 and 35 min depending on whether sham or ligated surgery. Post-operatively, the mice were observed daily for posture, wound care, movement and for the pattern of breathing, in a small animal colony unit with provision of standard chow and water.

2.2.4.4 Mouse clinical data

Total body weight (BWT) was recorded at baseline and weekly, thereafter. Heart rate (HR) and blood pressure (systolic and diastolic) were measured on conscious mice during daylight at baseline, and at day 28 post-surgery using a computerized blood pressure tail-cuff analysis system (Visitech Systems) and a mouse restraining chamber (Visitech

Systems). Mean arterial pressure (MAP) was calculated from the formula DBP + 1/3 (PP), where DBP denotes diastolic blood pressure and PP denotes pulse pressure, which is the difference between systolic and diastolic blood pressure (SBP and DBP respectively) [135, 136]. Each measurement was obtained from an average of 25 readings in a recording session.

2.2.4.5 Echocardiogram

Acquisition of the echocardiogram technique from an expert clinical echocardiographer (Ms Juliet Jensen, Waikato Hospital, Hamilton, New Zealand) took four months. For the purpose of this project, the 2D and M-Mode techniques [137] were used to calculate left ventricular end diastolic and systolic diameters (LVEDD and LVESD respectively) and FS. The study was performed using a Philips HDI 5000 Sono CT ultrasound, with a 10 MHz broadband compact linear array transducer that had a rate of up to 500 frames per second. Animals were lightly anaesthetized with the afore-mentioned anaesthetic combination at a dose of 0.05ml/10g body weight. Echocardiography was performed on a heated pad at 37°C to avoid hypothermia. To obtain an optimal image quality, the chest was shaved and swabbed with 75% alcohol. The study was performed at baseline, days 1 and 28 post-surgery and three readings were obtained for each measurement and then averaged. Left ventricular end diastolic and systolic diameters were calculated from 2D imaging in the parasternal short axis view by M-mode analysis at the level of the papillary muscle. Both FS and EF were calculated based on the formulae [(LVEDD-LVESD)/LVEDD] x 100% and [($LVEDD^2$-$LVESD^2$)/$LVEDD^2$] x 100% respectively [137,

[138]. Echocardiography was performed with the operator blinded to the surgical procedure (i.e. sham vs. MI), but the genotype was known due to the unmistakably larger body mass of the $Mstn^{-/-}$ mice.

2.2.4.6 Histological analysis

A post-MI period of 28 days was chosen as the time required to observe an effect based on previous experience [16]. At the end of this study period, the mice were weighed and anti-5-Bromo-2'-deoxyuridine (BrdU) was injected intra-peritoneally at a dose of 0.1 ml/10g body weight two hours before euthanasia. Mice were killed with carbon dioxide asphyxiation. The hearts were then rapidly excised, weighed and fixed in formalin and embedded in paraffin wax for histological examination.

Sections from the hearts were cut at 7 μm in thickness in a longitudinal plane and stained with haematoxylin and eosin (H&E). Sections were consistently taken at the same site in the centre of the infarct. Each section was digitally photographed using a computerised microscope (Leica DMI6000 B inverted microscope, Leica Microsystems, Germany) and the size of the infarct was calculated using Image J Software (NIH).

Figure 2-1. A representative mouse that has been anaesthetized, ventilated and positioned on the heated pad ready for surgery

2.3 Laboratory experiments

2.3.1 Extraction of RNA from tissue samples

RNA from sheep peri-infarct and distant cardiac muscle was extracted using Trizol according to the manufacturer's protocol (Invitrogen, Life Technologies). Tissue samples were kept on ice at all times to avoid degradation of RNA. One millilitre of the Trizol solution was added to 100 mg of tissue in a sterile eppendorf for analysis. Samples were centrifuged at 10,000 x *g* at 4°C for 5 min and the supernatant was transferred to a fresh tube to remove the insoluble debris. Chloroform (200 µl) was added to each tube to assist in the separation between the phenol phase and the aqueous phase which contained the RNA material. Following 3 min of incubation at room temperature, samples were centrifuged at 10,000 x *g* for 15 min. At this stage, three phases were observed in the tube: the upper aqueous phase, the interphase and the lower organic phase. The upper aqueous phase was transferred to fresh tubes using a 1 ml pipette. Care was taken to avoid contact with the interphase or the lower organic phase. Isopropanol (0.5 ml) was added to each tube in order to precipitate the RNA. Samples were then mixed by shaking and then incubated at room temperature for 15 min followed by centrifuged at 10,000 x *g* at 4°C for 15 min. By this time, the RNA pellet was evident and could be transferred to a fresh eppendorf using a 1 ml pipette. The RNA pellet was then washed with 1 ml of 75% ethanol and centrifuged at 10,000 x *g* for at least 5 min. The ethanol solution was carefully removed using a 1 ml pipette and the tubes were then left to dry at room temperature for 5 min. The pellets were then re-suspended in RNase-free water. The

volume used was dependent upon the size of the pellets obtained, and generally a 10-15 µl volume was sufficient. The tubes were vortexed gently to dislodge and help solubilise the pellets. Samples were then put in a 55°C water bath to aid re-suspension of the pellet. At this stage, the samples were stored on ice in preparation for quantification of RNA purity using a Nanodrop spectrophotometer.

2.3.2 Nucleic acid measurement using a Nanodrop mini-spectrophotometer

The spectrophotometer was cleaned with Milli-Q water before and after use. Using a 10 µl pipette, 2 µl of Milli-Q water was used to obtain a basal reading and a blank was obtained by using 2 µl of RNase-free water followed by measurement of 2 µl of the sample of interest and the concentration of RNA was determined from a reading at a wavelength of 260 nm.

2.3.3 cDNA synthesis

Total RNA (2.5 µg) was reversed transcribed into cDNA using first strand cDNA synthesis according to the manufacture's protocol. Each component was mixed and centrifuged briefly before use. Total RNA of 2.5 µg was diluted to a volume of 8 µl using diethylpyrocarbonate (DEPC) treated water. One microliter each of the Oligo(dT) (50

µM) and dNTP mix (10 mM) were added to the RNA solution and samples were incubated at 65°C for 5 min, then placed on ice for at least 1 min. During the incubation period, a cDNA synthesis master mix was prepared. For each reaction, a 2 µl 10x RT buffer, 4 µl 25 nM $MgCl_2$, 2 µl 0.1M DTT, 1 µl RNaseOUT (40U/µl) and 1 µl Superscript III RT (200U/µl) were mixed. A total of 10 µl of the master mix was added to each RNA sample and collected by brief centrifugation. Samples were then incubated for 50 min at 50°C and terminated at 85°C for 5 min before chilling on ice. The reaction was completed by adding 1 µl RNase H to each sample and incubated for 20 min at 37°C. The samples were ready for quantitation of gene expression using the quantitative polymerase chain reaction (qPCR).

2.3.4 Quantitative polymerase chain reaction (qPCR)

Quantitative real-time PCR was used to determine the concentration of myostatin mRNA. A standard curve was prepared from sheep skeletal muscle and was observed to have an efficiency of 1.97. The following primers were used for sheep myostatin sequence: forward primer – GATCTTGCTGTAACCTTCCC, reverse primer – GTGGAGTGCTCATCACAATC. The PCR conditions included an initial denaturation at 95°C for 10 min, followed by 45 cycles of 95°C for 5 min, annealing temperature at 65°C for 10 min and extension at 72°C for 7 sec, melt curve at 95°C, 60°C and 98°C, and cooling at 40°C for 20 min (LightCycler 2.0, Roche Diagnostic GmbH, Germany). Prior to PCR, the content of cDNA in each RT sample was determined using Quant-it OliGreen

ssDNA kit (Invitrogen) and data were normalised to obtain an arbitrary concentration of myostatin mRNA [139].

2.3.5 Immunohistochemistry (IHC)

Immunohistochemistry was performed on sections of the mouse cardiac tissue, which were fixed in formalin and embedded in wax. Prior to immunohistochemistry, samples were deparaffinised and rehydrated in a graded series of ethanol solutions for 5 min at each step according to standard procedures.

For antigen retrieval, the slides were immersed in a pre-heated water bath to 80°C containing 10mM sodium citrate buffer solution and incubated for 30 min. The slides were allowed to cool for 20 min before continuing. Slides were rinsed four times (5 min each) in tris-buffered saline (TBS). To reduce the endogenous peroxidase activity, the slides were then incubated in 3% H_2O_2 in distilled water (dH_2O) for 15 min and rinsed four times in TBS before blocking in TBS/Tween 20 (TBST) with 5% Normal Goat Serum (NGS) (eg. 0.5 ml NGS in 10 ml TBST) for 30 min at room temperature. Slides were then incubated overnight at 4°C in primary antibody of interest with optimal dilution determined from a serial dilution. Primary antibodies examined included anti-cleaved caspase-3 (1:300) (Cell Signalling, #9664), anti-PARP-1 (1:10,000) (Roche, Cat No. 1835238), anti-pAkt^{s473} (1:100) (Cell Signalling, #4058), anti-pAkt1/2/3^{s473} (1:2,000) (Santa Cruz, SC-7985) and anti-pAkt1/2/3^{t308} (1:1,000) (Santa Cruz, SC-16646). For a

negative control, a mouse IgG1 antibody (Dako, Code No. X0931) was used at the same dilution as the primary antibody of interest.

Slides were retrieved the following day, and rinsed 3 x 5 min in TBS before incubation in secondary biotinylated polyclonal goat anti-rabbit antibody (Dako, Code No. E0432) (1:500, 1.5h, room temperature). Slides were rinsed 3 x 5 min in TBS and incubated for 1 h in avidin-biotin complex using Vectastain Elite ABC-Peroxidase kits (Vector Laboratories, VEPK6100) followed by detection with Vector DAB substrate kit (Vector Laboratories, VESK4100) as per the manufacturer's protocol (incubation time ranged from 2 to 5 min). Slides were then counterstained with haematoxylin for morphologic orientation before dehydration and mounting with coverslips.

2.3.6 Immunofluorescence

An indirect immunofluorescent method was used to identify myofibroblasts using a mouse monoclonal α-smooth muscle actin antibody (Santa Cruz, SC-32251). Following deparaffinisation, antigen retrieval and blocking with NGS (described in the earlier section), samples were incubated with α-smooth muscle actin antibody at a dilution of 1:100 overnight at 4°C. Samples were retrieved the following day and incubated with Alexa Fluor 546 goat anti-mouse IgG (Molecular Probes Cat. No. A-11030) at a dilution factor of 1:300 for 2 hr. All incubation and rinsing processes were performed in the dark from this point onwards to avoid quenching of the signal. Samples were then incubated

for 5 min in DAPI at a dilution of 1:1000 before mounting with fluorescence mounting media and cover-slipped. Samples were sealed around the edges with nail polish. Once the sections were dried, samples were examined using the appropriate excitation wavelength.

2.4 Statistical analysis

Data were subjected to analysis of variance (ANOVA) using the statistical software package Genstat (release 15.0). Factors of genotype ($Mstn^{-/-}$ or WT), treatment (sham or ligation of LAD) and their interaction were included in the treatment term. Data were logarithmically transformed when required, to stabilise the variance and a geometric mean was derived (Section 3.3). All data were presented as mean ± standard error of the means (SEM). Data were considered to be statistically significant when a $P < 0.05$.

3

Temporal expression of myostatin mRNA post-MI in ovine cardiac muscle

3.1 Introduction

Several studies have reported that the expression of myostatin is increased in cardiac pathology, with CHF being the most widely studied (see Chapter one for details). However, the significance of this up-regulation in the expression of myostatin remains to be elucidated. Specifically, the question remains whether this increased expression of myostatin is a result of a direct release from the damaged cardiac cells and, therefore, serves as a prognostic indicator, or is a result of a counter-regulatory negative feedback mechanism limiting the growth of muscle mass following injury, or both.

Sharma and co-workers reported that the immunointensity of myostatin protein was increased in the peri-infarct region of the heart 12 h post-MI, which was the earliest time they studied, and that this increased immunointensity persisted throughout the 30 days post-MI of that study [16]. Conversely, the immunostaining of myostatin protein was at a very low abundance in the viable myocardium and similar to that of sham-operated controls [16]. The expression of myostatin mRNA, however, was not examined in this earlier work. A later study by Rodgers and co-workers investigated the expression of myostatin mRNA in WT mice at 28 days post-MI, and found no difference in the expression of myostatin mRNA between the infarcted, border-infarcted and non-infarcted cardiac tissue [122]. That study, however, did not include sham-operated controls and a time-series study post-MI was not conducted to establish whether dynamic changes in the expression of myostatin occurred.

Therefore, the aims of the current study are twofold. Firstly, to validate the study by Sharma *et al*. by measuring the expression of myostatin mRNA in the peri-infarct and distant viable myocardium post-MI and compared with non-infarcted controls. The second and more important aim is to examine the expression of myostatin mRNA at various time points post-MI, in particular with more frequent sampling at time points earlier than 12 h post-MI. This earlier period is critical as it represents the initiation of the ventricular remodelling process post-injury.

3.2 Methods

Cardiac muscle from three year old Romney ewes that had been collected previously were used for quantification of myostatin mRNA. Induction of MI was performed by Dr G. Devlin (interventional cardiologist, Hamilton, New Zealand) and the surgical procedure has been described previously [130] (for details, see also Chapter 2, section 2.2). Sheep were sacrificed at 0.125, 0.25, 0.5, 1, 2, 4, and 8 days post-infarct (n = 3 per group). Three sheep with no surgery were killed at time 0 and served as baseline controls. Following death, hearts were rapidly excised and the peri-infarct and distant viable cardiac muscle were collected and snap frozen in liquid nitrogen for qPCR analysis.

Total RNA was extracted from 100 mg of cardiac tissue using Trizol reagent (Invitrogen, Life Technologies). RNA (2.5 µg) was reverse transcribed into cDNA using first strand cDNA synthesis according to the manufacture's protocol (Invitrogen, Life Technologies).

PCR was carried out with 2.5 µl of a 1:50 dilution of the reverse transcriptase reaction using (see Chapter 2, section 2.3 for details). The primer sequences for sheep myostatin were: forward primer – GATCTTGCTGTAACCTTCCC, reverse primer – GTGGAGTGCTCATCACAATC at the following conditions: denaturation at 95°C for 10 min, amplification for 45 cycles at 95°C, annealing at 65°C for 10 min, and extension at 72°C for 7 sec (LightCycler 2.0, Roche Diagnostic GmbH, Germany).

3.3 Statistical analysis

Data for each sample were normalized to the concentration of cDNA in each RT sample using Quant-it OliGreen ssDNA kit (Invitrogen) [139]. All 'corrected' expressions were logarithmically transformed to stabilise the variance and a geometric mean was calculated for each time point (n = 3). The data reported and shown on the graphs are the geometric means which are expressed as a ratio relative to the non-infarcted controls. A $P < 0.05$ was considered to be statistically significant.

3.4 Results

When compared with non-infarcted controls, the concentrations of myostatin mRNA were different between the peri-infarct and distant viable cardiac tissue (Figure 3-1). In the peri-infarct region, a reduction in the concentrations of myostatin mRNA, which reached nadir at day one was observed, before progressively increasing to a concentration

similar to that of controls (i.e. day 0), at day eight post-MI ($P < 0.01$). By contrast, in the distant viable cardiac muscle, the concentration of myostatin mRNA was reduced within three hours (0.125 day) and remained low throughout the study period when compared with non-infarcted controls ($P < 0.01$).

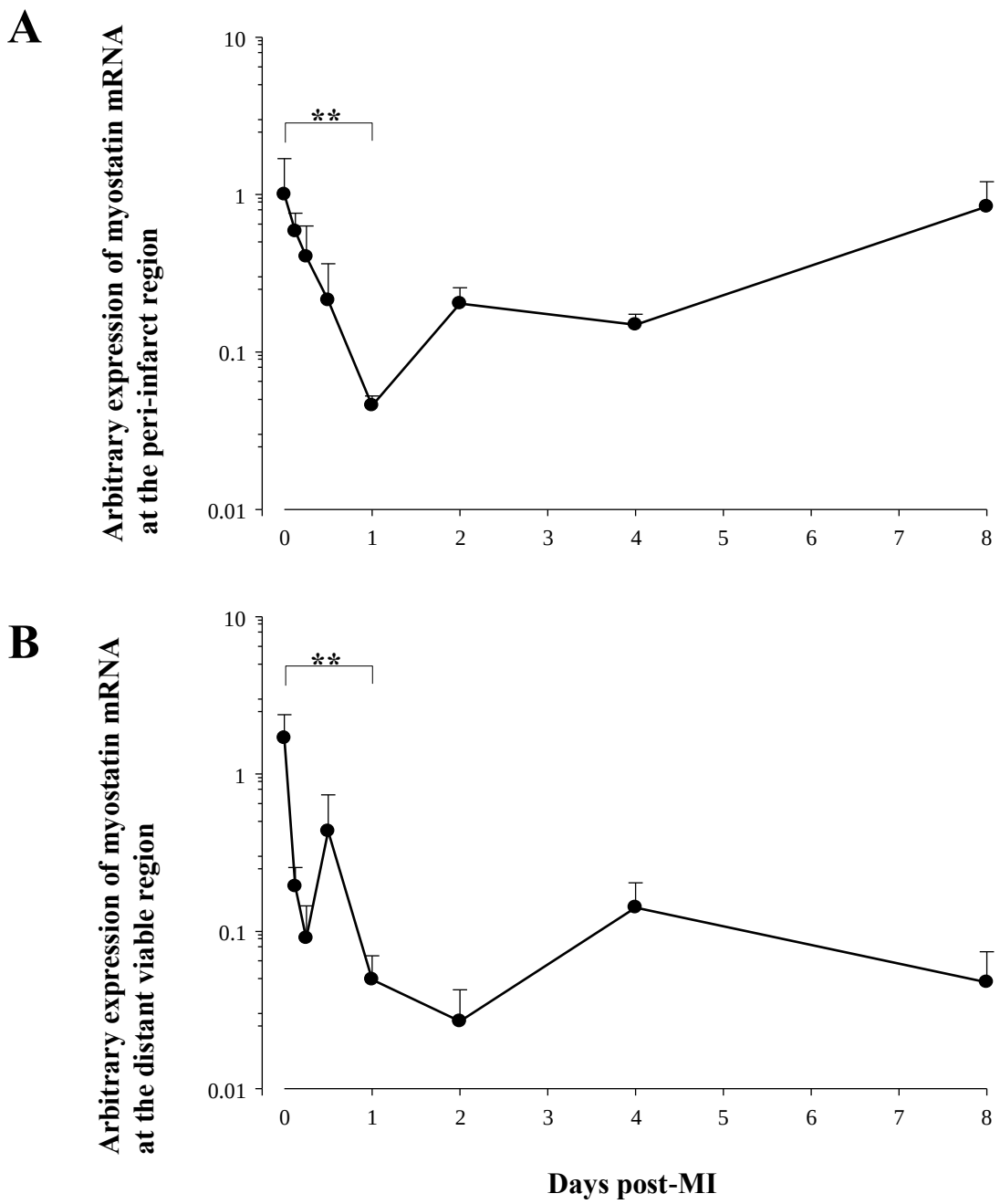

Figure 3-1. Arbitrary expression of the sheep myostatin mRNA at the peri-infarct (A) and distant viable (B) cardiac muscle at various time points post-MI. Data were log transformed and presented as mean ± SEM (n = 3 per group). ($^{**}P <$ 0.01 at day one from non-infarcted controls at day 0)

3.5 Discussion

This study extends the observations of Sharma *et al*. who showed that the expression of myostatin was increased in the peri-infarct region of the heart post-MI. However, contrary to this earlier report, the current study demonstrated an initial decline in the concentration of myostatin mRNA, which reached a nadir at day one post-MI, before a progressive increase back to that of controls at the end of the study at day eight post-MI. It is possible that the concentration of myostatin mRNA may continue to increase until it is higher than controls as demonstrated by Sharma *et al*, but the current study focused on the early period post-MI and, therefore, did not extend to time points beyond day eight post-MI. Secondly, the current study demonstrated that the expression of myostatin is dependent on the location of the cardiac tissue whereby dynamic changes were seen in the peri-infarct region, but a persistently low concentration was observed in the distant viable myocardium.

The initial reduction in the concentration of myostatin mRNA observed in this study was unexpected, and the reason for this is unclear. The expression of myostatin has frequently been reported to be increased in cultured cardiomyocytes following stress (eg. using phenylephrine or Akt stimulation), as well as in humans and animal models of heart failure [18, 19, 51, 124, 140]. A reduction of myostatin in cardiac tissue has not been previously reported. Jeanplong and co-workers did report a reduction in myostatin mRNA in the skeletal muscle of sheep after one week of underfeeding followed by restoration of myostatin mRNA to pre-treatment values by week four [141]. Those authors suggested that

myostatin may act as chalone in the regulation of skeletal mass [141]. The concept of 'chalones' was described by Bullough in the 1960s, who explained that organ or tissue-specific mitotic inhibitors exist in a manner to provide a direct negative feedback mechanism in order to control mitosis and cell growth [142]. Myostatin, has been considered a '*cardiac chalone*' following pathological stimulation of the cardiomyocytes [143]. One of the examples was demonstrated by Shyu and co-workers using cyclic stretch of neonatal rat cardiomyocytes and measured the concentration of myostatin mRNA and the abundance of myostatin protein [140]. A 20% stretch of the cultured neonatal cardiomyocytes resulted in a significant increase in the expression of myostatin mRNA and protein concentration as early as 6 h compared with non-stretched cells (three- and fourfold increased respectively) [140]. A decline in the concentration of myostatin mRNA and abundance of myostatin protein was observed from 18 h through to 48 h, but these changes were not significant [140]. Concomitantly, concentrations of IGF-1 were increased following cyclic stretch of cultured cardiomyocytes, and administration of recombinant IGF-1 to non-stretched cardiomyocytes induced the expression of myostatin similar to that seen in stretched cardiomyocytes [140]. Conversely, addition of monoclonal antibodies to IGF-1 and IGF-1 receptor significantly blocked the expression of myostatin by cyclic stretch [140]. Taken together, Shyu and co-workers concluded that IGF-1 acts as an autocrine factor and mediates the cyclic stretched-induced up-regulation of myostatin expression in cultured cardiomyocytes. Given the known effect of myostatin in limiting the growth of muscle mass, the up-regulation of myostatin post-cyclic stretch was thought to represent a negative feedback mechanism to counteract secretion of IGF-1. In patients with chronic osteoarthritis and wasting of the quadriceps muscle who underwent elective total hip joint replacement, an increase in the concentration of myostatin mRNA in

skeletal muscle along with an increase in the concentration of IGF-1 mRNA in a counter-regulatory fashion were observed pre- and post-operatively when compared with healthy controls [144]. Similarly, overexpression of activated Akt in transgenic mice significantly increased the expression of myostatin [145]. The serine-threonine kinase, Akt (or protein kinase B) is a critical protein kinase for cellular growth and survival [146]. Transgenic mice with a cardiac-specific overexpression of an active mutant of Akt (myr-Akt) were shown to have hypertrophy (concentric) of the myocardium compared with control littermates [147]. As Akt is essential for promoting the growth of cardiomyocytes, it is postulated that the up-regulation of myostatin serves as a negative feedback loop to limit the size of the heart [145]. By extrapolating these results to the current study, it can be assumed that the restoration of the concentration of myostatin mRNA at day 8 post-MI in the peri-infarct region is a result of counter-regulatory feedback loop to limit the growth of cardiac muscle from excessive hypertrophy following an MI. The initial decline in concentration of myostatin mRNA may be viewed as a means to facilitate recovery post-MI. During ventricular remodelling, hypertrophy of cardiomyocytes occurs to compensate for the loss of myocyte following MI. The enlargement of cardiomyocytes and formation of new sarcomeres initially serve to maintain cardiac function post-injury [148]. This adaptive response can be regulated by several factors, one of which is TGF-β [110]. Hence, it is reasonable to speculate that the initial decline in the expression of myostatin mRNA facilitates the hypertrophy of cardiomyocytes to maintain cardiac function. However, as the remodelling process continues, and the underlying pathology is not corrected, further loss of cardiac cells occurs, resulting in greater release of myostatin and up-regulation in the expression.

The second observation derived from this study is the selective expression and dynamic changes in the concentration of myostatin mRNA in the peri-infarct region, and not the distant viable myocardium, suggesting the preferential role of myostatin in the injured myocardium. This is not surprising given the inherently low concentration of myostatin in normal, uninjured myocardium and an enhanced expression in diseased state as discussed in Chapter one.

In conclusion, this study validated data from previous reports that a temporal relationship exists between the expression of myostatin and duration post-MI, and that this expression is restored in the peri-infarct region of the myocardium back to that of baseline controls. However, contrary to the previous observation, an initial decline in the expression of myostatin was seen prior to the restoration of the expression of myostatin. This is likely an adaptive response to injury to facilitate the initial physiological hypertrophy of the myocardium. However, as the remodelling of the ventricle progresses, an imbalance between the contractile demand and the contractile capacity of the heart may occur, triggering a cascade of signalling mechanism that may have promoted the up-regulation of myostatin. It remains unclear whether limiting the growth of cardiac muscle post-MI is a beneficial or detrimental phenomenon. Moreover, the significance of the frequently reported increased expression of myostatin following injury remains to be determined. It is likely that more work is needed to clarify this feedback mechanism. Nevertheless, by using genetically modified mice with a deletion in myostatin gene, the following chapters may help to provide a better insight to the functional relevance of myostatin following acute MI.

4

Absence of myostatin improves survival and cardiac function post-MI

4.1 Introduction

Since the detection of myostatin in the heart 15 years ago [16], an increasing number of studies have focused on the role of myostatin in the heart. Specifically, the expression of myostatin (protein or mRNA or both) was found to be up-regulated following a hypertrophic stress response using phenylephrine (PE), angiotensin II (AngII) or the cyclic-stretch of cultured cardiomyocytes [50, 51, 124, 140]. Similarly, the expression of myostatin was increased in the myocardium and/or serum in humans and animal models of heart failure and MI [16, 19, 20]. However, whether these changes in the expression of myostatin translate into a change in heart function following an acute MI remains to be elucidated. Furthermore, the absence of myostatin was reported to induce hypertrophy of the myocardium in response to stressful stimulus [122]. Therefore, it is hypothesized sthat the absence of myostatin reduces the severity of MI and improves the prognosis after such event.

To test the hypothesis, genetically engineered $Mstn^{-/-}$ mice will be subjected to an induction of acute MI and the clinical responses will be compared with WT controls. Ligation of the LAD artery is a well-established approach to induce MI in a murine model [133, 134, 149]. However, the conventional method of ligating proximal to the origin of the LAD artery is associated with a high post-operative mortality of up to 70% [134]. A more distal ligation of LAD artery, at a level midway between the left atrial appendage and the apex, is associated with a lower mortality of 20-30% [150]. Therefore, in the current study, the latter approach was employed by ligating the LAD artery midway between the left

atrium and the apex of the left ventricle as previously described [131]. A detailed description of the surgical and echocardiogram techniques can be found in Chapter 2, section 2.2.

4.2 Study design

Adult male WT and Mstn$^{-/-}$ mice (12 weeks old) were randomly assigned to either ligation of the LAD artery to induce MI (Lig) or sham-control (Sham) group (n = 12 per genotype and procedures), resulting in four cohorts in this study. The clinical data were measured at different time points (Figure 4-1) and mice were euthanized at the conclusion of the study at day 28.

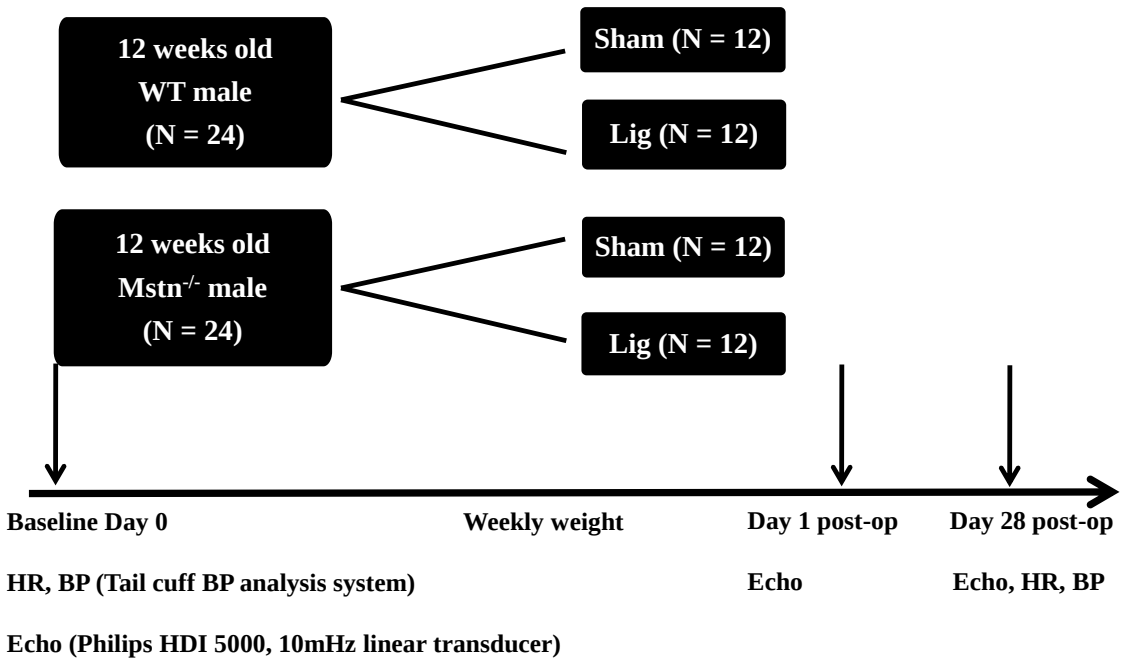

Figure 4-1. Study design indicating the intended numbers of animals used and the clinical data measured at various time points during the study.

4.3 Results

4.3.1 Mortality

Six WT mice died following surgery, which required the recruitment of an additional six mice, and resulted in a disproportionate increased mortality in the WT mice compared with $Mstn^{-/-}$ mice (20% vs 0%, $P < 0.05$). The majority of the WT mice (five out of six) died within the first day post-MI, while one died in the sham-operated group. The mean time to carry out the procedure of ligating the LAD artery was similar for the WT and $Mstn^{-/-}$ ligation groups (29.8 ± 1.4 min vs 27.8 ± 1.0 min respectively, $P = 0.24$). The number of cotton sticks used as an estimate of the amount of blood loss was similar between the two groups. No difference in the infarct size was observed between the two ligation groups (for details, see Chapter 5). The mean time for the procedure in sham animals was shorter and no difference was observed between the two genotypes (WT sham 24.0 ± 1.5 min vs $Mstn^{-/-}$ sham 23.8 ± 1.0 min, $P = 0.89$).

4.3.2 Total body weight and heart weight

The changes in BWT throughout the study period are summarised in Figure 4-2. As expected, $Mstn^{-/-}$ mice were consistently larger than WT littermates and remained so throughout the study period. Induction of a myocardial injury did not alter BWT of the

$Mstn^{-/-}$ mice over the 28 day period post-MI. Conversely, an almost 7% increase in BWT was observed in WT mice at the end of the study period, irrespective of whether the mice were assigned to the sham or ligation groups ($P < 0.001$).

At the end of the 28 day study period, the mice were weighed and euthanized. The hearts were rapidly excised, blotted and weighed. The hearts were then sectioned longitudinally and photographs taken before fixation in formalin. The heart weights (HW) of $Mstn^{-/-}$ mice were about 20% larger than WT mice ($P < 0.001$), while the HW/BWT ratio was smaller in $Mstn^{-/-}$ than in WT mice ($P < 0.001$). However, no difference in the HW or HW/BWT ratio was seen between the sham and ligation groups within genotype (Figure 4-3).

4.3.3 Heart rate and mean arterial blood pressure

Baseline resting HR on conscious mice was higher in the $Mstn^{-/-}$ group compared with WT littermates (575.5 ± 11.3 bpm vs 535.9 ± 12.0 bpm, $P < 0.05$), while the opposite was observed at day 28 post-surgery (599.1 ± 12.0 bpm vs 645.4 ± 6.5 bpm, $P < 0.01$), indicating the development of post-operative tachycardia in the WT mice, irrespective of surgical procedures (Figure 4-4). Meanwhile, the MAP was significantly greater in WT mice both at baseline and at day 28 post-MI compared with $Mstn^{-/-}$ mice (Figure 4-4). Induction of MI resulted in a 9% reduction of MAP in the $Mstn^{-/-}$ mice, whilst an increase of almost 6% in MAP was seen in the WT ligation group ($P < 0.05$).

4.3.4 Left ventricular end systolic and diastolic diameters

Both the LVESD and LVEDD obtained on lightly anaesthetised mice were consistently greater in Mstn$^{-/-}$ than WT mice throughout the study period (Figure 4-5). There were no differences in the LVESD between the groups over time, although a trend towards a greater LVESD at day 28 was observed in the WT mice (P = 0.07) (Data not shown). However, induction of MI resulted in a more pronounced reduction in the LVEDD from baseline in the WT mice compared with Mstn$^{-/-}$ mice ($P < 0.05$). By day 28, the LVEDD had returned to baseline, but a trend was observed with WT mice having a greater LVEDD post-surgery (P = 0.09) (Data not shown).

4.3.5 Fractional shortening and ejection fraction

Cardiac function, as determined by FS or EF using echocardiography, was similar between the groups at baseline (P = 0.162 and P = 0.15, respectively). Induction of MI resulted in a 6% and 8 % reduction in FS and EF respectively, in both groups of mice compared with sham-operated mice ($P < 0.05$). This reduction in FS and EF was not different between the groups suggesting a similar degree of cardiac insult (P = 0.7). At the end of the 28 day study period, cardiac function, both the FS and EF had restored to baseline in the ligated Mstn$^{-/-}$ mice, a finding which was not observed in WT counterparts ($P < 0.05$ and $P < 0.01$ respectively) (Figure 4-6).

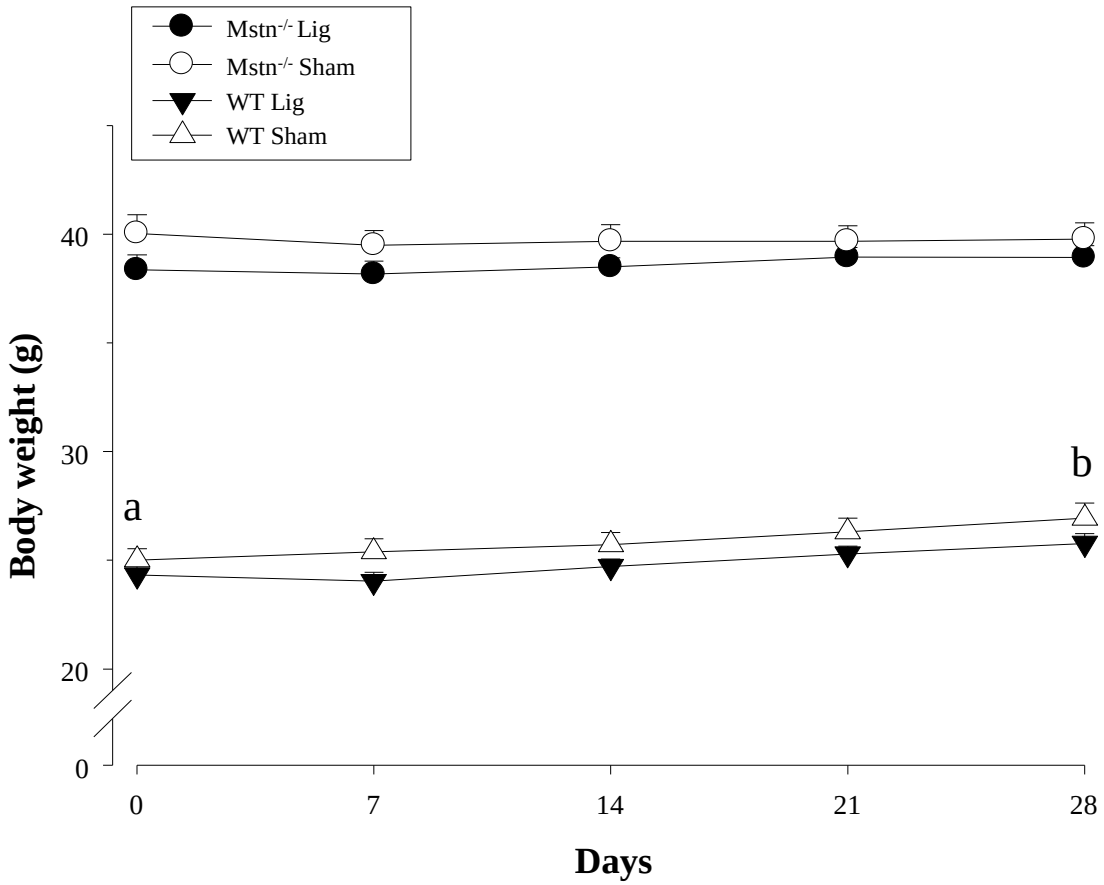

Figure 4-2. Mean body weight (± SEM) during the study period. The different letters (a & b) denote significant difference in body weight between the baseline and day 28 post-surgery irrespective of surgical procedures in the WT mice ($P < 0.001$).

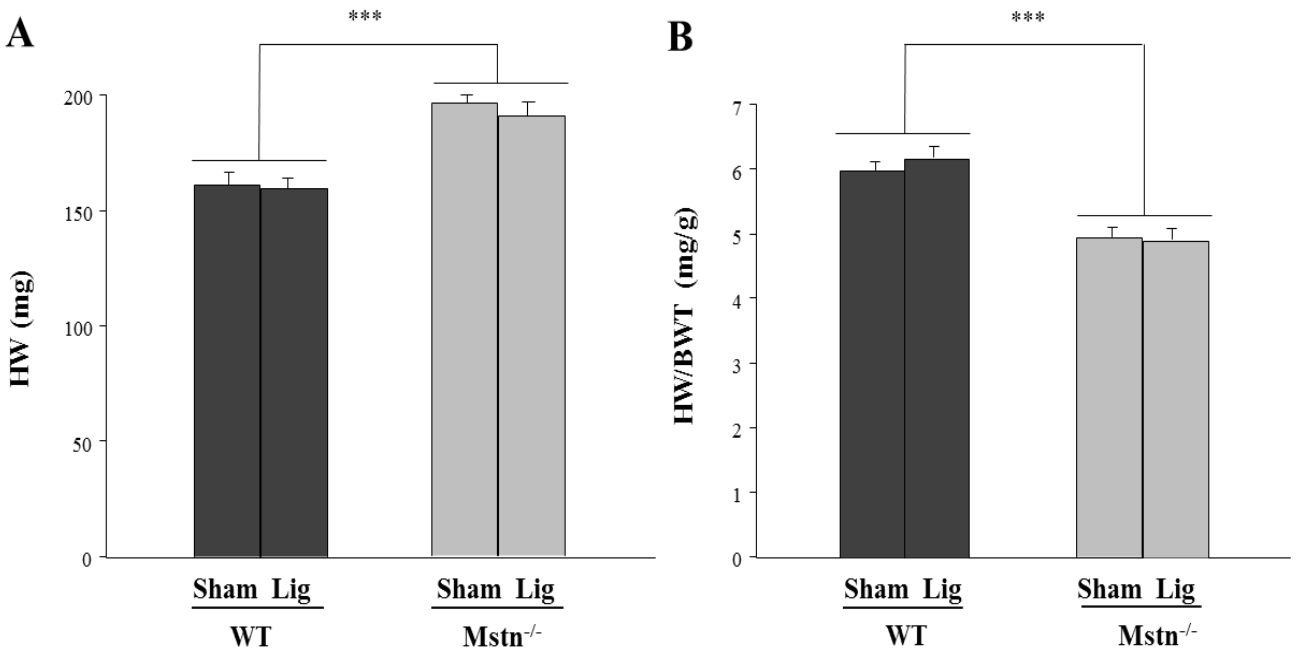

Figure 4-3. Heart weight (HW) analysis at the end of the study (mean ± SEM). (A) Total HW, and (B) Ratio of HW to BWT (***$P < 0.001$).

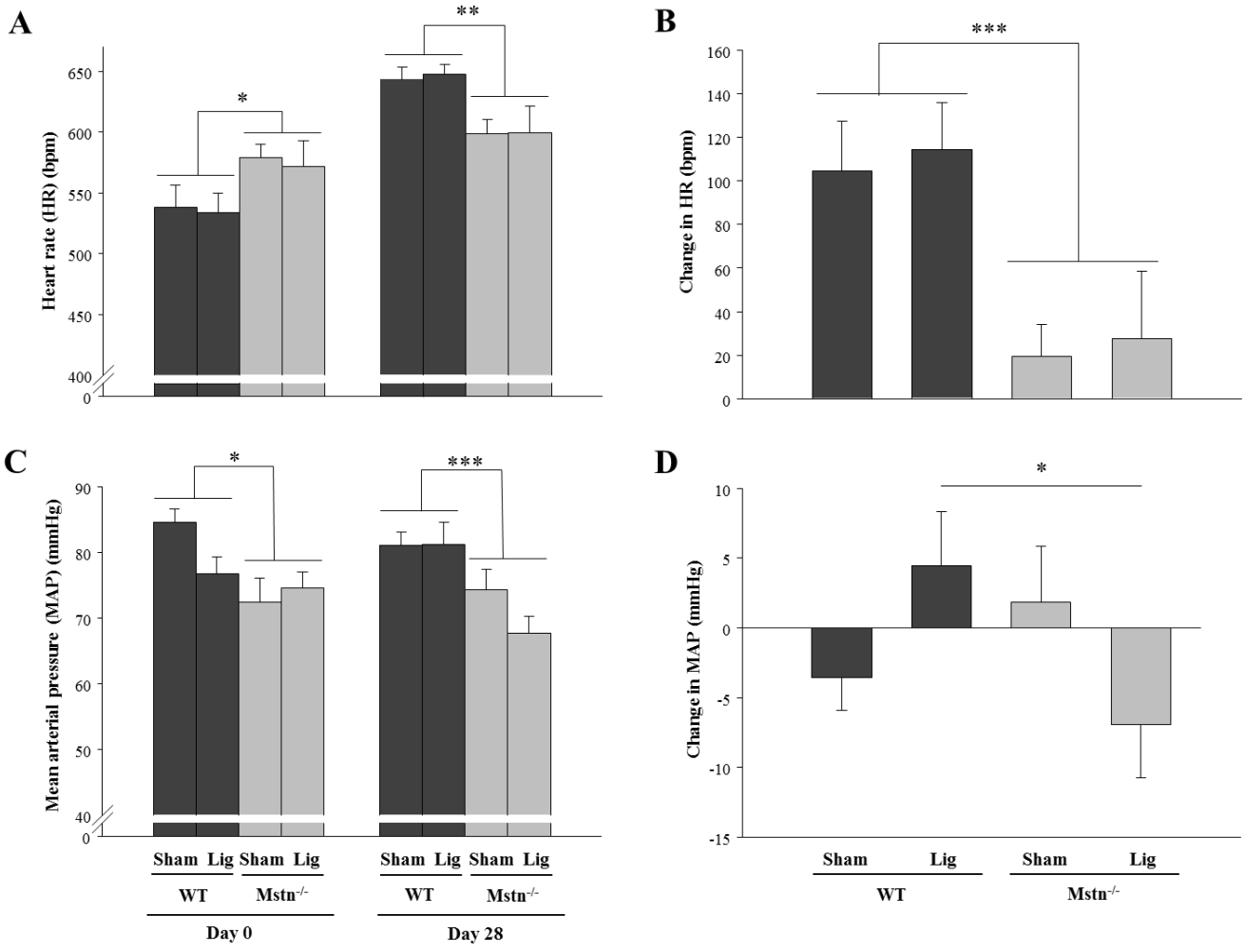

Figure 4-4. Haemodynamic changes during the study period. (A) Heart rate (HR), (B) Change in HR at day 28 from baseline, (C) Mean arterial blood pressure (MAP), (D) Change in MAP at day 28 from baseline. Data are presented as mean ± SEM (**P* <0.05, ***P* < 0.01, ****P* < 0.001).

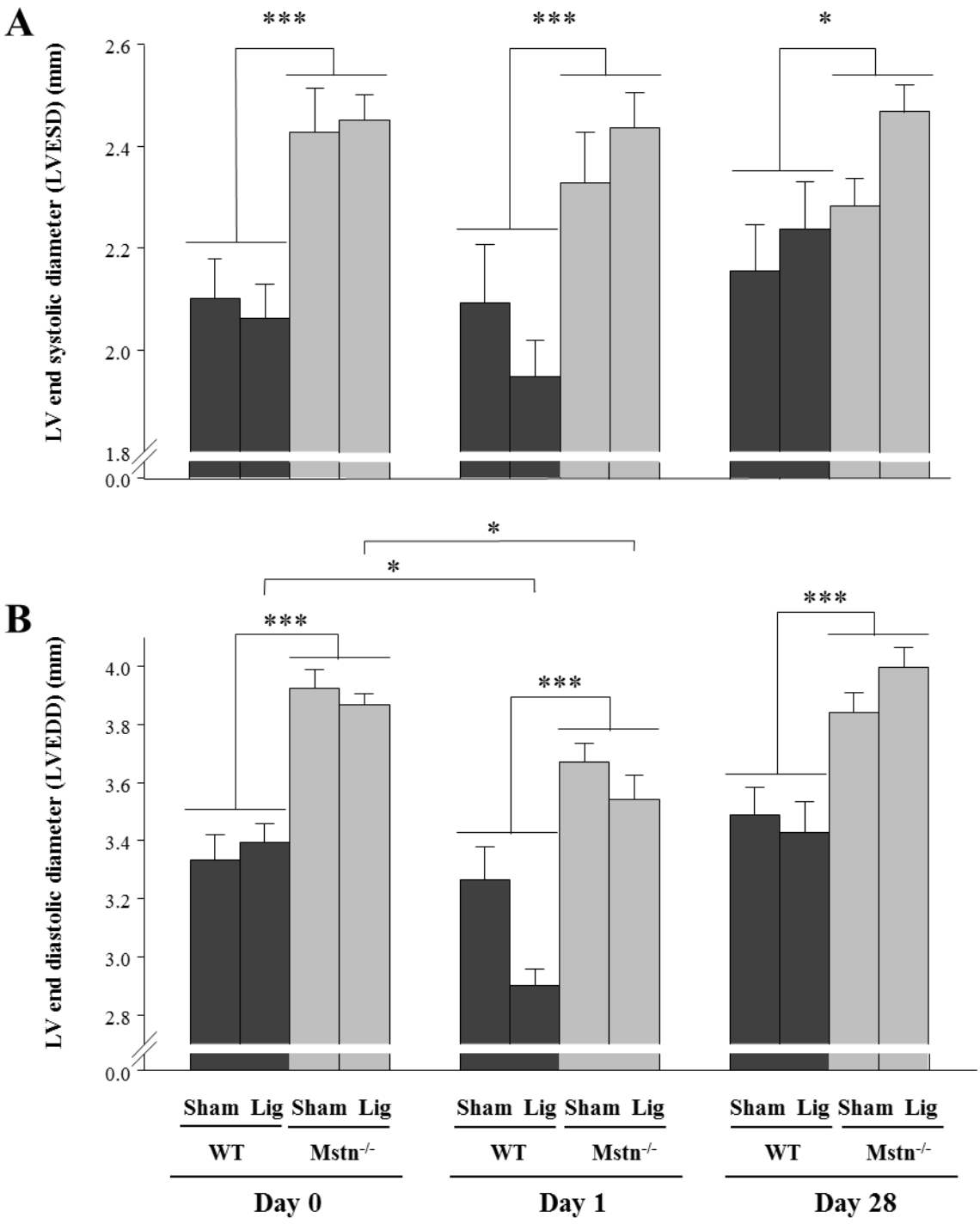

Figure 4-5. Measurements of the left ventricular dimensions at end systole (A) and diastole (B) at baseline, days 1 and 28 post-surgery. Data are presented as mean ± SEM (*$P < 0.05$, ***$P < 0.001$)

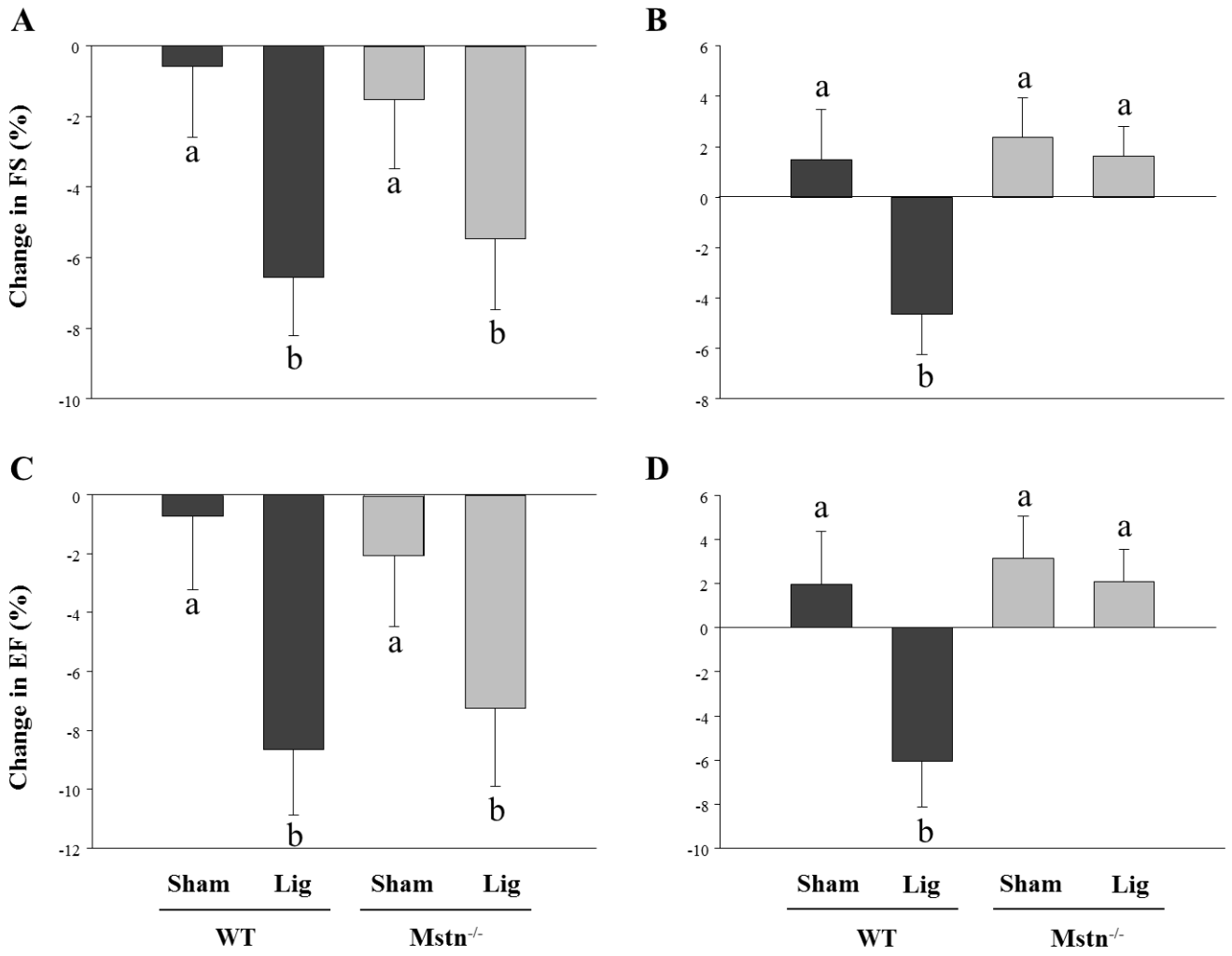

Figure 4-6. Measurements of the changes in fractional shortening (FS) from baseline to day one (A) and baseline to day 28 (B). Changes in ejection fraction (EF) from baseline to day one (C) and baseline to day 28 (D). Data are presented as mean ± SEM. Different letters denote a significant difference of $P < 0.05$.

4.4 Discussion

The expression of myostatin was shown to be up-regulated in several animal models and in human subjects with cardiac pathologies such as CHF or acute MI [16, 19, 20]. However, whether such up-regulation is associated with a change in cardiac function remains unclear. In this study, a number of key observations were identified: (1) a favourable survival outcome post-cardiac surgery in $Mstn^{-/-}$ mice compared with WT controls, (2) an improvement in ventricular function to near baseline level post-MI in the $Mstn^{-/-}$ mice which was not observed in the WT mice, and (3) haemodynamic changes in $Mstn^{-/-}$ mice which is suggestive of a better compensatory mechanism post-injury. To the best of my knowledge, this is the first time a primary clinical endpoint has been described in the absence of myostatin and an improvement in cardiac function following an acute MI demonstrated.

The lack of mortality in the $Mstn^{-/-}$ mice post-MI was unanticipated and is an important observation not reported previously. Mortality rate in C57BL/6 mice following ligation of LAD artery has been reported to range from <10% to 40% [133, 151, 152]. The mortality of 20% observed in WT mice in the current study is consistent with that reported in the literature. While the majority of the deaths in the WT mice occurred post-MI (within the first 24 hr), one animal died following the sham-operated procedure, suggesting that the susceptibility to death in WT mice is not confined to MI, but to open thoracic surgery in general. The cause of death was not apparent at autopsy, with no excessive bleeding, lung injury or cardiac rupture and, therefore, was presumed to result from a fatal ventricular

arrhythmia or severe acute heart failure as reported previously [149]. On the other hand, the literature on the mortality of Mstn$^{-/-}$ mice post-MI is limited due to the lack of numbers of these mice undergoing an induction of MI. Nevertheless, the reason for the discrepancy in mortality between the genotypes in the current study is unknown. All mice assigned to the MI procedure were treated equally and in the surviving cohort, the reduction in ventricular function and infarct size were similar. Therefore, the increased rate of survival in Mstn$^{-/-}$ mice cannot be attributed to a bias in the surgical procedure. It is also unlikely to be explained solely by the larger heart and body weights in Mstn$^{-/-}$ mice because Swiss Iffa Credo mice, which have a comparable body weight to that of Mstn$^{-/-}$ mice, had a 23% mortality post-MI [153]. As such, it is plausible to speculate that the absence of myostatin alone may be an independent prognostic indicator of survival.

The mean BWT in Mstn$^{-/-}$ mice remained constant throughout the study period, indicating that cardiac cachexia did not occur post-MI in this cohort. As discussed earlier, cachexia is an independent risk factor for mortality in patients with chronic heart failure [87]. While loss of weight was also absent in WT mice, a significant increase in mean BWT of almost 7% was evident, irrespective of sham or ligation procedure. A previous study using C57BL/6 mice (two months old at time of MI) also demonstrated an increase in body weight eight weeks post-MI both in sham-operated and ligated groups [154]. Those authors concluded that weight loss associated with the heart failure syndrome did not occur in these young mice. It is not known if an alteration in energy intake or expenditure was present in these mice. It is also unclear if the weight gain is due to an increase in fat or lean mass or extracellular fluids such as water and salt retention. However, this study was

not designed to investigate the weight changes in mice following an acute MI. Therefore, further investigation was not undertaken and the cause of the changes in BWT may warrant further study.

The HW in Mstn$^{-/-}$ mice has been reported to be increased [121, 122], unchanged [123] or decreased [124], depending upon the age and size of animals used. In this study, HW was significantly greater in Mstn$^{-/-}$ mice compared with WT mice, which is likely a genotypic effect. When HW was normalised to BWT, which is also larger in Mstn$^{-/-}$ mice, the opposite was seen with Mstn$^{-/-}$ mice developing a lower HW/BWT ratio compared with WT mice. Importantly, no difference was observed between the sham and ligation groups within the genotype, implying that induction of MI did not result in pathological hypertrophy of the myocardium, both in the Mstn$^{-/-}$ and WT mice.

Heart rate and MAP are two of the most easily accessible cardiovascular parameters that provide positive correlations with the haemodynamic changes in mice. Although these measurements are highly variable according to the circadian rhythms, a resting HR of ± 500 bpm and a blood pressure of ± 100 mmHg are generally accepted as being physiological in mice [155]. The baseline HR in WT mice in this study is consistent with the physiological range reported. However, a significant resting tachycardia developed post-operatively in the WT mice, both in the sham and ligated groups. Monitoring of ECG, which was not available for this study, would have been informative to determine whether a tachyarrhythmia had occurred. By contrast, the relatively similar HR between baseline and day 28 post-operatively in the Mstn$^{-/-}$ mice suggests that these mice were

able to maintain HR despite thoracic (sham) or cardiac surgery. It is not known if myostatin affects the autonomic nervous system, which is a key determinant of HR, but treatment with carvedilol in rats with an aorto-caval shunt significantly inhibited the up-regulation of myostatin mRNA induced by the shunt [19]. This causal relationship may imply the potential role of myostatin in the regulation of sympathetic or parasympathetic stimulation.

Mean arterial pressure is a function of left ventricular contractility, HR and vascular resistance and represents the steady flow of the arterial system and is often calculated as the sum of diastolic blood pressure and 1/3 of pulse pressure [136]. A genotype difference was observed wherein WT mice had a greater MAP at baseline and post-surgery compared to Mstn$^{-/-}$ mice. However, after an MI, the opposite was seen with Mstn$^{-/-}$ mice developing a lower MAP compared with WT ligated group, while no difference was observed in the sham-operated groups. The reason for this difference is unclear and, whether this is related to the alteration in HR, is also not known. An increase in MAP is an adverse predictor of further cardiovascular events in humans [135, 156]. Therefore, one can speculate that the increased MAP seen in WT mice post-MI may predispose them to recurrent cardiovascular events while the lower MAP in Mstn$^{-/-}$ mice may be protective.

A comparison of echocardiographic findings between studies is difficult given the difference in genetic backgrounds and age of animals used and the presence or absence of anaesthesia [124, 157, 158]. Nevertheless, several studies reported similar lseft ventricular dimensions and functions between Mstn$^{-/-}$ and WT mice [121, 123, 124]. Rodgers and co-

workers, however, reported that in Mstn$^{-/-}$ mice, the left ventricular dimensions were greater, but was associated with a depressed resting FS and EF compared with WT mice [122]. When challenged with chemical stress test using isoproterenol, an enhanced cardiac performance with greater increases in FS and EF were observed in Mstn$^{-/-}$ mice compared with WT mice [122]. In the current study, both the LVESD and LVEDD were greater but unchanged throughout the study, in the anaesthetised Mstn$^{-/-}$ mice compared with their own control littermates. The resting FS and EF were similar at baseline among the groups, but Mstn$^{-/-}$ mice was associated with a significantly better functional recovery 28 days post-MI compared with WT littermates. Together with the greater HW observed in Mstn$^{-/-}$ mice, these findings support that of Rodgers *et al*. that an eccentric hypertrophy of the myocardium exists in the Msnt$^{-/-}$ mice and the greater LVESD and LVEDD and functional improvement would be consistent with a physiological, and not pathological hypertrophy of the heart in these mice [122]. These data also extend previous observations that in myostatin deficient mice, cardiac performance is enhanced not only following chemical stress, but also in diseased hearts such as occurring after MI. Coupled with the stable HR and lower MAP post-MI, this study supports the hypothesis that the absence of myostatin protects the heart following acute MI.

In conclusion, the absence of myostatin is associated with a favourable survival outcome following open-chest surgery in mice. While baseline resting FS and EF were similar between the groups, Mstn$^{-/-}$ mice had a functional recovery to near baseline level 28 days post-MI whilst the cardiac function remained depressed in WT mice. The maintenance of a physiological HR post-surgery and lower MAP in Mstn$^{-/-}$ mice may imply a better

compensatory mechanism to injury seen in these mice. Further analyses are warranted to confirm and determine whether this apparent protective mechanism in the $Mstn^{-/-}$ mice is a result of a reduction in the formation of fibrosis, a change in cardiomyocyte size and/or numbers or an alteration in function in the subcellular level following acute MI, which will be discussed in Chapter Five.

5

Absence of myostatin is associated with a reduction in cardiac fibrosis

5.1 Introduction

In the previous chapter, it was shown that 28 days after an acute MI, the absence of myostatin improves survival and ventricular function of $Mstn^{-/-}$ mice, compared with WT mice. The mechanism underlying this beneficial role of myostatin is unclear.

As an inhibitor of muscle development, the absence of myostatin results in an increase in skeletal muscle mass by a combination of hyperplasia and hypertrophy of muscle cells and fibres [11]. *In vitro* studies support the role of myostatin in inhibiting cellular proliferation, differentiation and protein synthesis, both in skeletal muscle myoblasts and cardiomyocytes [52, 53, 119]. In cultured cardiomyocytes, an increase in the numbers and/or size of cells was demonstrated in the absence of myostatin through an inhibition of p38 and Akt phosphorylation [124] or Erk-dependent pathways [51].

Furthermore, the role of myostatin may influence the formation of fibrosis, in a manner similar to that of TGF-β [159]. Indeed, several animal studies of skeletal muscular dystrophies have shown a reduction in fibrosis in the absence of myostatin [12, 14]. Li and co-workers have demonstrated that myostatin (both protein and mRNA concentration) is produced by normal primary muscle fibroblasts [21]. Addition of recombinant myostatin directly stimulates the proliferation of normal skeletal muscle fibroblasts through the canonical Smad signalling pathway, as well as p38 MAPK and PI3K/Akt/mTOR signalling pathways, all of which mediate the proliferation of fibroblasts [21]. The same

authors subsequently demonstrated that myostatin resists apoptosis in fibroblasts *in vitro* and, by inhibiting myostatin using a soluble activin IIB receptor (ActRIIB.Fc), apoptosis of fibroblast was enhanced in *mdx* mice [22]. However, it is unknown whether the effects of myostatin on cardiac fibroblasts or myofibroblasts are similar to that observed in skeletal muscle fibroblasts.

It is, therefore, hypothesized that the functional improvement observed in $Mstn^{-/-}$ mice results from one (or more) of the following mechanisms: (1) an alteration in the number and/or size of the cardiomyocytes, (2) a reduction in the expression of myofibroblasts and hence, a reduction in fibrosis and (3) an enhanced survival or reduced apoptosis of cardiomyocytes resulting in more viable myocardium. Using immunohistochemistry and immunofluorescence, the aim of the current study is to examine each of these mechanisms in an attempt to understand the molecular mechanism resulting in the improvement in cardiac function post-MI, observed in $Mstn^{-/-}$ mice.

5.2 Materials and methods

All the sections of the myocardium used for the following analyses were randomly coded and calculations were performed with the operator blinded to the identification and treatment of the mice. In addition, all sections were performed in the same batch for each analysis to ensure uniformity of staining between the slides.

5.2.1 Assessment of infarct size

All histological sections were obtained from the hearts of mice that were euthanized at 28 days after either a sham procedure or ligation of the LAD artery (n= 4 to 6 per group). Sections were cut consistently in the longitudinal plane in the centre of the infarct (7 µm thick). Sections were stained with haematoxylin and eosin following a standard dewaxing and rehydration procedure. Sections were then examined at 200x magnification and images were captured using a computerised microscope (Leica DMI6000 B inverted microscope, Leica Microsystems, Germany). The size of the infarct was determined using a method previously described [160]. Briefly, the midline of the length of infarct which included over 50% of the whole thickness of the myocardial wall was traced manually and the size of the infarct is expressed as a percentage of the midline infarct length to the midline circumference of the LV in each section through the heart. The measurements were performed using Image J software (NIH).

5.2.2 Measurements of DNA synthesis

Estimation of the amount of DNA synthesis was made from the incorporation of 5-Bromo-2'-deoxyuridine (BrdU) according to the manufacturer's protocol (GE Healthcare Amersham cell proliferation kit, Code: RPN20). Briefly, BrdU was injected intra-peritoneally two hours before euthanasia. Following a standard dewaxing and rehydration procedure, and blocking with hydrogen peroxide and normal goat serum, samples were

incubated in primary mouse anti-BrdU antibody (1:100, 1.5 h, room temperature) and secondary goat anti-mouse $IgG_{2\alpha}$ (HRP labelled) (30 min, room temperature). Sections were rinsed with TBST (4 rinses, at 5 min each) between steps. Finally, sections were incubated in 3,3'-diaminobenzadine (DAB) with nickel chloride as the chromogen. Samples were counterstained with nuclear fast red before dehydration and mounting in DPX medium. For negative controls, primary antibodies were omitted on a different section on the same slide.

The total labelling fraction was calculated as a ratio of the BrdU positive cells to the total number of cells counted in each field [153]. Six fields per section in the border region of the infarcted ventricle were randomly selected for the calculation. For sham animals, the six fields were taken randomly throughout the left ventricle. Each section was examined at 400x magnification using a computerised microscope (Leica DMI6000 B inverted microscope, Leica Microsystems, Germany) and data were analysed using Image J software (NIH).

5.2.3 Quantification of the size of cardiomyocytes

To quantify the size of the cardiomyocytes, cells were stained with laminin (Dako, Code No. Z0097) to highlight the cell membrane and sections were counterstained with haematoxylin to visualise the nuclei. Whole-section images were sampled to a final resolution of 0.5µm/pixel. A point-counting system was used where a grid of equal

spacing was overlaid onto the section. Only cells with well-defined cell membrane and visible nuclei that sit on the 'crosses' of the grid were selected. Two different parameters were calculated to determine the cross-sectional size of the cardiomyocytes: (1) the 'cross-sectional area' and (2) the minimal 'Feret's diameter' as described previously [123, 161, 162]. A total of at least 300 consecutive cells were measured from each section using image J (NIH) software.

5.2.4 Measurement of collagen deposition

Van Gieson staining was used to determine the amount of scar tissue by estimating the deposition of collagen formation. Following dewaxing and rehydration, samples were stained in a mixed solution of Weigert's solution A and B for 10 min and rinsed well in water before staining with van Gieson for 10 min. Slides were then rinsed in water and then washed firstly in 90% ethanol with saturated picric acid for 30 sec followed by 100% ethanol with saturated picric acid for 1 min. Samples were then dehydrated and mounted with coverslips.

A modified grid-counting system was used to estimate the amount of collagen deposition in the peri-infarct region, where viable cardiomyocytes were still present [163]. A grid of equal spaces (distance - 140μm) was created over the region of interest (ie. Infarcted and peri-infarcted areas) on each sample. Grids that had over 50% of infarcted scar tissue (stained red) were graded as 1, while grids with over 50% of viable tissue (stained

yellow/light brown) interspersed with collagen were graded as 2. Grids with only viable cardiomyocytes were not counted as this represents the distant non-infarcted myocardium. The amount of collagen deposition was, therefore, given by the following calculations:

$$\text{Collagen deposition (\%)} = \frac{\text{Grade 1 (infarcted scar tissue)}}{\text{Grades 1 + 2 (infarcted + viable)}} \times 100\%$$

5.2.5 Determination of the number of myofibroblasts

An indirect immunofluorescence method was adopted to localise myofibroblasts using α-smooth muscle actin antibody (α-SMA) at a dilution of 1:100 and overnight incubation (Santa Cruz, SC-32251). This antibody is specific for α-smooth muscle actin, which is expressed in myofibroblasts and vascular smooth muscle cells but is non-reactive with actin from fibroblasts, myocardium and striated muscle. After incubation in primary antibody and rinsing, a secondary antibody (Alexa Fluor 546 goat anti-mouse IgG (H+L), Molecular Probes Cat. No. A-11030) was applied at a dilution of 1:300 for 1.5 h, before counterstaining with DAPI (1:1000, 5 min) and mounting (Dako Cytomation Fluorescence Mounting Media). The incubation and rinsing processes were done in the dark for optimal results.

The number of myofibroblasts was calculated using the grid-counting system as described earlier, where grids with immunofluorescence positivity (orange/red) was graded as 1, and grids with only DAPI (blue) was graded as 2. The number of myofibroblasts was estimated using the following calculations:

$$\text{Estimated amount of myofibroblasts} = \frac{\text{Grade 1 (positive)}}{\text{Grades 1 + 2 (total)}} \times 100\%$$

Grids with blood vessels were excluded from the analysis.

5.2.6 Immunohistochemistry for cellular apoptosis, programmed necrosis and survival

Immunohistochemistry was carried out to examine the immunointensity of various cellular markers of apoptosis (cleaved caspase-3, 1:300), programmed necrosis (anti-PARP-1, 1:10,000) and survival (anti-pAkt^{s473}, 1:100, anti-pAkt1/2/3^{s473}, 1:2,000, and anti-pAkt1/2/3^{t308}, 1:1000) (see section 2.3.6 for procedures). The immunointensity of the antibodies was obtained semi-quantitatively using a multiplicative quickscore method [164]. Briefly, the analysis takes into account both the proportion of positive cells (termed category A and assigned scores from 1 to 6) and the intensity of the staining (termed category B, and scores from 0 to 3). A quickscore is then derived from the following calculation:

Quickscore = Category A x Category B

5.3 Results

5.3.1 The size of the infarction was similar between the two genotypes

Ligating the LAD artery midway between the left atrial appendage and the apex produced an infarct size of approximately 11% of the left ventricle (Figure 5-1A). No difference was observed between the genotypes, suggesting that the cardiac injury was of similar extent (P = 0.38). Histopathological examinations of the cardiac tissue at 28 days post-MI revealed an area of ischaemia, and replacement of cardiomyocytes by inflammatory cells and scar tissue (Figure 5-1B). Although an objective quantification was not made, the appearance of fat vacuoles was more noticeable in the WT hearts, and was not frequently seen in the hearts of $Mstn^{-/-}$ mice. As expected, no histological abnormalities were seen in sham-operated mice in both the $Mstn^{-/-}$ and WT groups, in which the architecture of the myocardium was preserved.

5.3.2 Lack of myostatin does not affect the number of newly synthesized cells post-MI

An increase in the labelling fraction of BrdU was observed in all groups of mice at 28 days post-surgery, with a greater increment in the post-MI mice compared with sham-operated groups ($P < 0.01$) (Figure 5-2). In the MI-induced groups, the majority of the positive nuclei were located in the infarcted myocardium, whilst in the sham-operated groups, positive nuclei were largely scattered in the interstitium. These observations indicated that the majority of the newly synthesized DNA replicating cells are non-cardiomyocytes. Nevertheless, there was no difference in the number of BrdU-positive nuclei between the WT and $Mstn^{-/-}$ ligated mice, indicating that the lack of myostatin does not affect the number of replicating cells at 28 days post-MI.

5.3.3 Deletion of myostatin resulted in greater size of cardiomyocytes which did not change post-MI

The size of cardiomyocytes was increased in the absence of myostatin as measured by both the cross-sectional area and the minimal 'Feret's diameter ($P < 0.05$) (Figure 5-3). However, induction of MI did not result in an alteration in the size of cardiomyocytes within the groups, suggesting that further hypertrophy of the myocardium did not occur post-MI ($P = 0.2$). Microscopically, the integrity of the cardiomyocytes and cell-cell interaction were preserved in sham-operated mice while, in contrast, there was an obvious disarray of myocardial fibres and cellular infiltration seen in the myocardium of the MI-induced mice (Figure 5-4).

5.3.4 Absence of myostatin is associated with less fibrosis and with greater amount of viable myocardium in the peri-infarct region of the ventricle

Although the size of the infarct relative to the LV was similar between the genotypes, the hearts of $Mstn^{-/-}$ mice had less scar tissue and a greater amount of viable myocardium in the border region of the infarcted area compared with WT mice ($P < 0.05$) (Figure 5-5A). Microscopically, following MI, the amount of collagen (which stained red) was greater in the WT mice compared to $Mstn^{-/-}$ mice (Figure 5-5B). As a result, the number of viable cardiomyocytes (which stained brown) was proportionally greater in the peri-infarct region of the myocardium of the $Mstn^{-/-}$ mice as compared with that of the WT mice.

5.3.5 The α-SMA immunofluorescence positivity was a sensitive marker for identification of myofibroblasts

Immunofluorescence of α-SMA has been widely used as a marker of myofibroblasts. Although the immunofluorescence of α-SMA can be positive in blood vessels, the pattern of positivity is distinctly different from that of myofibroblasts with a distribution around a lumen that is surrounded by a layer of DAPI-positive endothelial cells. Interestingly, a similar amount of α-SMA immunofluorescence was observed in the blood vessels of all four groups ($P = 0.2$) and these area were excluded from the analysis. Importantly, an increase in the immunofluorescence of α-SMA was observed in the MI groups compared

to sham-operated controls, which corresponded to the infarcted zone ($P < 0.001$) (Figure 5-6). This is consistent with the understanding that myofibroblasts are only present in injured myocardium. The immunofluorescence of α-SMA in the ligated $Mstn^{-/-}$ mice tended to be lower compared with WT ligated mice, although statistical significance was not achieved ($P = 0.15$).

5.3.6 The reduction in fibrosis is not a result of an alteration in apoptosis, programmed necrosis or cellular survival

The immunointensity of anti-PARP-1 and cleaved caspase-3 antibodies were absent in the sham-operated mice, and was present in the peri-infarct region of the $Mstn^{-/-}$ and WT mice at 28 days post-MI (Figure 5-7 and Figure 5-8). The immunointensity was not different between the two groups, suggesting that absence of myostatin does not affect apoptosis or programmed necrosis at 28 days post-MI. On the other hand, the immunointensities of phospho-Akt^{t308} and phospho-Akt^{s473} were present in all four groups of mice, and a greater expression of phospho-Akt^{t308} was observed in the ligated mice compared to sham-operated controls ($P < 0.05$). However, no difference in the immunointensity of phospho-Akt^{t308} (and phosphor-Akt^{s473}) was observed between the two genotypes (Figure 5-9).

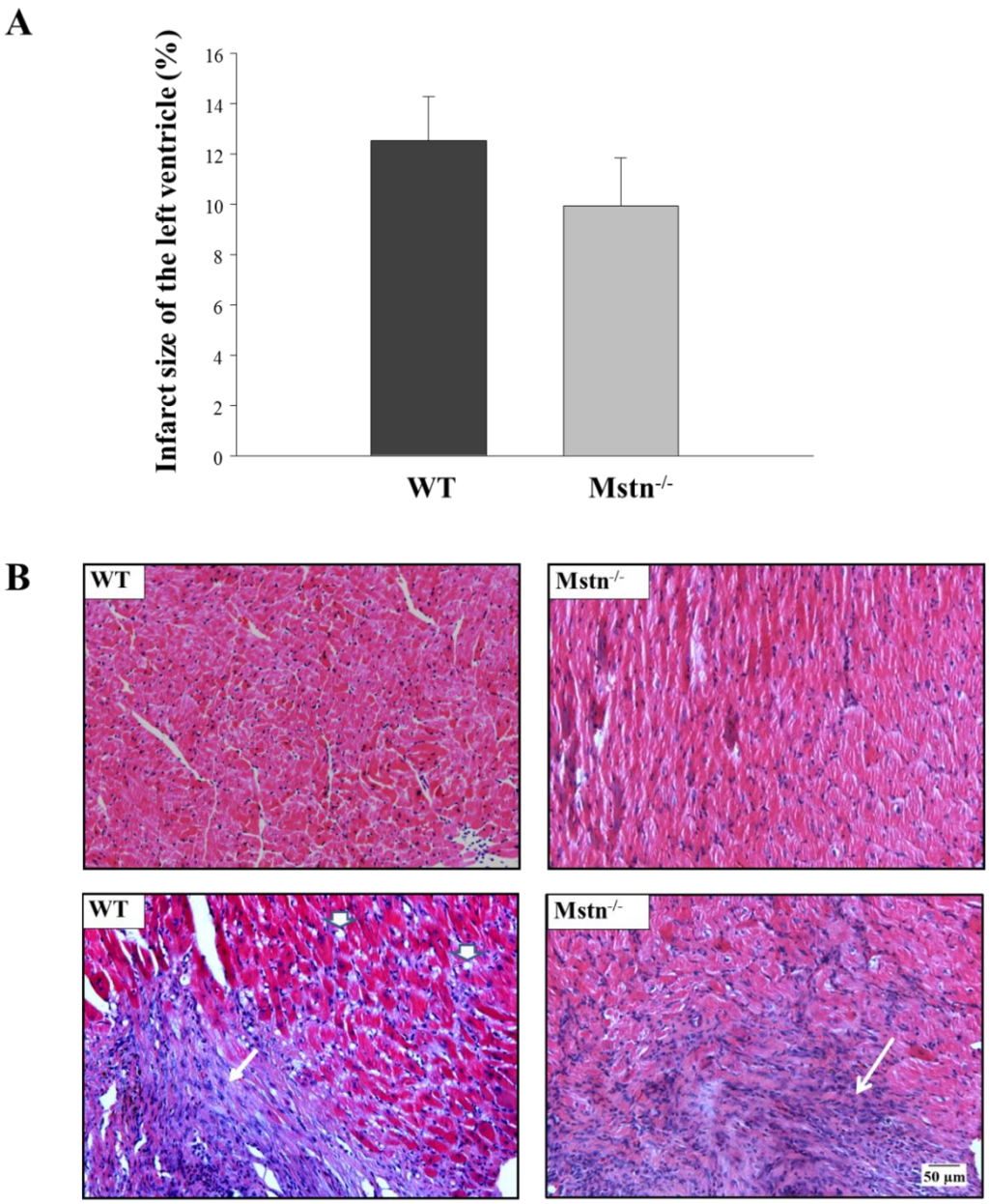

Figure 5-1. Size of the infarct of the left ventricle. (A) Percentage of infarct size between WT and Mstn$^{-/-}$ mice at day 28 post-MI. Data are presented as mean ± SEM. (B) Representative sections of sham-operated (upper panels) and MI (lower panels) obtained in the study. The increased in inflammatory infiltrates were present in the infarcted region of both the WT and Mstn$^{-/-}$ mice (arrows). Fat vacuoles were seen in the peri-infarct region of the representative WT animal (arrow heads) (H & E stain, 200x magnification)

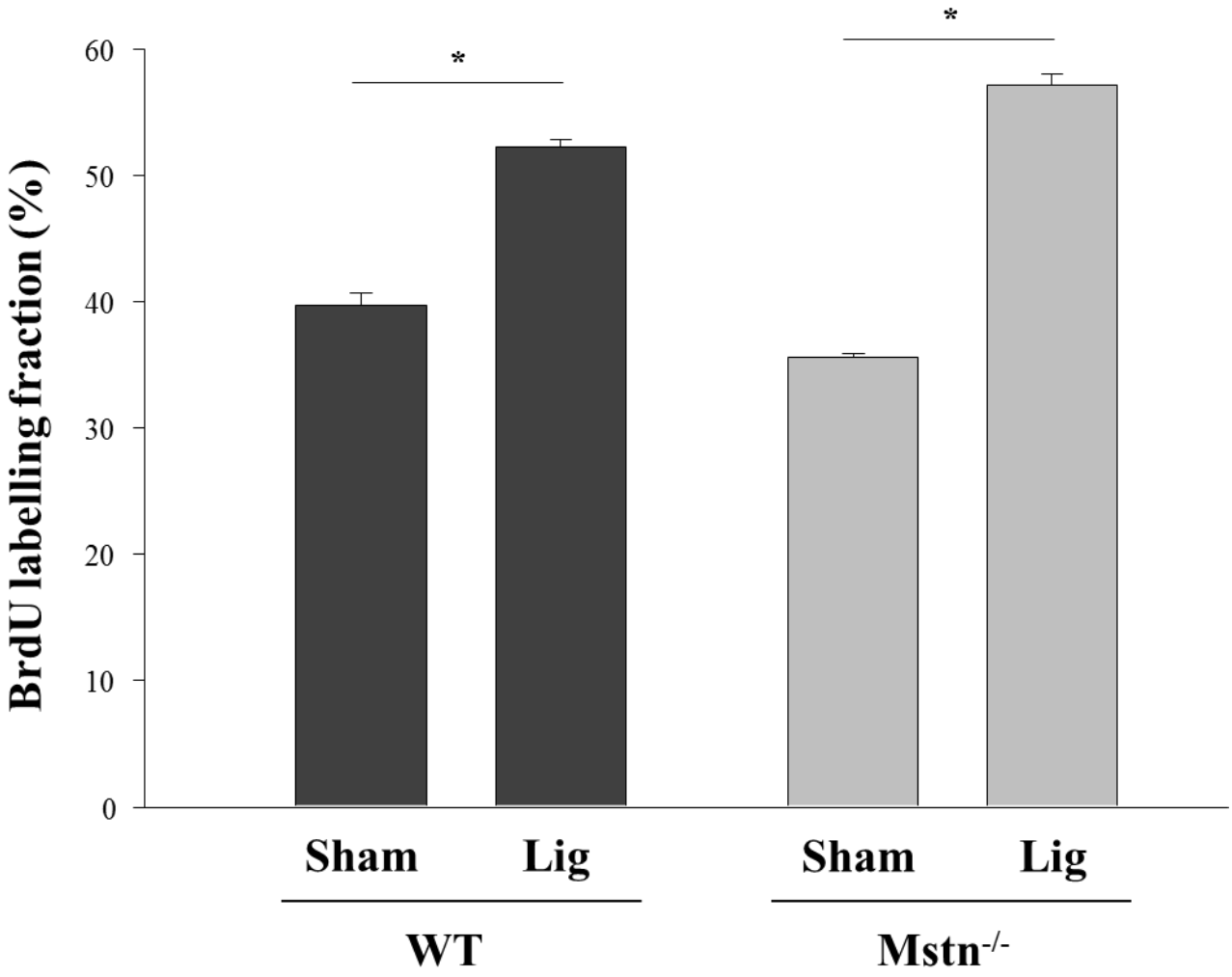

Figure 5-2. Percentage of BrdU positive nuclei (BrdU labelling fraction) in the border region of the infarcted ventricle. Data are presented as mean ± SEM ($^{*}P < 0.01$).

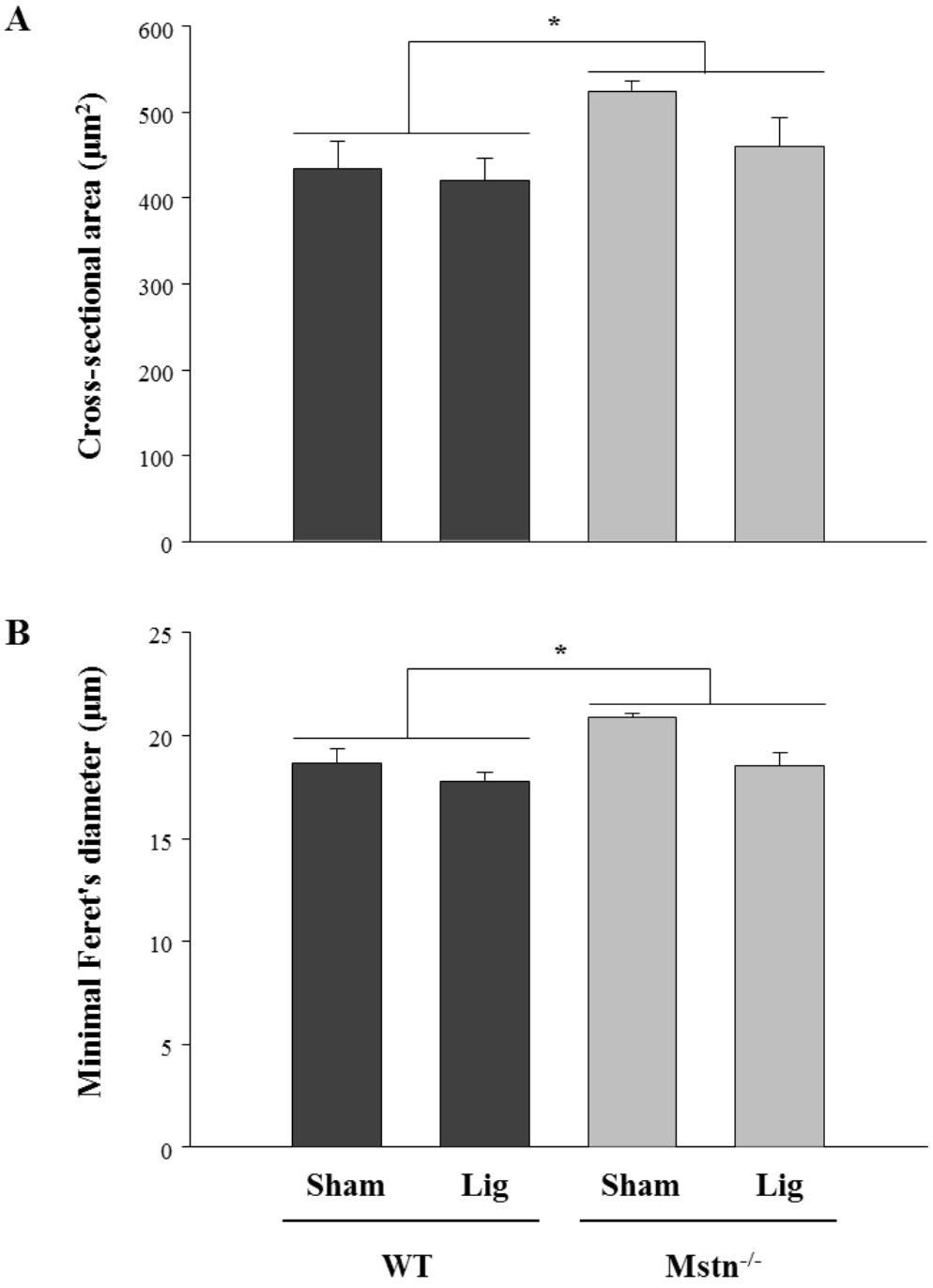

Figure 5-3. Size of the cardiomyocytes as measured by (A) cross-sectional area, and (B) minimal 'Feret's diameter'. Data are presented as mean ± SEM ($^{*}P < 0.05$)(See also Figure 5-4).

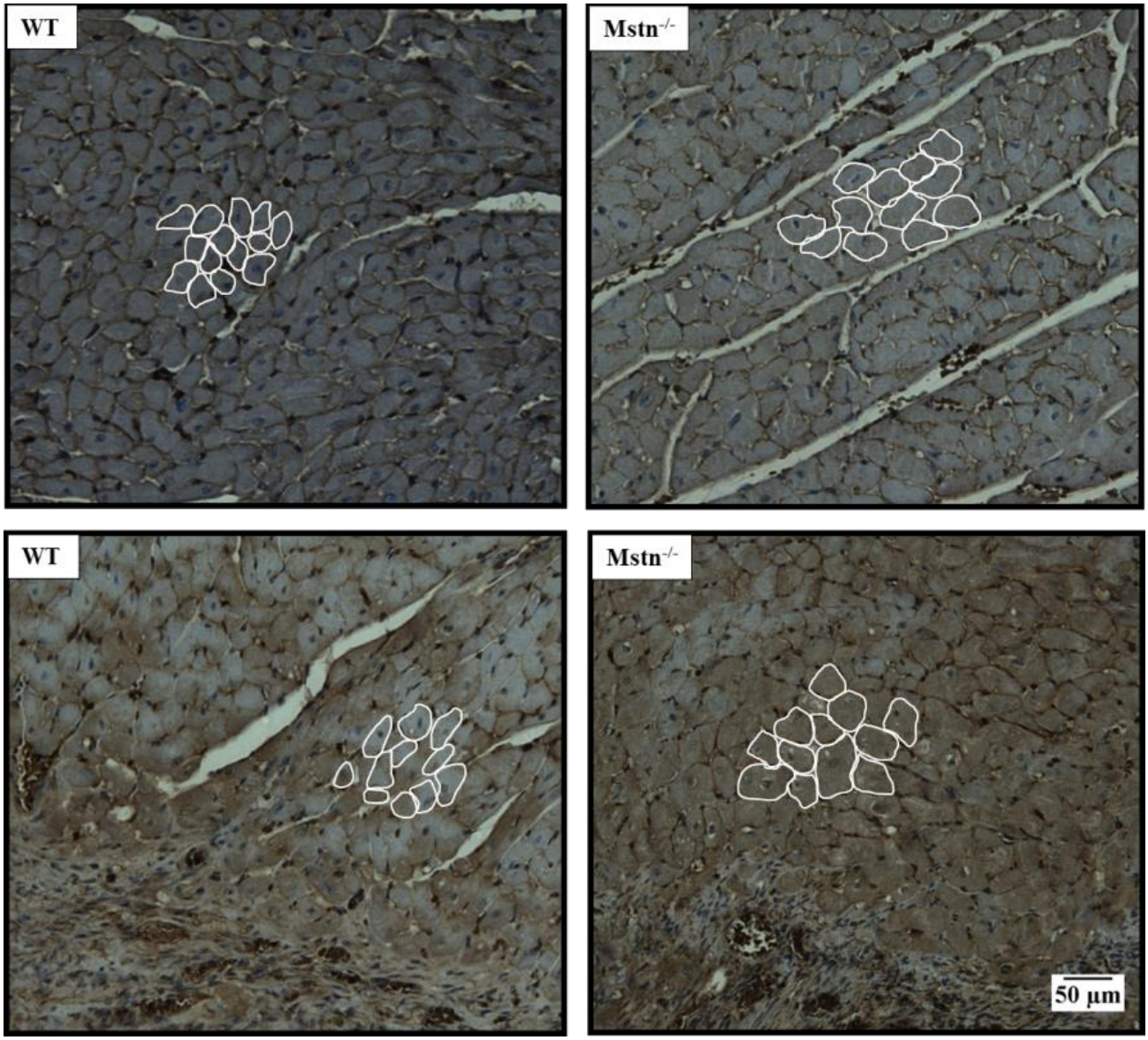

Figure 5-4. Representative sections of the cardiac tissue in sham-operated (upper panels) and MI (lower panels) mice which were stained with laminin to delineate the cell membrane of cardiomyocytes. Sections were counterstained with haematoxylin to visualise the nuclei. The size of cardiomyocytes were larger in $Mstn^{-/-}$ mice compared with WT mice, however, induction of MI did not change the size of cardiomyocytes within the groups (200x magnification)(see also Figure 5-3).

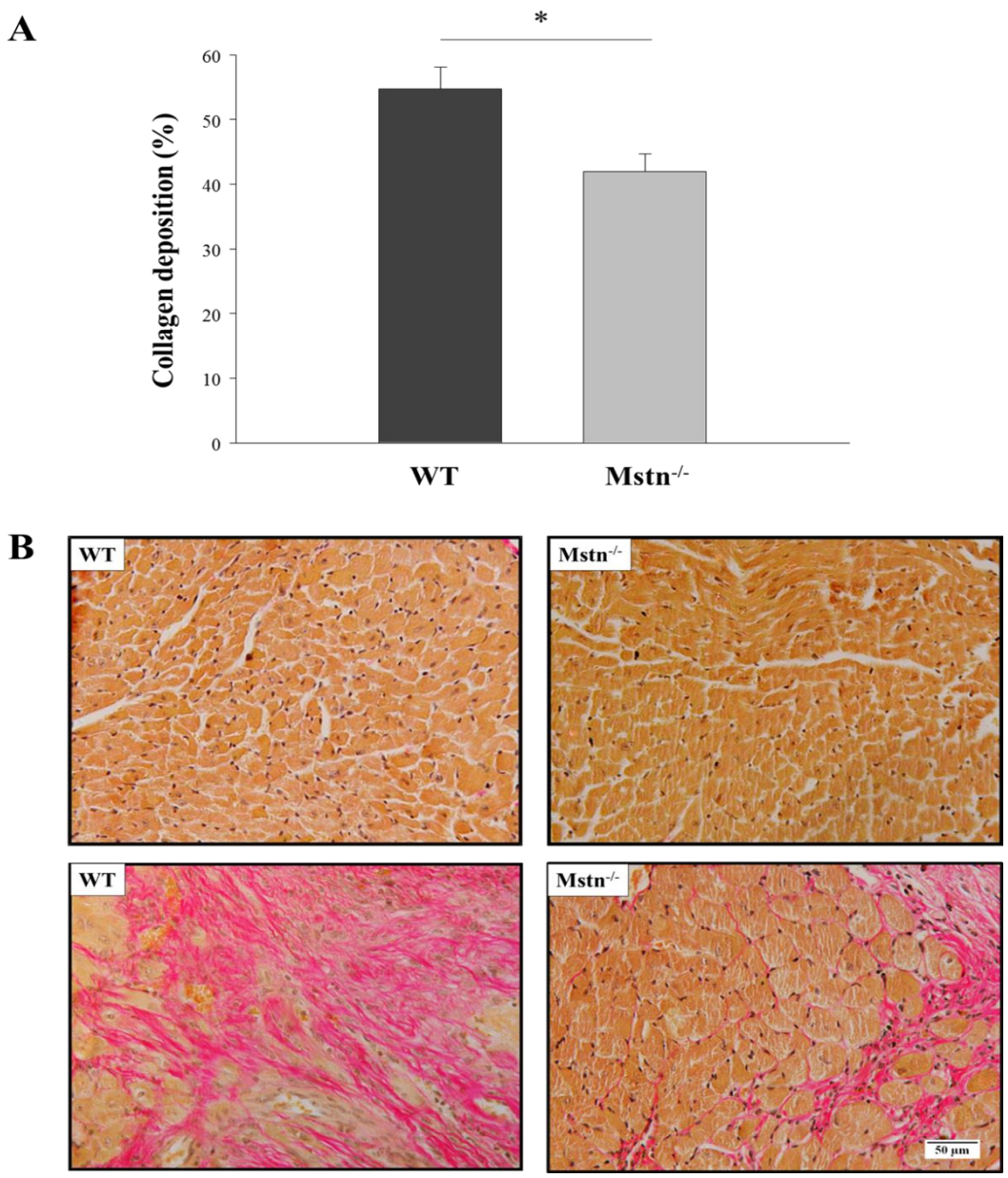

Figure 5-5. Collagen deposition in the infarcted left ventricle between Mstn$^{-/-}$ and WT mice. (A) Percentage of collagen deposition in the infarcted region relative to the peri-infarct area. Data are presented as mean ± SEM ($^{*}P < 0.05$). (B) Representative sections of the myocardium showing the deposition of collagen using Van Gieson staining in sham-operated (upper panels) and MI-induced (lower panels) mice. The collagen content (red) was absent in the sham animals, but significantly greater in the peri-infarct region of the WT mice, whilst more viable myocardium (brown) was present in Mstn$^{-/-}$ mice (200x magnification).

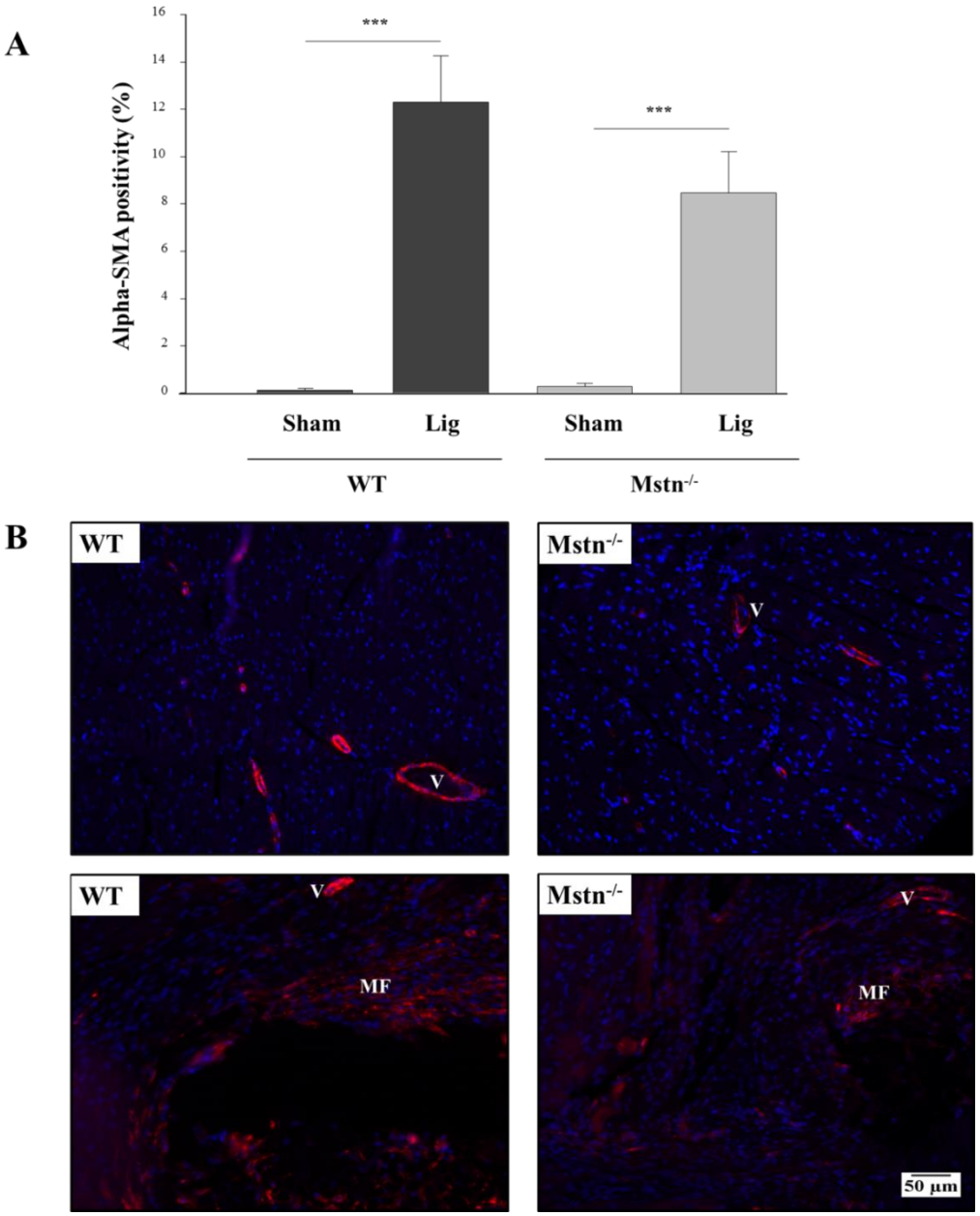

Figure 5-6. Immunofluorescence of alpha-smooth muscle actin (α-SMA) in the myocardium. (A) Percentage of cells expressing α-SMA immunofluorescence. Data are presented as mean ± SEM ($^{***}P < 0.001$). (B) Representative immunofluorescent sections of the cardiac tissue in sham-operated (upper panels) and MI-induced mice (lower panels) showing immune-positivity in the blood vessels (V) and myofibroblasts (MF) using α-SMA antibody. Note the increased in immunofluorescence in the MI-induced WT group (200x magnification)

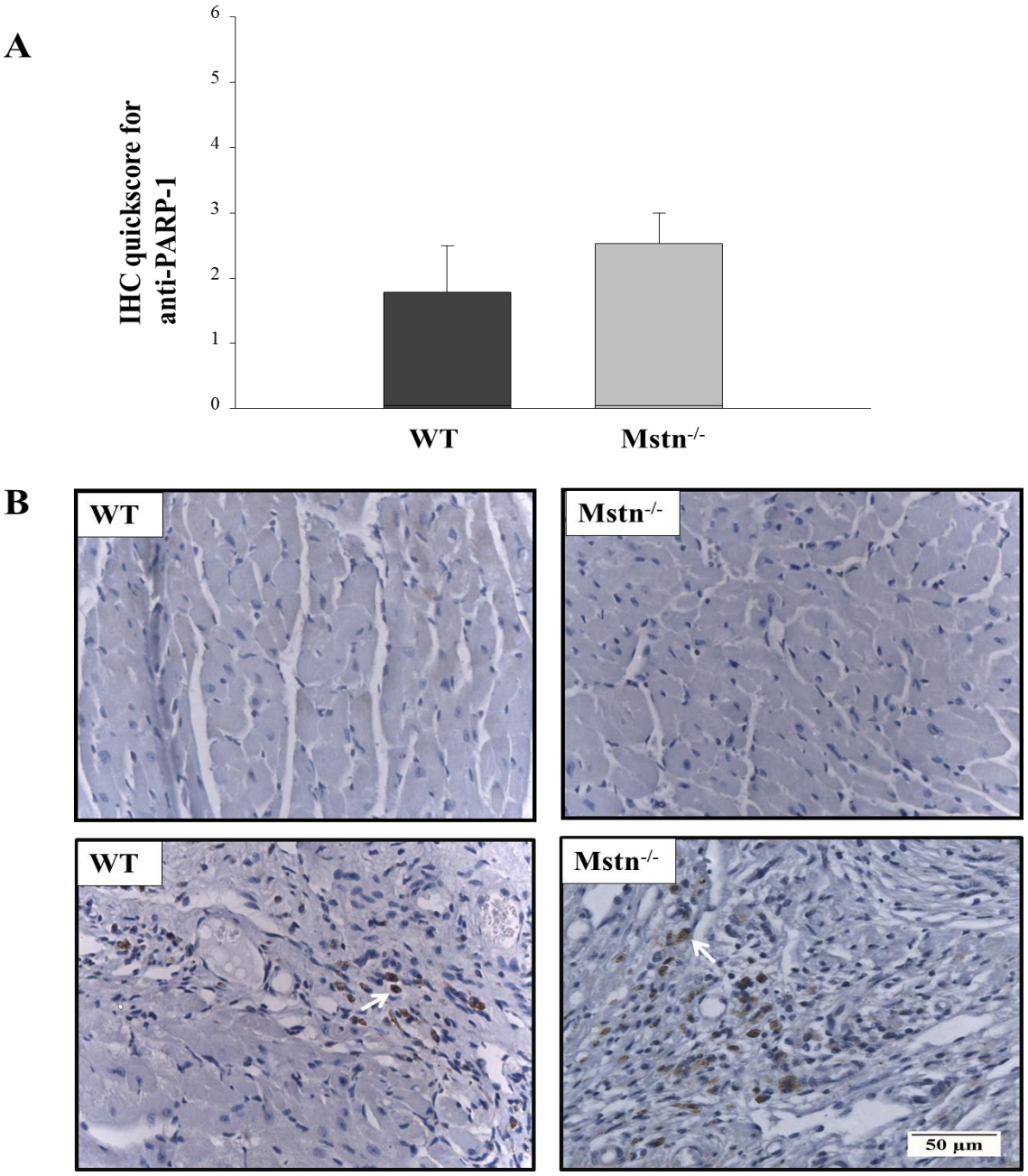

Figure 5-7. (A) Semiquantitative IHC analysis of the anti-PARP-1 antibody in the peri-infarct region of the WT and Mstn$^{-/-}$ mice post-MI. (B) Representative IHC sections of the cardiac tissue in sham-operated (upper panels) and MI-induced (lower panels) mice for anti-PARP-1 antibody. Note the nuclear localisation of the DAB-positive cells (arrows) in the MI groups but not the sham-operated animals (haematoxylin counterstaining, 400x magnification)

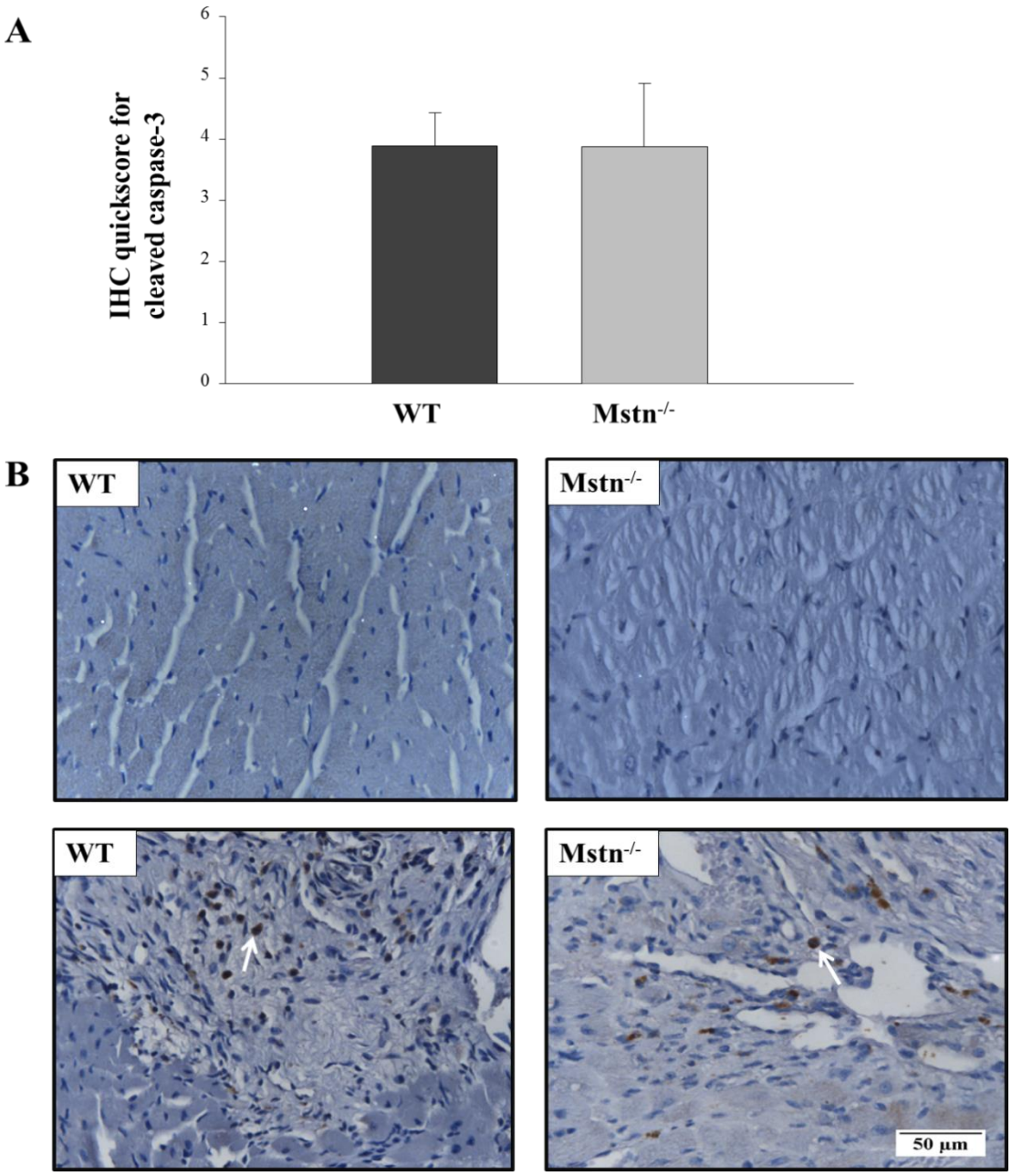

Figure 5-8. (A) Semiquantitative IHC analysis of the anti-cleaved caspase-3 antibody in the peri-infarct region of the WT and Mstn$^{-/-}$ mice post-MI. (B) Representative IHC sections of the cardiac tissue in sham-operated (upper panels) and MI-induced (lower panels) for anti-cleaved caspase-3 antibody. Immunointensity for cleaved caspase-3 was absent in sham animals and present in a similar intensity in MI-induced mice (arrows) (haematoxylin counterstaining, 400x magnification).

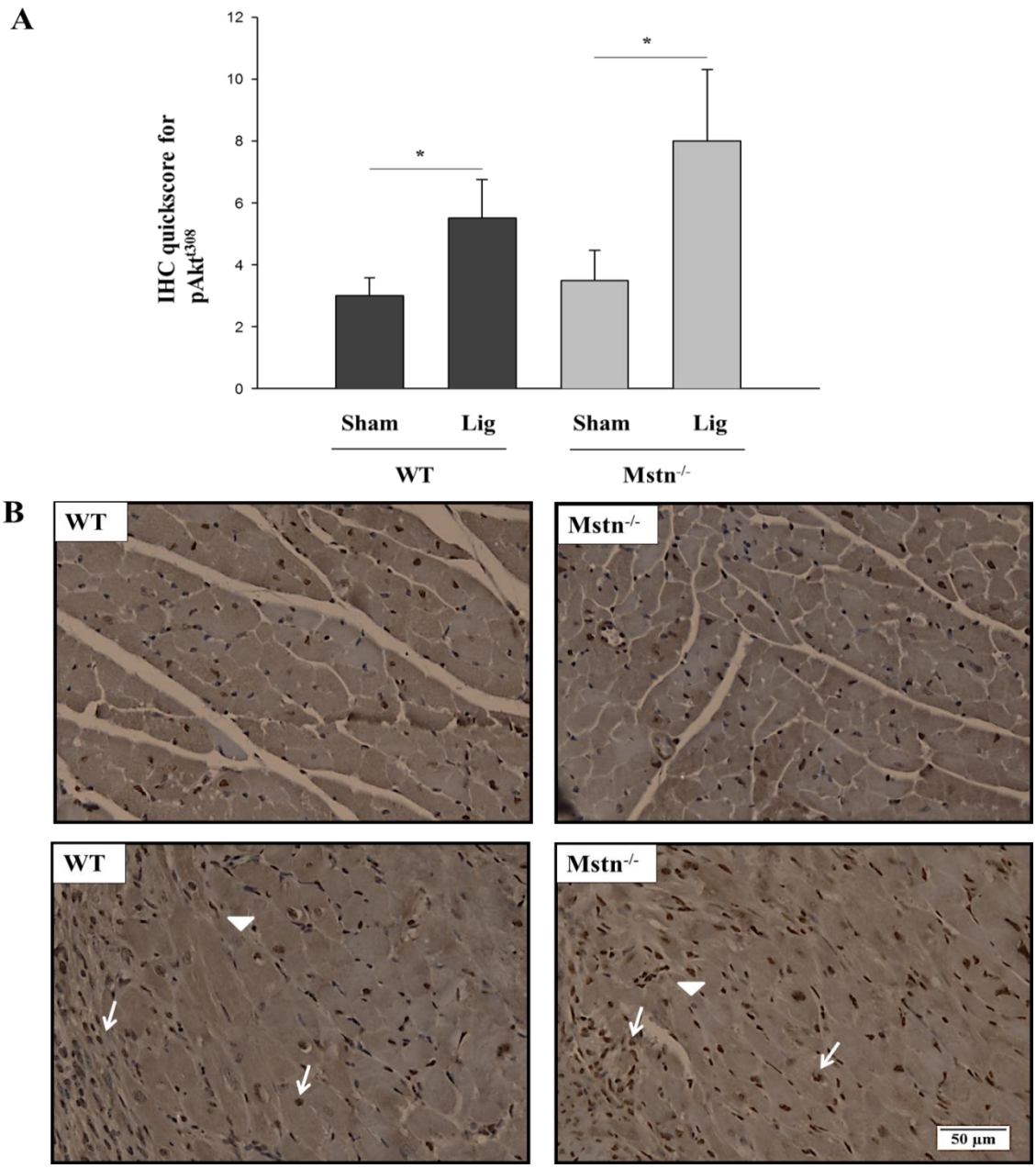

Figure 5-9. (A) Semiquantitative IHC analysis of the pAkt^{t308} antibody (*P < 0.05). (B) Representative IHC sections of the cardiac tissue in sham-operated (upper panels) and MI-induced (lower panels) mice post-surgery. DAB-positive cells were present in all groups of mice post-surgery (arrows). Sections were counterstained with haematoxylin to visualise the nuclei (arrow heads) (400x magnification).

5.4 Discussion

This chapter sought to explore the potential mechanism(s) which may have accounted for the clinical improvement seen in $Mstn^{-/-}$ mice at 28 days post-MI. By using semi-quantitative immunohistochemistry and immunofluorescence, it was shown that, while the size of the infarct was similar between the WT and $Mstn^{-/-}$ mice post-MI, the amount of collagen deposition was significantly less in the hearts of $Mstn^{-/-}$ mice. Furthermore, it can be speculated that this reduction in collagen is likely the result of a reduction in myofibroblasts in the $Mstn^{-/-}$ mice, although the level of significance was not achieved. In contrast, induction of MI did not alter the number and size of the cardiomyocytes, and there was no difference in apoptosis or cellular survival signalling between the two genotypes at 28 days post-MI.

Whilst cardiomyocytes account for at least 75% of the normal myocardial volume [165], they contribute to only 30% of the total cell numbers [166]. The remaining cells in the heart are non-cardiomyocytes, with cardiac fibroblasts being the most abundant cell type [113]. Cardiac fibroblasts are critical for the maintenance of homeostasis of the extracellular matrix [113]. In a diseased state such as ischaemia or MI, cardiac fibroblasts become a key player in the myocardial remodelling process by promoting excessive collagen deposition and/or inhibiting degradation at the site of the infarct through various cytokines and growth factors such as matrix metalloproteinases (MMPs) and TGF-β [167]. Once considered inert, an infarct scar is now regarded as living tissue with a population of terminally differentiated fibroblast-like cells known as the myofibroblasts, which are

nourished by a neovasculature, and whose function is to regulate the turnover of collagen and contraction of scar tissue [168]. The origin of myofibroblasts is debated, but their presence only in pathological wounds such as the infarcted myocardium together with the expression of α-SMA, have made them a specific class of cells distinguished from that of fibroblasts [169, 170]. Indeed, the current study has supported these findings by demonstrating that (1) α-SMA is expressed in myofibroblasts and not cardiac fibroblasts in general, and (2) positive expression is only found in injured myocardium, and not in sham-operated mice. Importantly, the current study has demonstrated that genetic deletion of the myostatin gene behaves in a similar manner to that of the WT controls with positive expression of myofibroblasts in infarcted cardiac tissue.

Upon injury, fibroblasts evolve firstly into proto-myofibroblasts and then into myofibroblasts under the influence of various growth factors, the most well-studied being TGF-β1 [169, 171]. It is widely accepted that TGF-β promotes formation of the extracellular matrix and is a potent stimulator of fibrosis, whilst inhibition of TGF-β leads to a reduction in collagen content and fibrosis [159, 172]. By using genetically knock-out mice, the current study confirms that inhibition of myostatin also resulted in a reduction in cardiac fibrosis, an effect consistent with other members of the TGF-β superfamily. Indeed, emerging evidence has shown that myostatin is pro-fibrotic in skeletal muscle [21, 173]. The mechanisms of the pro-fibrotic nature of myostatin in skeletal muscle have been proposed. Specifically, these include a direct stimulation of the proliferation of fibroblasts and expression of extracellular matrix proteins by myostatin [21], a switch to a fibrotic synthetic phenotype with intensive production of collagen to aid in the progression of

fibrosis [174], and an enhanced differentiation of fibroblasts to myofibroblasts [173]. It is also thought that a co-stimulatory relationship exists between TGF-β1 and myostatin in promoting the formation of fibrosis [173]. Using immunofluorescence, this study has demonstrated that the activity of α-SMA is induced in the infarcted cardiac tissue, and the level of α-SMA activity is lower in Mstn$^{-/-}$ mice, compared with WT mice post-MI, suggesting a lower amount of myofibroblasts in the Mstn$^{-/-}$ mice. Although a level of significance was not achieved, coupled with the reduction in collagen deposition observed in Mstn$^{-/-}$ mice, one could speculate that the absence of myostatin reduces the formation of fibrosis in the myocardium and most likely does so by preventing/reducing the differentiation of fibroblasts to myofibroblasts, an effect previously reported in skeletal muscle fibroblasts [173].

Several studies have previously reported variable results between cardiac fibrosis and myostatin [73, 123]. Morissette and colleagues reported a reduction in cardiac fibrosis in normal hearts of the senescent Mstn$^{-/-}$ mice compared with WT mice, although a mechanism for the reduction was not proposed [73]. Cohn and co-workers had shown that myostatin does not regulate cardiac hypertrophy or fibrosis in the double mutant *mdx*/Mstn$^{-/-}$ mice compared with *mdx* mice [123]. However, their study needs to be interpreted with caution. Firstly, the mean body weights of Mstn$^{-/-}$ and WT mice were similar (40.3 ± 2.1g vs 37.4 ± 0.9g) which is interesting, and may have explained the lack of difference between the size of cardiomyocytes and heart weight. Secondly, the assessment of collagen deposition was performed at rest, and this result may differ from that when the heart is stimulated under pathological conditions such MI. Thirdly, the

underlying mechanism for cardiac fibrosis in *mdx* mice or DMD may be different from that observed following myocardial ischaemia, and possibly accounts for the lack of difference in fibrosis between the groups. It is also possible that the severe cardiomyopathic changes in *mdx* mice circumvent the effects of the absence of myostatin in the heart and thereby, negate any possible benefit that the myostatin knockout imparts.

To examine if the absence of myostatin affects the size of the cardiomyocytes following cardiac surgery, cells were stained with laminin to delineate the cell membrane and the cross-sectional area and minimal 'Feret's diameter' of the cells were measured. Both parameters correlated well with each other and showed that the size of cardiomyocytes were greater in the absence of myostatin compared with WT mice, irrespective of whether the procedure was a sham operation or ligation of the LAD artery. This is consistent with the results from the earlier chapter demonstrating an increased in heart weight in the $Mstn^{-/-}$ mice, indicating that the increase in heart weight is likely due to the increase in the size of the cardiomyocytes. Importantly, a further increased in the size of cardiomyocytes was not observed post-MI suggesting the absence of a pathological hypertrophy of the myocardium.

To investigate if DNA synthesis was increased post-MI, the labelling fraction of BrdU was determined. Following thoracic cardiac surgery (sham or ligation of the LAD artery), BrdU-incorporation was increased in all groups of mice. However, the increased in BrdU-positive nuclei was significantly greater in the MI-induced mice, with the major positive distribution within the infarcted myocardium. In contrast, in the sham-operated mice,

BrdU-positive nuclei were mainly found in the interstitium of the myocardium. An earlier study had similarly reported an increased in BrdU labelling fraction in the non-infarcted septum and right ventricle of mice [153]. In rats following ligation of the LAD artery, a transient increased in the BrdU labelling fraction was observed mainly in the interstitium of the ventricles, indicating that the majority of the new DNA synthesising cells were non-cardiomyocytes, and by deduction, was likely to be fibroblasts and endothelial cells [175]. Although a detailed characterisation of the BrdU-positve cells was not performed in this study, the location of the positive cells also indicates that the majority of these cells are likely to be non-cardiomyocytes. Collectively, these data suggest that induction of MI does not alter the number and/or size of cardiomyocytes and that the clinical improvement seen in $Mstn^{-/-}$ mice is unlikely a change in the number and/or size of cardiomyocytes.

To determine if the restoration of cardiac function in $Mstn^{-/-}$ mice a result of the alteration in the pathways of cellular growth and apoptosis, immunohistochemistry was performed. While a previous study reported that Akt may lie down stream of the effects of myostatin [124], this study did not find any significant changes in the Akt pathway. Similarly, while reduction in post-infarct apoptosis has been shown to reduce the expansion of infarct in mechano-growth factor (a splice variant of IGF-1) [130], the immunointensity for cleaved caspase-3 was similar between the WT and $Mstn^{-/-}$ mice in this study. Taken together, it appears that the improvement in cardiac function in $Mstn^{-/-}$ mice is independent of an alteration in cellular growth and apoptosis pathway. However, it is possible that the effects of myostatin on these pathways occurs earlier on post-MI (i.e. during the early

hours or days post-MI) and a difference not observed at day 28 post-MI. It is likely that more studies are needed to provide further insight into these pathways.

In conclusion, the absence of myostatin improves cardiac function post-MI. The improvement is likely due to a reduction in the formation of cardiac fibrosis in the absence of myostatin. While a level of significance was not achieved, it is speculated that a reduction in the differentiation of fibroblasts to myofibroblasts in the absence of myostatin is the mechanism accounting for the reduction in the formation of cardiac fibrosis.

6

Final discussion

6.1 Discussion

In the introduction to this thesis, a hypothesis was developed, that "the absence of myostatin protects the heart against an acute MI". Using a murine model with a genetic deletion in the myostatin gene, and induction of an acute myocardial infarction by ligation of the LAD artery, the studies presented in this thesis support the proposed hypothesis.

In chapter one, an overview of myostatin, its receptors and signalling pathways were described. What is clear from literature is that myostatin, like other members of the TGF-β superfamily, is regulated at several levels. Moreover, myostatin shares similar serine/threonine transmembrane receptors and signalling pathways with other members of the TGF-β superfamily. These characteristics, which are common among this superfamily suggest that caution is needed when an inhibitor of myostatin is to be developed, in an attempt to reduce any undesirable effect of antagonising other growth factors. For instance, follistatin, while capable of blocking the activity of myostatin, is also able to inhibit the activities of activin and growth and differentiation factor-11 (GDF-11) [176]. Activin is critical in gonadal function and reproduction [177], whilst GDF-11 affects the development of pancreatic islet cells [178]. Therefore, it is prudent to develop a targeted antagonist that, in this case, reduces the activity of myostatin, but preserves that of activin and GDF-11.

Myostatin was initially discovered as a regulator of the development of skeletal muscle [11]. Naturally, the role of myostatin in skeletal muscle is better established. It is understood that an absence or a reduction in myostatin results in an increase in the mass of skeletal muscle [11]. Conversely, overexpression of myostatin causes wasting of skeletal muscle commonly seen in cachexia [27]. However, when it comes to the effects of myostatin on the function of skeletal muscle, the evidence is less clear, with conflicting and disproportionate effects reported [61-63]. Similarly, published data on longevity in the absence of myostatin is also lacking, although unpublished results from our group demonstrated no difference in lifespan between $Mstn^{-/-}$ and WT mice (n = 24 per genotype). Nonetheless, it appears that the absence of myostatin, while not correcting the underlying pathology of the skeletal muscle disorders, is capable of increasing the mass and strength of these illnesses [12, 14]. Moreover, mounting research has demonstrated a potential benefit of the absence of myostatin in organs other than skeletal muscle. The findings of two different pools of myostatin (i.e. local vs systemic) has further substantiated that the role of myostatin is broader than previously thought.

It is widely accepted that myostatin is expressed in the heart, but literature review in chapter one suggests that myostatin appears to have a minor physiological role in normal cardiac development. In a diseased state, however, the expression of myostatin is increased. The literature to date supports a role of myostatin in mediating cardiac cachexia, and likely contributes to the weight loss seen in chronic heart failure [128]. However, it was unclear if a decrease in the expression of myostatin would result in a

detectable improvement in cardiac function. It is with this in mind that led to the design of the current studies.

Chapter three addressed the presence of a dynamic change in the expression of myostatin mRNA in the peri-infarct cardiac tissue of the sheep following an acute MI. Importantly, an initial decline in the concentration of myostatin mRNA, which reached a nadir at day 1 post-MI, was observed before a progressive restoration to a concentration similar to non-infarcted controls at day eight post-MI. This reduction in the concentration of myostatin mRNA may represent an adaptive response to injury to facilitate the initial physiological hypertrophy of the myocardium commonly encountered during the early remodelling process of the left ventricle. This is a potentially important finding and suggests that if an effective antagonist to myostatin is to be developed and administered, it is possible that a dose given immediately post- and prior to day 1 post-MI will result in the maximum gain in efficacy. Further studies are warranted to support this theory.

Another observation derived from chapter three is the selective expression of the concentration of myostatin mRNA. A persistently low concentration of myostatin mRNA was observed in the distant viable part of the myocardium which was different from that observed in the peri-infarct region. In retrospect, it would have been useful to have measured the abundance of myostatin protein in order to establish a correlation between myostatin mRNA and protein. Nevertheless, this temporal relationship between the expression of myostatin mRNA and duration post-MI further increases our understanding of the role of myostatin.

Chapter four demonstrated the functional relevance of the absence of myostatin when an acute MI was induced in $Mstn^{-/-}$ mice and the findings compared with WT littermates. An increase in survival and an improvement in cardiac function post-MI were observed in the absence of myostatin, despite a similar size of infarct in the two groups. Mortality in WT mice occurred early and within the first 24 hr post-surgery (sham or ligation). This observation further supports earlier speculation that an inhibitor of myostatin, if given, is best administered within the first 24 hr post-MI. To date, several pharmaceutical companies have developed a number of inhibitors of myostatin, predominantly tested in Phase I/II trials and in patients with muscular dystrophy [64]. The concept of using myostatin inhibitors is also increasingly popular in the bodybuilding and sporting industry (albeit unlicenced) given the excessive muscle mass observed in the $Mstn^{-/-}$ mice and animals with a naturally mutation in the myostatin gene. However, the safety and efficacy of such inhibitors remain to be tested in large trials for clinical practice. Three distinct inhibitors of myostatin have been developed, all of which administered either subcutaneously or intravenously. Stamulumab or MYO-29 is the first neutralizing antibody to myostatin produced by Wyeth Pharmaceuticals [13]. A two-weekly intravenous injection of MYO-29 for six months was reported to be safe and well tolerated, but an improvement in strength and function was not observed in the study of patients with primary muscle diseases [13]. AMG-745 is a peptibody produced by Amgen [179]. A phase I clinical trial on AMG-745 was undertaken but results were not made public [180]. A subsequent phase II trial to evaluate the safety and efficacy of AMG-745 in humans with age-associated muscle loss was conducted in 2009, but was withdrawn by the investigators prior to enrolment [181]. The third inhibitor of myostatin, ACE-031, is a

soluble activin receptor type IIB produced by Acceleron Pharma [182]. A single subcutaneous dose of ACE-031 to healthy post-menopausal women was shown to be safe, and resulted in an increase in lean mass and muscle volume in the highest dose cohort (3mg/kg) compared with placebo [182]. However, an earlier trial with ACE-031 in boys with DMD was terminated due to minor adverse effects (e.g. nose and gum bleeding) (press release in Muscular Dystrophy Association) [183]. Collectively, these data indicate that while efforts in developing a safe inhibitor of myostatin remain disappointing to date, it is appreciated that the nature of trials involving experimental drugs are inherently risky. Therefore research is continuing to identify an effective and safe myostatin antagonist.

Other difference in the clinical outcomes measured in chapter four, including total body weight, heart rate, mean arterial pressure and left ventricular diameters, could be attributed to a genotypic effect (i.e. WT vs $Mstn^{-/-}$) and not a consequence of the MI. An additional control cohort (i.e. without open chest surgery) may have helped to clarify these differences. Moreover, ECG monitoring, which would have been useful, was unavailable at the time of the study to document the presence of arrhythmias. While using a 10MHz transducer is sufficient to obtain satisfactory 2D and M-mode echocardiographic analysis, a higher frequency transducer (eg. 15-25MHz) may have improved resolution and permitted more precise determination of the ventricular dimensions and volumes to be obtained. Despite these limitations, a beneficial effect of the absence of myostatin on cardiac function post-MI was documented in the current study. Future studies using a larger number of animals and incorporating an additional control cohort without having a thoracotomy will be important to confirm these findings.

In these studies, continuous ECG monitoring will be essential to monitor for any tachyarrhythmias that may occurs peri- and post-operatively.

Chapter five investigated the potential cellular mechanism(s) that might explain an improvement in cardiac function in the absence of myostatin. Histological examination of the cardiac sections confirmed a similar size of infarct (~ 11%) between the two groups of mice. While the size of infarct is not large, it was demonstrated that the amount of collagen deposition was significantly less in the $Mstn^{-/-}$ mice compared to WT mice, which suggested a reduction in cardiac fibrosis in the absence of myostatin. It is widely accepted that a specific class of fibroblasts, the myofibroblasts, are responsible for the formation of fibrosis in injured tissue including that of the myocardium. The current study highlighted that the effects of myostatin on cardiomyocytes and myofibroblasts differ from that of skeletal muscle. While the size of cardiomyocytes was greater in the absence of myostatin, induction of MI does not increase the size of cardiomyocytes further. The number of newly synthesized cells in the myocardium was similar between the groups following MI. Although the characteristics of the newly synthesized cells were not identified in this study, the distribution of the cells indicated the likely candidates were non-cardiomyocytes. This observation was at least in part supported by the *in vitro* studies by Morissette *et al.* which demonstrated that myostatin regulates the growth of cultured neonatal cardiomyocytes but does not affect the number of cardiomyocytes [124]. In contrast, while a level of significance was not achieved, the reduction in the immunointensity of α-SMA suggests that fewer myofibroblasts are activated following

MI in the absence of myostatin, which is likely contributed to the reduction in cardiac fibrosis.

Apoptosis and programmed necrosis of cardiomyocytes are thought to be two of the key phenomenon in cardiac diseases [184]. Signalling pathways such as cleaved-caspase-3 and poly(ADP-ribose) polymerase (PARP-1) involving in these processes were examined using immunohistochemistry. The lack of difference observed in these pathways between the groups was not unexpected, given that apoptosis and necrosis of cardiomyocytes tend to occur early following a cardiac injury [9]. It is also possible that other pathways or enzymes (eg. cellular Ca^{2+} concentrations, caspase 8 etc.) are involved which were not examined in this work. Similarly when the growth and survival factor Akt was examined, the greater immunointensity of $pAkt^{t308}$ was observed in the ligated animals with no difference observed between $Mstn^{-/-}$ and WT mice. Collectively, these data suggest that while cellular survival may be important in the early development of remodelling process, the role is less critical at 28 days post-MI when the formation of scar tissue and fibrosis becomes a more prominent feature. Nevertheless, studies in the future will need to focus on different time points post-MI (eg. from early hours through to three months post-MI) to delineate these differences. It will also be important to incorporate immunohistochemistry data with western blot analysis of the abundance of myostatin protein, and qPCR for quatification of myostatin mRNA for a more complete view of the role of myostatin post-MI. Given the mounting data on the role of myostatin in other organs, collection of tissues other than cardiac sections (eg. skeletal muscle, liver, serum)

between Mstn$^{-/-}$ and WT mice will likely increase our understanding of the pathophysiology of this growth factor.

6.2 Area of uncertainty

While the absence of myostatin appears beneficial and improves survival in mice following an acute MI, the long-term effects of the absence of myostatin are unclear. Specifically, it is unclear if a reduction in mortality will also be observed in chronic cardiac disorders. Furthermore, while the phenotype of the absence of myostatin has been examined in aging Mstn$^{-/-}$ mice [73, 74], it remains unclear if this translates to an enhanced longevity in these mice.

As discussed earlier, the inhibition of myostatin can be achieved at several levels, and a targeted post-natal inhibition of myostatin in the myocardium has yet to be developed. A cardiac-specific genetic deletion of myostatin is thought to play a role in the atrophy of skeletal muscle seen in heart failure, suggesting that cardiac myostatin contributed to the systemic pool of myostatin [38, 128]. However, it is unclear if this systemic effect is contributing to the cardiac cachexia observed in humans.

6.3 Conclusion

In conclusion, this work has added valuable insights into our current understanding of the effects of myostatin, or the absence of it, in the heart following an acute MI. While basic research takes years to progress to clinical research in humans, and that the effect of pre-natal deletion of myostatin in genetically knockout mice may be different from post-developmental inhibition of myostatin, this study has, at least in part, demonstrated that the absence of myostatin may be potentially beneficial to the heart post-MI. Further studies in this area are warranted and ongoing efforts to develop an effective antagonist to myostatin are worthwhile to serve as a potential effective adjunct to the current treatment of acute MI.

References

1. Mortality and Demographic Data 2009. Wellington: Ministry of Health. In; Ministry of Health 2012.
2. Hospital Events 2008/09 and 2009/10. Wellington: Ministry of Health. In; Ministry of Health 2012.
3. O'Gara PT, Kushner FG, Ascheim DD, Casey DE, Jr., Chung MK, de Lemos JA, et al. 2013 ACCF/AHA guideline for the management of ST-elevation myocardial infarction: executive summary: a report of the American College of Cardiology Foundation/American Heart Association Task Force on Practice Guidelines. Circulation 2013;127(4):529-55.
4. Rosengren A, Wilhelmsen L, Hagman M, Wedel H. Natural history of myocardial infarction and angina pectoris in a general population sample of middle-aged men: a 16-year follow-up of the Primary Prevention Study, Goteborg, Sweden. J Intern Med 1998;244(6):495-505.
5. Bui QT, Reddy VS, Jacobs JR, Begelman SM, Frederick PD, Miller DP, et al. Previous Myocardial Infarction as a Risk Factor for In-Hospital Cardiovascular Outcomes (from the National Registry of Myocardial Infarction 4 and 5). Am J Cardiol 2013.
6. Mosterd A, Hoes AW. Clinical epidemiology of heart failure. Heart 2007;93(9):1137-46.
7. Ross R. The pathogenesis of atherosclerosis: a perspective for the 1990s. Nature 1993;362(6423):801-9.
8. Frantz S, Bauersachs J, Ertl G. Post-infarct remodelling: contribution of wound healing and inflammation. Cardiovasc Res 2009;81(3):474-81.
9. Fraccarollo D, Galuppo P, Bauersachs J. Novel therapeutic approaches to post-infarction remodelling. Cardiovasc Res 2012;94(2):293-303.
10. Shah AM, Mann DL. In search of new therapeutic targets and strategies for heart failure: recent advances in basic science. Lancet 2011;378(9792):704-12.
11. McPherron AC, Lawler AM, Lee SJ. Regulation of skeletal muscle mass in mice by a new TGF-beta superfamily member. Nature 1997;387(6628):83-90.
12. Wagner KR, McPherron AC, Winik N, Lee SJ. Loss of myostatin attenuates severity of muscular dystrophy in mdx mice. Ann Neurol 2002;52(6):832-6.
13. Wagner KR, Fleckenstein JL, Amato AA, Barohn RJ, Bushby K, Escolar DM, et al. A phase I/IItrial of MYO-029 in adult subjects with muscular dystrophy. Ann Neurol 2008;63(5):561-71.

14. Bogdanovich S, Krag TO, Barton ER, Morris LD, Whittemore LA, Ahima RS, et al. Functional improvement of dystrophic muscle by myostatin blockade. Nature 2002;420(6914):418-21.
15. Holzbaur EL, Howland DS, Weber N, Wallace K, She Y, Kwak S, et al. Myostatin inhibition slows muscle atrophy in rodent models of amyotrophic lateral sclerosis. Neurobiol Dis 2006;23(3):697-707.
16. Sharma M, Kambadur R, Matthews KG, Somers WG, Devlin GP, Conaglen JV, et al. Myostatin, a transforming growth factor-beta superfamily member, is expressed in heart muscle and is upregulated in cardiomyocytes after infarct. J Cell Physiol 1999;180(1):1-9.
17. Tu P, Bhasin S, Hruz PW, Herbst KL, Castellani LW, Hua N, et al. Genetic disruption of myostatin reduces the development of proatherogenic dyslipidemia and atherogenic lesions in Ldlr null mice. Diabetes 2009;58(8):1739-48.
18. Lenk K, Schur R, Linke A, Erbs S, Matsumoto Y, Adams V, et al. Impact of exercise training on myostatin expression in the myocardium and skeletal muscle in a chronic heart failure model. Eur J Heart Fail 2009;11(4):342-8.
19. Shyu KG, Lu MJ, Wang BW, Sun HY, Chang H. Myostatin expression in ventricular myocardium in a rat model of volume-overload heart failure. Eur J Clin Invest 2006;36(10):713-9.
20. George I, Bish LT, Kamalakkannan G, Petrilli CM, Oz MC, Naka Y, et al. Myostatin activation in patients with advanced heart failure and after mechanical unloading. Eur J Heart Fail 2010;12(5):444-53.
21. Li ZB, Kollias HD, Wagner KR. Myostatin directly regulates skeletal muscle fibrosis. J Biol Chem 2008;283(28):19371-8.
22. Bo Li Z, Zhang J, Wagner KR. Inhibition of myostatin reverses muscle fibrosis through apoptosis. J Cell Sci 2012;125(Pt 17):3957-65.
23. Gonzalez-Cadavid NF, Taylor WE, Yarasheski K, Sinha-Hikim I, Ma K, Ezzat S, et al. Organization of the human myostatin gene and expression in healthy men and HIV-infected men with muscle wasting. Proc Natl Acad Sci U S A 1998;95(25):14938-43.
24. Patel K, Amthor H. The function of myostatin and strategies of myostatin blockade-new hope for therapies aimed at promoting growth of skeletal muscle. Neuromuscul Disord 2005;15(2):117-26.
25. Oldham JM, Osepchook CC, Jeanplong F, Falconer SJ, Matthews KG, Conaglen JV, et al. The decrease in mature myostatin protein in male skeletal muscle is developmentally regulated by growth hormone. J Physiol 2009;587(Pt 3):669-77.

26. Hill JJ, Davies MV, Pearson AA, Wang JH, Hewick RM, Wolfman NM, et al. The myostatin propeptide and the follistatin-related gene are inhibitory binding proteins of myostatin in normal serum. J Biol Chem 2002;277(43):40735-41.
27. Zimmers TA, Davies MV, Koniaris LG, Haynes P, Esquela AF, Tomkinson KN, et al. Induction of cachexia in mice by systemically administered myostatin. Science 2002;296(5572):1486-8.
28. McPherron AC, Lee SJ. Double muscling in cattle due to mutations in the myostatin gene. Proc Natl Acad Sci U S A 1997;94(23):12457-61.
29. Kambadur R, Sharma M, Smith TP, Bass JJ. Mutations in myostatin (GDF8) in double-muscled Belgian Blue and Piedmontese cattle. Genome Res 1997;7(9):910-6.
30. Mosher DS, Quignon P, Bustamante CD, Sutter NB, Mellersh CS, Parker HG, et al. A mutation in the myostatin gene increases muscle mass and enhances racing performance in heterozygote dogs. PLoS Genet 2007;3(5):e79.
31. Stinckens A, Luyten T, Bijttebier J, Van den Maagdenberg K, Dieltiens D, Janssens S, et al. Characterization of the complete porcine MSTN gene and expression levels in pig breeds differing in muscularity. Anim Genet 2008;39(6):586-96.
32. Johansen KA, Overturf K. Quantitative expression analysis of genes affecting muscle growth during development of rainbow trout(Oncorhynchus mykiss). Mar Biotechnol (NY) 2005;7(6):576-87.
33. Roberts SB, Goetz FW. Myostatin protein and RNA transcript levels in adult and developing brook trout. Mol Cell Endocrinol 2003;210(1-2):9-20.
34. Xu C, Wu G, Zohar Y, Du SJ. Analysis of myostatin gene structure, expression and function in zebrafish. J Exp Biol 2003;206(Pt 22):4067-79.
35. Schuelke M, Wagner KR, Stolz LE, Hubner C, Riebel T, Komen W, et al. Myostatin mutation associated with gross muscle hypertrophy in a child. N Engl J Med 2004;350(26):2682-8.
36. Lee SJ. Regulation of muscle mass by myostatin. Annu Rev Cell Dev Biol 2004;20:61-86.
37. Anderson SB, Goldberg AL, Whitman M. Identification of a novel pool of extracellular pro-myostatin in skeletal muscle. J Biol Chem 2008;283(11):7027-35.
38. Breitbart A, Auger-Messier M, Molkentin JD, Heineke J. Myostatin from the heart--local and systemic actions in cardiac failure and muscle wasting. Am J Physiol Heart Circ Physiol 2011.
39. Lee SJ, McPherron AC. Regulation of myostatin activity and muscle growth. Proc Natl Acad Sci U S A 2001;98(16):9306-11.

40. Thies RS, Chen T, Davies MV, Tomkinson KN, Pearson AA, Shakey QA, et al. GDF-8 propeptide binds to GDF-8 and antagonizes biological activity by inhibiting GDF-8 receptor binding. Growth Factors 2001;18(4):251-9.
41. Cash JN, Rejon CA, McPherron AC, Bernard DJ, Thompson TB. The structure of myostatin:follistatin 288: insights into receptor utilization and heparin binding. Embo J 2009;28(17):2662-76.
42. Newfeld SJ, Wisotzkey RG, Kumar S. Molecular evolution of a developmental pathway: phylogenetic analyses of transforming growth factor-beta family ligands, receptors and Smad signal transducers. Genetics 1999;152(2):783-95.
43. Attisano L, Wrana JL. Signal transduction by the TGF-beta superfamily. Science 2002;296(5573):1646-7.
44. Massague J. TGF-beta signal transduction. Annu Rev Biochem 1998;67:753-91.
45. Franzen P, ten Dijke P, Ichijo H, Yamashita H, Schulz P, Heldin CH, et al. Cloning of a TGF beta type I receptor that forms a heteromeric complex with the TGF beta type II receptor. Cell 1993;75(4):681-92.
46. Attisano L, Carcamo J, Ventura F, Weis FM, Massague J, Wrana JL. Identification of human activin and TGF beta type I receptors that form heteromeric kinase complexes with type II receptors. Cell 1993;75(4):671-80.
47. Massague J, Wotton D. Transcriptional control by the TGF-beta/Smad signaling system. EMBO J 2000;19(8):1745-54.
48. Rebbapragada A, Benchabane H, Wrana JL, Celeste AJ, Attisano L. Myostatin signals through a transforming growth factor beta-like signaling pathway to block adipogenesis. Mol Cell Biol 2003;23(20):7230-42.
49. Zhu X, Topouzis S, Liang LF, Stotish RL. Myostatin signaling through Smad2, Smad3 and Smad4 is regulated by the inhibitory Smad7 by a negative feedback mechanism. Cytokine 2004;26(6):262-72.
50. Wang BW, Chang H, Kuan P, Shyu KG. Angiotensin II activates myostatin expression in cultured rat neonatal cardiomyocytes via p38 MAP kinase and myocyte enhance factor 2 pathway. J Endocrinol 2008;197(1):85-93.
51. Bish LT, Morine KJ, Sleeper MM, Sweeney HL. Myostatin is upregulated following stress in an Erk-dependent manner and negatively regulates cardiomyocyte growth in culture and in a mouse model. PLoS One 2010;5(4):e10230.
52. Thomas M, Langley B, Berry C, Sharma M, Kirk S, Bass J, et al. Myostatin, a negative regulator of muscle growth, functions by inhibiting myoblast proliferation. J Biol Chem 2000;275(51):40235-43.

53. Taylor WE, Bhasin S, Artaza J, Byhower F, Azam M, Willard DH, Jr., et al. Myostatin inhibits cell proliferation and protein synthesis in C2C12 muscle cells. Am J Physiol Endocrinol Metab 2001;280(2):E221-8.
54. Rios R, Carneiro I, Arce VM, Devesa J. Myostatin regulates cell survival during C2C12 myogenesis. Biochem Biophys Res Commun 2001;280(2):561-6.
55. Langley B, Thomas M, Bishop A, Sharma M, Gilmour S, Kambadur R. Myostatin inhibits myoblast differentiation by down-regulating MyoD expression. J Biol Chem 2002;277(51):49831-40.
56. Megeney LA, Rudnicki MA. Determination versus differentiation and the MyoD family of transcription factors. Biochem Cell Biol 1995;73(9-10):723-32.
57. Joulia D, Bernardi H, Garandel V, Rabenoelina F, Vernus B, Cabello G. Mechanisms involved in the inhibition of myoblast proliferation and differentiation by myostatin. Exp Cell Res 2003;286(2):263-75.
58. Reisz-Porszasz S, Bhasin S, Artaza JN, Shen R, Sinha-Hikim I, Hogue A, et al. Lower skeletal muscle mass in male transgenic mice with muscle-specific overexpression of myostatin. Am J Physiol Endocrinol Metab 2003;285(4):E876-88.
59. Wheeler TL, Shackelford SD, Casas E, Cundiff LV, Koohmaraie M. The effects of Piedmontese inheritance and myostatin genotype on the palatability of longissimus thoracis, gluteus medius, semimembranosus, and biceps femoris. J Anim Sci 2001;79(12):3069-74.
60. Holmes JH, Ashmore CR, Robinson DW. Effects of stress on cattle with hereditary muscular hypertrophy. J Anim Sci 1973;36(4):684-94.
61. Whittemore LA, Song K, Li X, Aghajanian J, Davies M, Girgenrath S, et al. Inhibition of myostatin in adult mice increases skeletal muscle mass and strength. Biochem Biophys Res Commun 2003;300(4):965-71.
62. Personius KE, Jayaram A, Krull D, Brown R, Xu T, Han B, et al. Grip force, EDL contractile properties, and voluntary wheel running after postdevelopmental myostatin depletion in mice. J Appl Physiol (1985) 2010;109(3):886-94.
63. Amthor H, Macharia R, Navarrete R, Schuelke M, Brown SC, Otto A, et al. Lack of myostatin results in excessive muscle growth but impaired force generation. Proc Natl Acad Sci U S A 2007;104(6):1835-40.
64. Wagner KR. Clinical applications of myostatin inhibitors for neuromuscular diseases. Immunology, endocrine & metabolic agents - medicinal chemistry 2010;10(4):204-210.

65. Bish LT, Sleeper MM, Forbes SC, Morine KJ, Reynolds C, Singletary GE, et al. Long-term systemic myostatin inhibition via liver-targeted gene transfer in golden retriever muscular dystrophy. Hum Gene Ther 2011;22(12):1499-509.
66. Parsons SA, Millay DP, Sargent MA, McNally EM, Molkentin JD. Age-dependent effect of myostatin blockade on disease severity in a murine model of limb-girdle muscular dystrophy. Am J Pathol 2006;168(6):1975-85.
67. Li ZF, Shelton GD, Engvall E. Elimination of myostatin does not combat muscular dystrophy in dy mice but increases postnatal lethality. Am J Pathol 2005;166(2):491-7.
68. Ohsawa Y, Hagiwara H, Nakatani M, Yasue A, Moriyama K, Murakami T, et al. Muscular atrophy of caveolin-3-deficient mice is rescued by myostatin inhibition. J Clin Invest 2006;116(11):2924-34.
69. Bogdanovich S, McNally EM, Khurana TS. Myostatin blockade improves function but not histopathology in a murine model of limb-girdle muscular dystrophy 2C. Muscle Nerve 2008;37(3):308-16.
70. Krivickas LS, Walsh R, Amato AA. Single muscle fiber contractile properties in adults with muscular dystrophy treated with MYO-029. Muscle Nerve 2009;39(1):3-9.
71. Muscaritoli M, Anker SD, Argiles J, Aversa Z, Bauer JM, Biolo G, et al. Consensus definition of sarcopenia, cachexia and pre-cachexia: joint document elaborated by Special Interest Groups (SIG) "cachexia-anorexia in chronic wasting diseases" and "nutrition in geriatrics". Clin Nutr 2010;29(2):154-9.
72. Lang T, Streeper T, Cawthon P, Baldwin K, Taaffe DR, Harris TB. Sarcopenia: etiology, clinical consequences, intervention, and assessment. Osteoporos Int 2010;21(4):543-59.
73. Morissette MR, Stricker JC, Rosenberg MA, Buranasombati C, Levitan EB, Mittleman MA, et al. Effects of myostatin deletion in aging mice. Aging Cell 2009;8(5):573-83.
74. Jackson MF, Luong D, Vang DD, Garikipati DK, Stanton JB, Nelson OL, et al. The aging myostatin null phenotype: reduced adiposity, cardiac hypertrophy, enhanced cardiac stress response, and sexual dimorphism. J Endocrinol 2012;213(3):263-75.
75. Kawada S, Tachi C, Ishii N. Content and localization of myostatin in mouse skeletal muscles during aging, mechanical unloading and reloading. J Muscle Res Cell Motil 2001;22(8):627-33.
76. Haddad F, Adams GR. Aging-sensitive cellular and molecular mechanisms associated with skeletal muscle hypertrophy. J Appl Physiol 2006;100(4):1188-203.
77. Leger B, Derave W, De Bock K, Hespel P, Russell AP. Human sarcopenia reveals an increase in SOCS-3 and myostatin and a reduced efficiency of Akt phosphorylation. Rejuvenation Res 2008;11(1):163-175B.

78. Raue U, Slivka D, Jemiolo B, Hollon C, Trappe S. Myogenic gene expression at rest and after a bout of resistance exercise in young (18-30 yr) and old (80-89 yr) women. J Appl Physiol 2006;101(1):53-9.
79. Welle S, Bhatt K, Shah B, Thornton C. Insulin-like growth factor-1 and myostatin mRNA expression in muscle: comparison between 62-77 and 21-31 yr old men. Exp Gerontol 2002;37(6):833-9.
80. Yarasheski KE, Bhasin S, Sinha-Hikim I, Pak-Loduca J, Gonzalez-Cadavid NF. Serum myostatin-immunoreactive protein is increased in 60-92 year old women and men with muscle wasting. J Nutr Health Aging 2002;6(5):343-8.
81. Lakshman KM, Bhasin S, Corcoran C, Collins-Racie LA, Tchistiakova L, Forlow SB, et al. Measurement of myostatin concentrations in human serum: Circulating concentrations in young and older men and effects of testosterone administration. Mol Cell Endocrinol 2009;302(1):26-32.
82. LeBrasseur NK, Schelhorn TM, Bernardo BL, Cosgrove PG, Loria PM, Brown TA. Myostatin inhibition enhances the effects of exercise on performance and metabolic outcomes in aged mice. J Gerontol A Biol Sci Med Sci 2009;64(9):940-8.
83. Siriett V, Salerno MS, Berry C, Nicholas G, Bower R, Kambadur R, et al. Antagonism of myostatin enhances muscle regeneration during sarcopenia. Mol Ther 2007;15(8):1463-70.
84. Evans WJ, Morley JE, Argiles J, Bales C, Baracos V, Guttridge D, et al. Cachexia: a new definition. Clin Nutr 2008;27(6):793-9.
85. Morley JE, Thomas DR, Wilson MM. Cachexia: pathophysiology and clinical relevance. Am J Clin Nutr 2006;83(4):735-43.
86. Sharma R, Anker S. First Cachexia Symposium, Berlin, Germany, 1st-2nd December, 2000. Eur J Heart Fail 2001;3(6):751-4.
87. Anker SD, Ponikowski P, Varney S, Chua TP, Clark AL, Webb-Peploe KM, et al. Wasting as independent risk factor for mortality in chronic heart failure. Lancet 1997;349(9058):1050-3.
88. Dewys WD, Begg C, Lavin PT, Band PR, Bennett JM, Bertino JR, et al. Prognostic effect of weight loss prior to chemotherapy in cancer patients. Eastern Cooperative Oncology Group. Am J Med 1980;69(4):491-7.
89. Hoenig MR. Hypothesis: myostatin is a mediator of cardiac cachexia. Int J Cardiol 2008;124(2):131-3.

90. McFarlane C, Plummer E, Thomas M, Hennebry A, Ashby M, Ling N, et al. Myostatin induces cachexia by activating the ubiquitin proteolytic system through an NF-kappaB-independent, FoxO1-dependent mechanism. J Cell Physiol 2006;209(2):501-14.
91. McPherron AC, Lee SJ. Suppression of body fat accumulation in myostatin-deficient mice. J Clin Invest 2002;109(5):595-601.
92. Hamrick MW, Pennington C, Webb CN, Isales CM. Resistance to body fat gain in 'double-muscled' mice fed a high-fat diet. Int J Obes (Lond) 2006;30(5):868-70.
93. Wilkes JJ, Lloyd DJ, Gekakis N. Loss-of-function mutation in myostatin reduces tumor necrosis factor alpha production and protects liver against obesity-induced insulin resistance. Diabetes 2009;58(5):1133-43.
94. Milan G, Dalla Nora E, Pilon C, Pagano C, Granzotto M, Manco M, et al. Changes in muscle myostatin expression in obese subjects after weight loss. J Clin Endocrinol Metab 2004;89(6):2724-7.
95. Guo T, Jou W, Chanturiya T, Portas J, Gavrilova O, McPherron AC. Myostatin inhibition in muscle, but not adipose tissue, decreases fat mass and improves insulin sensitivity. PLoS One 2009;4(3):e4937.
96. Kim WK, Choi HR, Park SG, Ko Y, Bae KH, Lee SC. Myostatin inhibits brown adipocyte differentiation via regulation of Smad3-mediated beta-catenin stabilization. Int J Biochem Cell Biol 2012;44(2):327-34.
97. Seale P, Lazar MA. Brown fat in humans: turning up the heat on obesity. Diabetes 2009;58(7):1482-4.
98. Vijgen GH, Bouvy ND, Teule GJ, Brans B, Schrauwen P, van Marken Lichtenbelt WD. Brown adipose tissue in morbidly obese subjects. PLoS One 2011;6(2):e17247.
99. Brandt C, Nielsen AR, Fischer CP, Hansen J, Pedersen BK, Plomgaard P. Plasma and muscle myostatin in relation to type 2 diabetes. PLoS One 2012;7(5):e37236.
100. Wang F, Liao Y, Li X, Ren C, Cheng C, Ren Y. Increased circulating myostatin in patients with type 2 diabetes mellitus. J Huazhong Univ Sci Technolog Med Sci 2012;32(4):534-9.
101. Doyle F, Brown J, Lachance C. Relation between bone mass and muscle weight. Lancet 1970;1(7643):391-3.
102. Hamrick MW, McPherron AC, Lovejoy CO. Bone mineral content and density in the humerus of adult myostatin-deficient mice. Calcif Tissue Int 2002;71(1):63-8.
103. Hamrick MW. Increased bone mineral density in the femora of GDF8 knockout mice. Anat Rec A Discov Mol Cell Evol Biol 2003;272(1):388-91.

104. Kellum E, Starr H, Arounleut P, Immel D, Fulzele S, Wenger K, et al. Myostatin (GDF-8) deficiency increases fracture callus size, Sox-5 expression, and callus bone volume. Bone 2009;44(1):17-23.
105. Teixeira R, Goncalves L, Gersh B. Acute myocardial infarction - historical notes. Int J Cardiol 2013.
106. Nikus KC, Eskola MJ, Virtanen VK, Harju J, Huhtala H, Mikkelsson J, et al. Mortality of patients with acute coronary syndromes still remains high: a follow-up study of 1188 consecutive patients admitted to a university hospital. Ann Med 2007;39(1):63-71.
107. ICD-10 Classification. In; 2010.
108. Nabel EG, Braunwald E. A tale of coronary artery disease and myocardial infarction. N Engl J Med 2012;366(1):54-63.
109. Pfeffer MA, Braunwald E. Ventricular remodeling after myocardial infarction. Experimental observations and clinical implications. Circulation 1990;81(4):1161-72.
110. Sutton MG, Sharpe N. Left ventricular remodeling after myocardial infarction: pathophysiology and therapy. Circulation 2000;101(25):2981-8.
111. Erlebacher JA, Weiss JL, Eaton LW, Kallman C, Weisfeldt ML, Bulkley BH. Late effects of acute infarct dilation on heart size: a two dimensional echocardiographic study. Am J Cardiol 1982;49(5):1120-6.
112. Theroux P, Ross J, Jr., Franklin D, Covell JW, Bloor CM, Sasayama S. Regional myocardial function and dimensions early and late after myocardial infarction in the unanesthetized dog. Circ Res 1977;40(2):158-65.
113. Camelliti P, Borg TK, Kohl P. Structural and functional characterisation of cardiac fibroblasts. Cardiovasc Res 2005;65(1):40-51.
114. Porter KE, Turner NA. Cardiac fibroblasts: at the heart of myocardial remodeling. Pharmacol Ther 2009;123(2):255-78.
115. van den Borne SW, Diez J, Blankesteijn WM, Verjans J, Hofstra L, Narula J. Myocardial remodeling after infarction: the role of myofibroblasts. Nat Rev Cardiol 2010;7(1):30-7.
116. Ostbye TK, Galloway TF, Nielsen C, Gabestad I, Bardal T, Andersen O. The two myostatin genes of Atlantic salmon (Salmo salar) are expressed in a variety of tissues. Eur J Biochem 2001;268(20):5249-57.
117. Rescan PY, Jutel I, Ralliere C. Two myostatin genes are differentially expressed in myotomal muscles of the trout (Oncorhynchus mykiss). J Exp Biol 2001;204(Pt 20):3523-9.

118. Kubota K, Sato F, Aramaki S, Soh T, Yamauchi N, Hattori MA. Ubiquitous expression of myostatin in chicken embryonic tissues: its high expression in testis and ovary. Comp Biochem Physiol A Mol Integr Physiol 2007;148(3):550-5.
119. McKoy G, Bicknell KA, Patel K, Brooks G. Developmental expression of myostatin in cardiomyocytes and its effect on foetal and neonatal rat cardiomyocyte proliferation. Cardiovasc Res 2007;74(2):304-12.
120. Torrado M, Iglesias R, Nespereira B, Mikhailov AT. Identification of candidate genes potentially relevant to chamber-specific remodeling in postnatal ventricular myocardium. J Biomed Biotechnol;2010:603159.
121. Artaza JN, Reisz-Porszasz S, Dow JS, Kloner RA, Tsao J, Bhasin S, et al. Alterations in myostatin expression are associated with changes in cardiac left ventricular mass but not ejection fraction in the mouse. J Endocrinol 2007;194(1):63-76.
122. Rodgers BD, Interlichia JP, Garikipati DK, Mamidi R, Chandra M, Nelson OL, et al. Myostatin represses physiological hypertrophy of the heart and excitation-contraction couping. J Physiol 2009.
123. Cohn RD, Liang HY, Shetty R, Abraham T, Wagner KR. Myostatin does not regulate cardiac hypertrophy or fibrosis. Neuromuscul Disord 2007;17(4):290-6.
124. Morissette MR, Cook SA, Foo S, McKoy G, Ashida N, Novikov M, et al. Myostatin regulates cardiomyocyte growth through modulation of Akt signaling. Circ Res 2006;99(1):15-24.
125. Mahmoudabady M, Mathieu M, Dewachter L, Hadad I, Ray L, Jespers P, et al. Activin-A, transforming growth factor-beta, and myostatin signaling pathway in experimental dilated cardiomyopathy. J Card Fail 2008;14(8):703-9.
126. Gruson D, Ahn SA, Ketelslegers JM, Rousseau MF. Increased plasma myostatin in heart failure. Eur J Heart Fail 2011;13:734-6.
127. Lenk K, Erbs S, Hollriegel R, Beck E, Linke A, Gielen S, et al. Exercise training leads to a reduction of elevated myostatin levels in patients with chronic heart failure. Eur J Prev Cardiol 2011;19(3):404-11.
128. Heineke J, Auger-Messier M, Xu J, Sargent M, York A, Welle S, et al. Genetic deletion of myostatin from the heart prevents skeletal muscle atrophy in heart failure. Circulation 2010;121(3):419-25.
129. Anker SD, Negassa A, Coats AJ, Afzal R, Poole-Wilson PA, Cohn JN, et al. Prognostic importance of weight loss in chronic heart failure and the effect of treatment with angiotensin-converting-enzyme inhibitors: an observational study. Lancet 2003;361(9363):1077-83.

130. Carpenter V, Matthews K, Devlin G, Stuart S, Jensen J, Conaglen J, et al. Mechano-growth factor reduces loss of cardiac function in acute myocardial infarction. Heart Lung Circ 2008;17(1):33-9.
131. Ellmers LJ, Scott NJ, Medicherla S, Pilbrow AP, Bridgman PG, Yandle TG, et al. Transforming growth factor-beta blockade down-regulates the renin-angiotensin system and modifies cardiac remodeling after myocardial infarction. Endocrinology 2008;149(11):5828-34.
132. Arras M, Autenried P, Rettich A, Spaeni D, Rulicke T. Optimization of intraperitoneal injection anesthesia in mice: drugs, dosages, adverse effects, and anesthesia depth. Comp Med 2001;51(5):443-56.
133. Salto-Tellez M, Yung Lim S, El-Oakley RM, Tang TP, ZA AL, Lim SK. Myocardial infarction in the C57BL/6J mouse: a quantifiable and highly reproducible experimental model. Cardiovasc Pathol 2004;13(2):91-7.
134. Michael LH, Entman ML, Hartley CJ, Youker KA, Zhu J, Hall SR, et al. Myocardial ischemia and reperfusion: a murine model. Am J Physiol 1995;269(6 Pt 2):H2147-54.
135. Kengne AP, Czernichow S, Huxley R, Grobbee D, Woodward M, Neal B, et al. Blood pressure variables and cardiovascular risk: new findings from ADVANCE. Hypertension 2009;54(2):399-404.
136. Safar ME. Pulse pressure in essential hypertension: clinical and therapeutical implications. J Hypertens 1989;7(10):769-76.
137. Anderson B. Echocardiography - the normal examination and echocardiographic measurements.: MGA Graphics, Australia; 2000.
138. Collins KA, Korcarz CE, Lang RM. Use of echocardiography for the phenotypic assessment of genetically altered mice. Physiol Genomics 2003;13(3):227-39.
139. Lundby C, Nordsborg N, Kusuhara K, Kristensen KM, Neufer PD, Pilegaard H. Gene expression in human skeletal muscle: alternative normalization method and effect of repeated biopsies. Eur J Appl Physiol 2005;95(4):351-60.
140. Shyu KG, Ko WH, Yang WS, Wang BW, Kuan P. Insulin-like growth factor-1 mediates stretch-induced upregulation of myostatin expression in neonatal rat cardiomyocytes. Cardiovasc Res 2005;68(3):405-14.
141. Jeanplong F, Bass JJ, Smith HK, Kirk SP, Kambadur R, Sharma M, et al. Prolonged underfeeding of sheep increases myostatin and myogenic regulatory factor Myf-5 in skeletal muscle while IGF-I and myogenin are repressed. J Endocrinol 2003;176(3):425-37.

142. Bullough WS. Mitotic and functional homeostasis: a speculative review. Cancer Res 1965;25(10):1683-727.
143. Gaussin V, Depre C. Myostatin, the cardiac chalone of insulin-like growth factor-1. Cardiovasc Res 2005;68(3):347-9.
144. Reardon KA, Davis J, Kapsa RM, Choong P, Byrne E. Myostatin, insulin-like growth factor-1, and leukemia inhibitory factor mRNAs are upregulated in chronic human disuse muscle atrophy. Muscle Nerve 2001;24(7):893-9.
145. Cook SA, Matsui T, Li L, Rosenzweig A. Transcriptional effects of chronic Akt activation in the heart. J Biol Chem 2002;277(25):22528-33.
146. Dudek H, Datta SR, Franke TF, Birnbaum MJ, Yao R, Cooper GM, et al. Regulation of neuronal survival by the serine-threonine protein kinase Akt. Science 1997;275(5300):661-5.
147. Matsui T, Li L, Wu JC, Cook SA, Nagoshi T, Picard MH, et al. Phenotypic spectrum caused by transgenic overexpression of activated Akt in the heart. J Biol Chem 2002;277(25):22896-901.
148. McMullen JR, Jennings GL. Differences between pathological and physiological cardiac hypertrophy: novel therapeutic strategies to treat heart failure. Clin Exp Pharmacol Physiol 2007;34(4):255-62.
149. Du XJ, Gao X, Ramsey D. Surgical methods of inducing transverse aortic stenosis and myocardial infarction in the mouse. Asia Pacific Heart Journal 1998;7:187-92.
150. Degabriele NM, Griesenbach U, Sato K, Post MJ, Zhu J, Williams J, et al. Critical appraisal of the mouse model of myocardial infarction. Exp Physiol 2004;89(4):497-505.
151. Michael LH, Ballantyne CM, Zachariah JP, Gould KE, Pocius JS, Taffet GE, et al. Myocardial infarction and remodeling in mice: effect of reperfusion. Am J Physiol 1999;277(2 Pt 2):H660-8.
152. Ahn D, Cheng L, Moon C, Spurgeon H, Lakatta EG, Talan MI. Induction of myocardial infarcts of a predictable size and location by branch pattern probability-assisted coronary ligation in C57BL/6 mice. Am J Physiol Heart Circ Physiol 2004;286(3):H1201-7.
153. Lutgens E, Daemen MJ, de Muinck ED, Debets J, Leenders P, Smits JF. Chronic myocardial infarction in the mouse: cardiac structural and functional changes. Cardiovasc Res 1999;41(3):586-93.
154. Gould KE, Taffet GE, Michael LH, Christie RM, Konkol DL, Pocius JS, et al. Heart failure and greater infarct expansion in middle-aged mice: a relevant model for postinfarction failure. Am J Physiol Heart Circ Physiol 2002;282(2):H615-21.

155. Doevendans PA, Daemen MJ, de Muinck ED, Smits JF. Cardiovascular phenotyping in mice. Cardiovasc Res 1998;39(1):34-49.
156. Sesso HD, Stampfer MJ, Rosner B, Hennekens CH, Gaziano JM, Manson JE, et al. Systolic and diastolic blood pressure, pulse pressure, and mean arterial pressure as predictors of cardiovascular disease risk in Men. Hypertension 2000;36(5):801-7.
157. Rottman JN, Ni G, Brown M. Echocardiographic evaluation of ventricular function in mice. Echocardiography 2007;24(1):83-9.
158. Roth DM, Swaney JS, Dalton ND, Gilpin EA, Ross J, Jr. Impact of anesthesia on cardiac function during echocardiography in mice. Am J Physiol Heart Circ Physiol 2002;282(6):H2134-40.
159. Leask A, Abraham DJ. TGF-beta signaling and the fibrotic response. FASEB J 2004;18(7):816-27.
160. Takagawa J, Zhang Y, Wong ML, Sievers RE, Kapasi NK, Wang Y, et al. Myocardial infarct size measurement in the mouse chronic infarction model: comparison of area- and length-based approaches. J Appl Physiol 2007;102(6):2104-11.
161. Wang J, Hoshijima M, Lam J, Zhou Z, Jokiel A, Dalton ND, et al. Cardiomyopathy associated with microcirculation dysfunction in laminin alpha4 chain-deficient mice. J Biol Chem 2006;281(1):213-20.
162. Briguet A, Courdier-Fruh I, Foster M, Meier T, Magyar JP. Histological parameters for the quantitative assessment of muscular dystrophy in the mdx-mouse. Neuromuscul Disord 2004;14(10):675-82.
163. Kitamura M, Shimizu M, Kita Y, Yoshio H, Ino H, Misawa K, et al. Quantitative evaluation of the rate of myocardial interstitial fibrosis using a personal computer. Jpn Circ J 1997;61(9):781-6.
164. Detre S, Saclani Jotti G, Dowsett M. A "quickscore" method for immunohistochemical semiquantitation: validation for oestrogen receptor in breast carcinomas. J Clin Pathol 1995;48(9):876-8.
165. Moore GW, Hutchins GM, Bulkley BH, Tseng JS, Ki PF. Constituents of the human ventricular myocardium: connective tissue hyperplasia accompanying muscular hypertrophy. Am Heart J 1980;100(5):610-6.
166. Vliegen HW, van der Laarse A, Cornelisse CJ, Eulderink F. Myocardial changes in pressure overload-induced left ventricular hypertrophy. A study on tissue composition, polyploidization and multinucleation. Eur Heart J 1991;12(4):488-94.
167. Souders CA, Bowers SL, Baudino TA. Cardiac fibroblast: the renaissance cell. Circ Res 2009;105(12):1164-76.

168. Sun Y, Kiani MF, Postlethwaite AE, Weber KT. Infarct scar as living tissue. Basic Res Cardiol 2002;97(5):343-7.
169. Gabbiani G. The myofibroblast in wound healing and fibrocontractive diseases. J Pathol 2003;200(4):500-3.
170. Leslie KO, Taatjes DJ, Schwarz J, vonTurkovich M, Low RB. Cardiac myofibroblasts express alpha smooth muscle actin during right ventricular pressure overload in the rabbit. Am J Pathol 1991;139(1):207-16.
171. Leask A. Potential therapeutic targets for cardiac fibrosis: TGFbeta, angiotensin, endothelin, CCN2, and PDGF, partners in fibroblast activation. Circ Res 2010;106(11):1675-80.
172. Ellmers LJ. The role of transforming growth factor-beta in cardiac fibrosis. Current Enzyme Inhibition 2010;6(2):78-86.
173. Zhu J, Li Y, Shen W, Qiao C, Ambrosio F, Lavasani M, et al. Relationships between transforming growth factor-beta1, myostatin, and decorin: implications for skeletal muscle fibrosis. J Biol Chem 2007;282(35):25852-63.
174. Artaza JN, Singh R, Ferrini MG, Braga M, Tsao J, Gonzalez-Cadavid NF. Myostatin promotes a fibrotic phenotypic switch in multipotent C3H 10T1/2 cells without affecting their differentiation into myofibroblasts. J Endocrinol 2008;196(2):235-49.
175. van Krimpen C, Smits JF, Cleutjens JP, Debets JJ, Schoemaker RG, Struyker Boudier HA, et al. DNA synthesis in the non-infarcted cardiac interstitium after left coronary artery ligation in the rat: effects of captopril. J Mol Cell Cardiol 1991;23(11):1245-53.
176. Schneyer AL, Sidis Y, Gulati A, Sun JL, Keutmann H, Krasney PA. Differential antagonism of activin, myostatin and growth and differentiation factor 11 by wild-type and mutant follistatin. Endocrinology 2008;149(9):4589-95.
177. Welt C, Sidis Y, Keutmann H, Schneyer A. Activins, inhibins, and follistatins: from endocrinology to signaling. A paradigm for the new millennium. Exp Biol Med (Maywood) 2002;227(9):724-52.
178. Harmon EB, Apelqvist AA, Smart NG, Gu X, Osborne DH, Kim SK. GDF11 modulates NGN3+ islet progenitor cell number and promotes beta-cell differentiation in pancreas development. Development 2004;131(24):6163-74.
179. http://www.amgenoncology-international.com/#/our-products/our-pipeline/. In.
180. Haas MJ. Muscling up in cancer cachexia. Science Business eXchange 2010.
181. http://clinicaltrials.gov/show/NCT00975104.

182. Attie KM, Borgstein NG, Yang Y, Condon CH, Wilson DM, Pearsall AE, et al. A single ascending-dose study of muscle regulator ACE-031 in healthy volunteers. Muscle Nerve 2013;47(3):416-23.
183. http://quest.mda.org/news/update-ace-031-clinical-trials-duchenne-md.
184. Kung G, Konstantinidis K, Kitsis RN. Programmed necrosis, not apoptosis, in the heart. Circ Res 2011;108(8):1017-36.